NGU Report 95.153

# Regional Geology of the Okstindene Area, the Rödingsfjäll Nappe Complex, Nordland, Norway

NGU
NORGES GEOLOGISKE UNDERSØKELSE
Geological Survey of Norway
P.O.Box 3006 - Lade
N-7002 Trondheim, Norway
Tel.: 47 73 90 40 11
Telefax 47 73 92 16 20

# REPORT

Report no.: 95.153 | ISSN 0800-3416 | Grading: Open

Title:
Regional Geology of the Okstindene Area, the Rödingsfjäll Nappe Complex, Nordland, Norway

Authors:
Terje Bjerkgård, Rune Larsen, Mogens Marker

Client: NGU, The Nordland Programme, Bleikvassli Gruber

| | |
|---|---|
| County: Nordland | Commune: Hemnes |
| Map-sheet name (M=1:250.000): Mo i Rana and Mosjøen | Map-sheet no. og -name (M=1:50.000): 1926-I Røssvatnet, 1927-II Korgen, 2026-IV Hjartfjellet, 2027-III Storakersvatnet |
| Deposit name and grid-reference: | Number of pages: 87  Price (NOK): 430<br>Map enclosures: Geology of the Okstindene Area |

| Fieldwork carried out: | Date of report: | Project no.: | Person responsible: |
|---|---|---|---|
| 1993, 1994, 1995 | December 1995 | 67.2543.29 | |

Summary:
This report presents preliminary results of regional fieldwork in the Okstindene Area, the Rödingsfjäll Nappe Complex (RNC), Uppermost Allochthon, Nordland, Norway. The area hosts the Bleikvassli sedimentary-exhalative Pb-Zn deposit, and the main objective with this work is to establish a geological basis for prospecting after new Pb-Zn deposits in the area. The area comprises four lithological units; the Kjerringfjellet(?), Anders Larsa/Lifjell and Kongsfjell Groups and the Målvatn Unit. All units are dominated by metasediments, mainly garnet-mica and calcareous mica schists. Calcite and dolomite marbles are abundant in the Anders Larsa and Lifjell Groups, whereas various quartz-feldspathic schists are typical of the Målvatn Unit. Amphibolites, which are metabasalts and andesites of probable transitional MORB to island arc affinity according to geochemistry, are present in all units. They are particularly abundant in the Kongsfjell Group close to the contacts to the Anders Larsa/Lifjell Groups and between calcareous mica schists and garnet-mica schists. Isolated bodies of ultramafics, partly chromite-bearing, are present within the Målvatn Unit, close to Kongsfjell Group. Taking into account the geochemistry of the amphibolites and the association with mainly continent-derived sediments, the the Okstindene lithologies have most probably formed in a spreading regime behind an ensialic arc. Sr-isotope analysis of the marbles, show that the sediments have an age of 590-600 Ma, in accordance with ages obtained elsewhere in the RNC. The area has been subjected to five major deformation phases, of which the first three have been very intense. The rock units have been folded into one megascale, recumbent fold, bounded by major thrusts. This structure has a major impact on prospecting after new deposits, meaning that the contact between the Lifjell and Kongsfjell Group is as important as the contact between the Anders Larsa and Kongsfjell Group, where the Bleikvassli deposit is situated.


| Keywords: Okstindene Area | Rödingsfjäll Nappe Complex | Sedimentary exhalative lead-zinc deposit |
|---|---|---|
| Bleikvassli Mine | Regional Geology | Geochemical analyses |
| Strontium Isotopes | REE Analyses | Ensialic arc environment |

# CONTENTS

## APPENDIX

1) Map with sample localitities

2) Complete XRF analyses of rock samples collected in 1994.

3) Geology of the Okstindane Area - Geological map 1 : 75 000

## INTRODUCTION

This report presents preliminary results of regional fieldwork in the Okstindene Area, the Rödingsfjäll Nappe Complex, Uppermost Allochthon, Nordland, Norway, until December 1995 (fig.1 and 2). The field work was carried out during the summers of 1993, 1994 and 1995.

The area, which all together has been mapped both in earlier days and during this project, extends from the northern shores of Røssvatnet in the south to the southern shores of Storakersvatnet in the north. In the west the area is mapped until the river Røssåga, while the eastern restriction is the Swedish border. The total area covered by mapping is close to 1100 km$^2$.

The areas south and partly west of the Bleikvassli mine were mapped before this project was initiated. This work were done by Ramberg (1967), I.J. Rui (internal reports for A/S Bleikvassli Gruber), several Danish and Norwegian students and others employed by the mining company. Correlation of these data and including mapping of the southern part of the area, close to Røssvatnet were done by Gustavson & Gjelle (Preliminary mapsheet 1:50000, Røssvatnet 1926 I).

The areas southeast and east of the mine (viz. the area between Røssvatnet and the Okstindene Glacier), the valley Spjeltfjelldalen and the area between the lakes Grasvatnet and Storakersvatnet were to a large degree mapped during the summer 1993 by Mogens Marker and Rune Larsen. In 1994, the authors of this report mapped the area between the northern shores of Bleikvatnet to Grasvatnet and westward to Målvatnet. In 1995, the first author of the report mapped the area around Målvatnet and westwards to Leirskardalen and the area north of Grasfjellet, while the second author worked in the Artfjellet area and Halvarddalen. The geological data have been interpreted and transformed into digital form and is found as a map in the appendix. Representative samples of the different lithologies were collected in order to reveal their geophysical properties as well as to carry out geochemical analyses (see appendix for complete analyses and map with sample localities.

The main objective of this work has been to establish a geological basis for prospecting after new lead-zinc ore deposits. Geology is, together with soil geochemistry and aerial geophysics, the basis for isolating anomalies or areas for further investigations.

The Bleikvassli deposit is a lead-zinc deposit of the proximal sedimentary-exhalative type (Skauli 1992), which means that it was formed above its exhalative conduit. Deposits may also form distal from the conduit. Proximal deposits are easier to find because of the possible association with alteration zones, proximity to igneous rocks and relation to inconformities such as larger fault

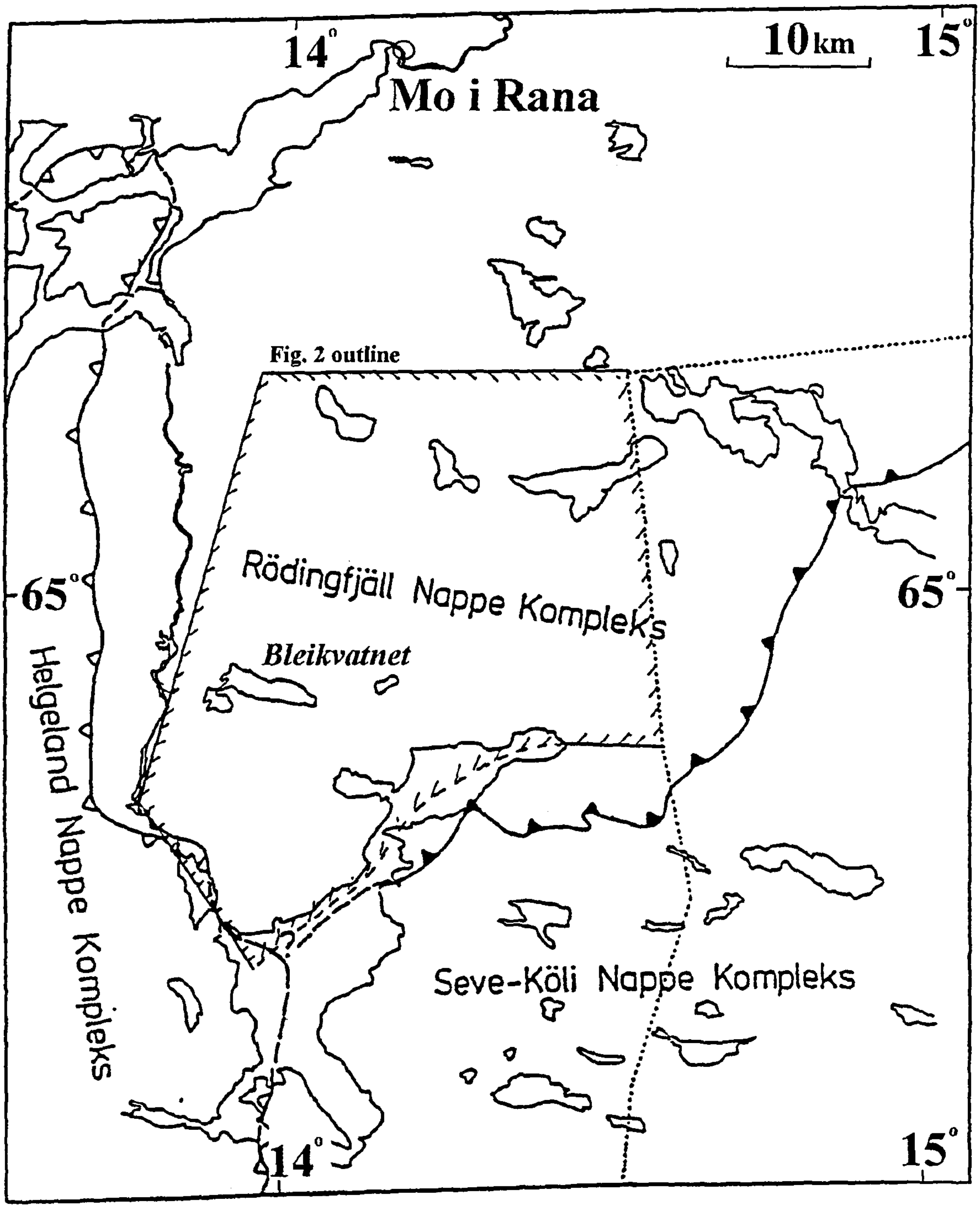


Figur 1: A simplified tectonostratigraphic of the Central-Northern Caledonides of Norway. The position of the Okstindene Area (Fig. 2) is outlined.

zones or primary unconformities. A distal deposit, even though it may be considerably larger, lacks lithological or structural features revealing its nearby presence. Thus, it is necessary to unravel the original morphology of the sedimentary basin as well as the nature and origin of the lithologies in order to restrict the investigations to areas where some of the above-mentioned criteria for proximal exhalations are fulfilled.

Earlier field work has shown that the Kongsfjell Group, which is the unit hosting the Bleikvassli deposit, has the best potential for finding new deposits and furthermore, a lot of smaller mineralizations are found in the vicinity of Bleikvassli. However, none of these seems to be economically viable. The other lithological units in the area are almost barren with respect to sulfide mineralizations. Thus, regional geological studies have been concentrated to the Kongsfjell Group and to follow and correlate promising lithologies in this unit.

Earlier work has shown that the region was affected by several deformational episodes having different imprint on the lithologies in the area, and it was necessary to undertake regional structural studies to understand the original structure and architecture of the sedimentary basin.

## TECTONOSTRATIGRAPHY AND STRATIGRAPHY OF THE RÖDINGSFJÄLL NAPPE COMPLEX

The Okstindene Area is situated within the Rödingsfjäll Nappe Complex, which is part of the Uppermost Allochthon of the Central-Norwegian Caledonides (fig.1). The nappe complex is placed above the Seve-Köli Nappe Complex in the Upper Allochthon and below the Helgeland Nappe Complex in the Uppermost Allochthon. The Rödingsfjäll Nappe Complex is bordered by extensive mylonites at the trust contacts to the other allochthons.

In the Okstindene Area, the Rödingsfjäll Nappe Complex comprises four lithological units. These are from the structural basis and upward the Mofjellet Group or the Kjerringfjell Group, the Anders Larsa Group/Lifjell Unit, the Kongsfjell Group and the Målvatnet Unit (fig.2). The position of the Målvatnet unit is, however, uncertain due to incomplete mapping and structural interpretation in the northernmost area, and it might be equivalent to units within the Mofjellet Group.

### The Mofjellet or Kjerringfjell Group

Felsic grey gneisses which either belong to the Mofjellet Group or the Kjerringfjell Group are found in the core of a dome structure in the northern part of Spjeltfjelldalen (center of dome ≈ UTM 478 7325). The structure has so far not been investigated in detail in this project and will not be addressed any further.

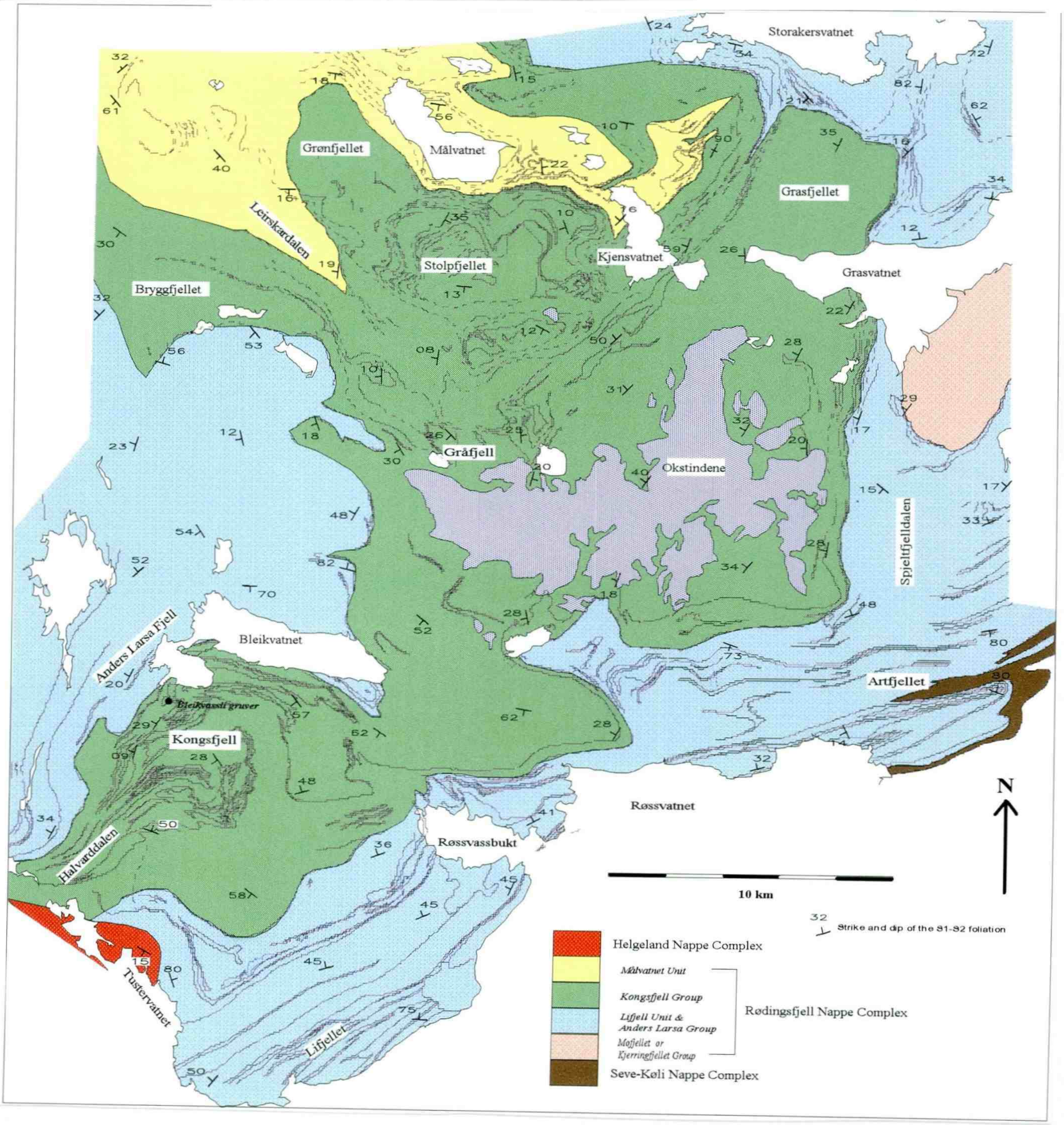


Figur 2: The main lithological units of the Okstindene area. The streaks within each unit mark rock boundaries and outline main structural patterns.

## The Lifjell unit

The lithologies at Lifjellet just north of Røssvatnet comprise garnet-mica schists and calcareous mica schists, extensive units of calcite marbles, dolomite marbles and quartz-feldspathic schists, the latter of which could represent felsic metavolcanics. This package of rocks continues eastwards partly across Artfjellet into Sweden, but reenters Norway north of Mofjellet, where it is named the Plurdal Group. Because of complex structural geometry, the rocks also branches into Spjeltfjelldalen and can be followed up to Grasvatnet and further to Storakersvatnet. These rocks seem to be separated from the Kongsfjell Group by a tectonic boundary and is therefore in this context referred to as the Lifjell Unit after the mountain just north of Røssvatnet. This unit is also very similar to, and could be correlated with the Anders Larsa Group (see below).

## The Anders Larsa Group

The Anders Larsa Group which are found in the northwestern part of the area, is dominated by thick units of marbles, separated by garnet-mica schists and calcareous mica schists. This unit is separated from the Kongsfjell Group by an unconformity or a tectonic boundary. The lithologic assemblage of the Anders Larsa Group and especially the high content of marbles, makes a correlation to the Plurdal Group and the units at Lifjell likely.

## The Kongsfjell Group

The Kongsfjell Group is totally dominated by garnet-mica schists, which occupy the central part of the mapped area. Very persistent units of calcareous mica schists with thickness up to several hundred meters occur in the upper part of the garnet-mica schists. The layers of calcareous schists have especially large thickness in Leirskardalen, due to repetitive folding (Fig.3). Amphibolites occur in the Kongsfjell Group both as extensive layers and as restricted and isolated bodies. The more extensive layers probably represent basaltic flows. Amphibolites are typically found at or close to the contact between garnet-mica schists and calcareous mica schists. Other rock types in the Kongsfjell Group are graphitic schists, typically associated with garnet-mica schists, and calcite marble, occurring in thin lenses, but exceptionally also as more extensive and thicker layers. Quartz-feldspathic schists are abundant at Kongsfjellet and Stolpfjellet and small isolated bodies of presumed orthogneisses are also found.

## The Målvatn Unit

The Målvatnet Unit is a field term given for a complex unit consisting of quartz-feldspathic schists (probably meta-sediments), garnet-mica schists, thin units of amphibolites, marbles and small bodies of ultramafic rocks, which have been mapped in the area around the lake Målvatnet, and also has been followed into Leirskardalen. The contact to the structurally overlying Kongsfjell Group is marked by a persistent thin layer of calcite marble, and the contact seems to be an unconformity rather than a tectonic boundary.

## THE POSITION OF THE BLEIKVASSLI DEPOSIT

The Bleikvassli deposit is situated in the structurally uppermost part of the Kongsfjell Group, close to the possible unconformity between this group and the structurally overlying Anders Larsa Group. The deposit is closely associated with extensive units of metabasalts or amphibolites, situated about 100 m structurally below the deposit. The rocks between the amphibolites and the stratiform massive ore are mainly kyanite-mica schists, impure quartzites and microcline gneiss. The ore itself is imbedded in quartz-muscovite schist. The high content of potassium in the microcline gneiss, and also silica and alumina in the other lithologies have been interpreted to be due to hydrothermal alteration (Skauli 1992). New work by Larsen et al. (in prep.) however, show that the microcline gneiss is an alkaline syenitic intrusive, and not a result of extensive alteration. A presumably precise magmatic age of 481 +/- 2 Ma has been obtained for this intrusion (Larsen et al., in prep.), which is more than 100 Ma younger than the surrounding sediments, and thereby also the ore deposit. Also stratigraphically below and above the ore are thick horizons of quartz-feldspathic mica schists. These schists extend for several kilometers southwards from the deposit and are best developed at Kongsfjellet, southeast of Bleikvassli, where they are partly altered to quartz-muscovite schists. In that area the quartz-muscovite schists typically contain minor iron sulfides and there are numerous small occurrences of lead and zinc sulfides.

## DESCRIPTION OF THE LITHOLOGIES

### The Lifjell Unit and Anders Larsa Group

Because of the many similarities between these two units, they are naturally described together (see also below).

#### Garnet-mica schists

Garnet-mica schists are abundant in these units. As opposed to the Kongsfjell Group, the garnet mica schists in this unit are more mafic as they contain amphibole and locally also chlorite as major phases. Another important difference is that the Anders Larsa/Lifjell garnet mica schists contain segregations of calcite in the central parts of lenses composed of quartz. This relationship is also known from calcareous mica schist, but in contrary to this lithology, calcite is absent in the matrix.

In the area around Artfjellet, where the eastern continuation of the Lifjell Unit appears, the garnet-mica schists obtain an almost gneissic appearance. Garnets are extremely coarse-grained, quartz-feldspathic leucosomes are developed and the schistosity is less pronounced compared to the Lifjell area. Finally, the garnet-mica schists in the Lifjell Unit contain horizons which are more than 50 m thick ( for example cropping out at Tustervassdammen; UTM 44460 730522), that are enriched in magnetite and, for this reason, is responsible for a strong magnetic anomaly. The major phases in a sample from Tustervassdammen are quartz, plagioclase, biotite, muscovite, garnet, hornblende, chlorite and staurolite. Apatite, magnetite and tourmaline are important accessory phases.

Calcareous mica schists

Calcareous mica schists are present in these units in thick horizons. Horizons with thicknesses of several hundred meters are present in the Lifjell Unit. One horizon is extending from Tustervatnet (UTM 450 7299) to Røssvassbukt (UTM 463 7309) where it wedges out toward a tectonic contact. Another thick unit has been mapped in the area between Över-Uman and Storakersvatnet. (UTM 477 7335 to 4785 7332). These two units can possibly be correlated. There are no differences between the calcareous mica schists in these units and the ones in the Kongsfjell Group (see below for mineralogy, description).

Amphibolites

Larger horizons of amphibolites are found in the Lifjell Unit north of Røssvatnet (at Steikfjellet and Artfjellet, e.g. horizon from ≈ UTM 466 7313 to 478 7314), close to Grasvatnet (from ≈ UTM 4732 73204 to 4787 73308) and finally, south of Storakersvatnet (westwards from ≈ UTM 4709 73337). As for the amphibolites in the Kongsfjell Group, the large extent of these units (5-20 km) strongly indicate that they represent volcanic flows rather than being intrusive. One large amphibolite within the Anders Larsa Group is found east of the Bleikvassli deposit, at the southern banks of Bleikvatnet (UTM 456 7312) and probably extending westward to Rapliåsen (UTM 450 7314) close to Bleikvassli. This unit is very interesting because it contain an ultramafic body (UTM 4564 73125). Otherwise, the amphibolites in these units are quite similar in appearance to those in the Kongsfjell Group (see below).

Marbles

Marbles are present in all the units in the Okstindene area, but are particularly abundant in the Anders Larsa Group and the Lifjell Unit. Marbles of the Anders Larsa Group are well exposed in road cuts along the main road from Bleikvassli to Korgen. The marbles are both dolomite and calcite marbles, usually of relatively high purity. Dolomite marble is dominant, occurring sometimes in more than 100 meter thick beds. The calcite marble beds are usually less than 10 meter thick. Along the Bleikvassli-Korgen road, the marbles alternate with garnet-mica schists, calcareous mica schists and amphibolites.

In the Lifjell Unit thick beds of calcite and dolomite marbles are also found in the northern part of Spjeltfjelldalen (about UTM 474 7324) and continue northward across Grasvatnet where they turn eastward into Sweden. The beds disappear under the mountain Grasfjellet, but crop out again at the northern slopes of the mountain, south of Storakersvatnet. In this area, beds of several hundred meters thickness of both calcite and dolomite marble occur with some intercalations of mainly amphibolite, especially in the structurally upper part. These marble beds cover the banks of the Storakersvatnet, especially in the north and south. The outcrop pattern is mainly due to interplay between the fold phases $F_4$ and $F_5$, which create domes and depressions (see structural geology section).

The calcite and dolomite marbles are relatively easy to distinguish in the field. The calcite marble is coarse grained (2-10 mm calcite grains), often characterized by a graphite-banding, yellowish to white hue and no calc-silicates. However, at the border to schist units a contact skarn is often present containing diopside and/or actinolite/tremolite. The dolomite marbles are very massive, fine-grained (less than 1 mm), homogeneous or with bands rich in calc-silicates and usually have a bluish white tint. Calc-silicate minerals, usually tremolite, are abundant, and at Storakersvatnet tremolite occur in up to 50 cm long needles, sometimes in stellate aggregates (fig.3).

Figure 3: Tremolite crystals in dolomite marble. Locality: north of Grasfjellet (UTM 474300 7333600). Length of ruler is 15 cm.

Where the dolomite and calcite marbles are in contact, there is a sharp boundary between them. For example, in the Grasvatnet - Storakersvatnet area, the calcite marbles make up the structurally upper part of a several hundred meters thick unit comprising both calcite and dolomite marble. The boundary between the two marbles is well defined.

Typically, the calcite marbles have a grain-size of 1-3 mm and occur in a somewhat irregular granoblastic texture. Accessory quartz occur as small, rounded inclusions in the calcite grains, whereas muscovite occur as minute laths. Pyrite occur as minute rounded grains as well. The dolomite marbles generally have a grain-size around 0.5 mm, and the dolomite grains occur in a well crystallized granoblastic texture. Accessory tremolite and diopside are typically poikiloblastic with quartz inclusions. Muscovite is occasionally present.

In the Lifjell Unit in the Røssvatnet area, thin horizons (few meters) of very magnetite-rich rocks, creating strong magnetic anomalies, occur intercalated in calcite marble. At one locality (UTM 44873 730178) a magnetite-quartzite rock is strongly sheared, containing quartz in a typical ribbon texture and magnetite twisted into fish-shapes. Some amphibole is also present. The shearing is most likely due to the position close to the contact to the Seve-Köli Nappe Complex. At another locality near Røssvassbukt (UTM 45820 730697) the rock is a magnetite-quartz-hornblende-biotite schist. These magnetite-rich rocks may represent small equivalents to the banded iron formations in Dunderlandsdalen, which are also hosted by carbonates.

The marbles in the Lifjell - Artfjell area are quite similar to those described from the Grasvatnet-Storakersvatnet area. Either they are composed of dolomite, occasionally with 1-2 cm thick bands of coarse-grained white tremolite, or they are largely composed of calcite ± graphite ± calcsilicate minerals. One particular calcite marble cropping out south of Artfjellet is extremely rich in graphite giving it a dark grey appearance and a well defined slaty schistosity. As in the Anders Larsa group, the contact between the calcite and dolomite marbles is sharp and welldefined. Individual layers of marble vary in thickness from a few meters and up to 400 meters and can normally be followed for kilometers to tens of kilometers along strike.

### The Kongsfjell Group

*Garnet-mica schists*

Garnet-mica schists are the dominating lithology of the Kongsfjell Group and especially occupy the central and north-eastern part of the area, underlying and encircling the Okstindene Glacier. This massive and weather-resistant rock is responsible for the high altitude and alpine character of the glacier area.

Figure 4: Typical garnet-mica schists from the Kongsfjell Group, with biotite, quartz and quartz-feldspar-rich lenses. Red spots are garnets. Length of ruler is 15 cm. Locality: East of Kjennsvatnet (UTM 464390 7329850).

The schists are generally characterized by mm to cm thick laminae and layers composed mostly of quartz in a micaceous matrix, dominated by muscovite, with smaller, but significant amounts of biotite (fig.4). At some localities, for example at Artfjellet, the garnet-mica schists obtain a gneissic appearance characterized by quartz-feldspathic leucosomes and a non-penetrative foliation, consisting of biotite and muscovite. Generally, garnets are evenly distributed, in both mm to cm aggregates of smaller grains and as single crystals. Larger lenses or veinlets of quartz are common, containing coarse-grained feldspar, amphibole, biotite, and sometimes kyanite.

The garnet-mica schists are particularly rich in kyanite in the high areas in the northern part of the Okstindene Glacier (from about UTM 458 7320) and extending northwards and westwards to Grasfjellet (UTM 471 7333). Similar schists are also found at the highest peaks of Tverrfjellet (UTM 4615 73252) and Stolpfjellet (UTM 4595 73285).

The kyanite-rich schists consist of cm-scale alternating bands rich in muscovite, kyanite and quartz. The high content of kyanite gives the rocks a conspicuous bluish colour. Up to several cm long crystals of blue kyanite are found within the numerous quartz-segregations in the schists. These schist generally have a variable content of garnet and in the slopes of the high peaks Okstinden (UTM 466200 7320220) and Oksskolten (UTM 470060 7321850), there are strata composed of garnet-free kyanite-muscovite schists, intercalated or folded together with more typical garnet-mica schists, also containing a lot of kyanite. The boundary between kyanite-rich and almost kyanite-free schists is sharp, which indicates that it was a primary feature in the sediments, probably due to an initially higher content of alumina (see geochemistry section).

South of Stolpfjellet, in an area from Svarttinden (UTM 4547 73297) to Grønfjellet (UTM 4533 73313) and Kviturdfjellet (UTM 4550 73342), extending eastwards from there along Målvatnet (UTM 4578 73305) to Kjennsvatnet (UTM 4635 73300), and close to the contact to the Målvatnet Unit, there is a very light variety of garnet-mica schist with a high content of feldspar and muscovite. Garnets have a characteristic white rim of quartz, which in high strain zones form extended haloes around the garnets or fine-grained garnet-aggregates (fig.5). The content of garnet is variable, but generally lower than in ordinary garnet-mica schists, and in zones which can be up to 10-20 meter thick, there are no garnets present. This variety also show a weathering surface which is irregular due to small pits, which is indicative of a rather high content of carbonate (fig.6). Structurally above, there is a well defined contact to garnet-mica schist which is darker because of a higher content of mica, especially biotite and a much lower content of feldspar, which also makes it more schistose. The content of garnet is quite low and it is partly rusty because of small amounts of sulfides.

Close to the contact with carbonate-rich lithologies such as the calcareous mica schist and marbles, the garnet mica schists has a strong schistosity, and contain small amounts of sulfides as indicated by its rusty appearance. They may also contain some graphite. The rusty schists are especially found at Gråfjell, north of Okstinden and Oksskolten, all north of the Okstindene Glacier

Figure 5: Garnet-mica schist containing garnets with rims of mainly quartz. Locality: Kjelbekkskaret (UTM 457670 7330600). Length of ruler is 15 cm.

(about UTM 459 7321 to UTM 472 7325). The content of garnet is commonly low in the most rusty schists. Where the contact is not marked by rusty schists, the garnets in the garnet-mica schists are often much bigger than elsewhere (up to 2-3 cm). The reason could be that Ca from the calcareous schists is readily taken up by the garnet (grossular-component).

The occurrence of rusty, schistose, garnet-mica schists at the contact to the calcareous schists is most probably due to the effect of increasing pH because of the presence of carbonates, which leads to deposition of sulfides.

Generally the garnet-mica schists consist of quartz, muscovite and biotite as main phases. There is generally a diffuse to discrete banding between bands of mainly granoblastic quartz and bands of muscovite-biotite. Muscovite is always growing at expense of biotite. Kyanite is present as poikiloblastic, large grains, and often, also as a major phase. Garnet is a subordinate to major phase, always porphyroblastic. Important accessory phases are tourmaline, alkalifeldspar, plagioclase and rutile.

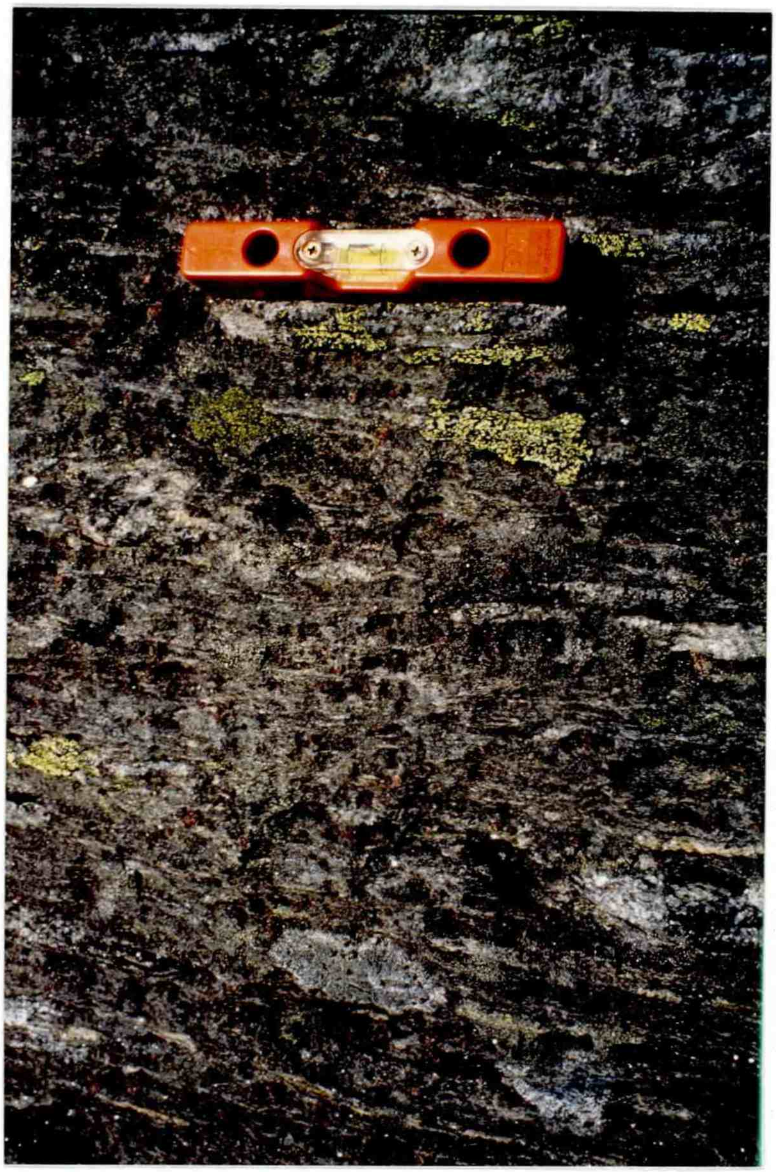

Figure 6: Garnet-mica schist with weathering pits after carbonate. Locality: North of Måltinden (UTM 461700 7334240). Length of ruler is 15 cm.

Figure 7 a): Well defined contact between light garnet-mica schist and dark calcareous mica schist. Locality: Tverrfjellet (UTM 464560 7325640). Photo towards the South. Length of hammer shaft is 35 cm.

Figure 7 b): Typical calcareous mica schist, with dark color and a weathering surface with many pits. Locality: Top of Gråfjell (UTM 459250 7321690). Photo towards the North. Length of hammer shaft is 35 cm.

Calcareous mica schists

The calcareous mica schists occur as persistent layers within the peripheral parts of the units of garnet-mica schists in the Kongsfjell Group and may obtain thicknesses of several hundred meters. The contact to the garnet-mica schists is typically very sharp (fig.7 a). The largest abundance of these schists are in Leirskardalen, at Kongsfjellet and northwest of Grasvatnet. At least regarding the first two localities, the great thickness is partly due to folding (see below).

The schists consist mainly of quartz, calcite, feldspar and biotite, while muscovite and/or amphibole and/or epidote are subordinate. Garnet is mostly accessory, but is locally very abundant. The high content of biotite gives the rock a dark color, and together with a high content of calcite, giving a weathering surface with many pits, makes it easy to distinguish the rock in the field (fig.7 b). The content of calcite is variable and locally it grades into impure marble. The content of calc-silicate minerals (i.e. epidote, diopside and amphibole) is locally high, such as at Tverrfjellet (UTM 4610 73254) and the major unit at Kjennsvassfjellet (about UTM 467 7330 to about UTM 469 7334), giving the rock a conspicuous greenish color.

Amphibolites

Amphibolites occur in all the lithological units as concordant layers or horizons of variable extent and thickness. They typically have a dark green to black color and are usually schistose. Color differences are mainly due to variations in the content of epidote and biotite. Larger amphibolites which belong to the Kongsfjell Group are found about 100 m structurally and probably also stratigraphically below the Bleikvassli deposit. This very thick unit is tightly folded and can be traced for 5-10 km eastward on Kongsfjell. Another thick unit is followed from Halvarddalen northward to the southern part of Kongsfjell, a total length of more than 15 km. Another 2.5 km long, but relatively thin unit is found north of Kjennsvatnet. The large extent of these units makes a formation as flows reasonable.

The only locality where an amphibolite seems to be intrusive is at a locality between Stolpfjellet and Grønfjellet (UTM 456360 7330320), where an amphibolite body contains angular stretched xenoliths of a felsic rock (fig.8).

Small and intensively folded bodies are abundant at Stolpfjellet and Tverrfjellet (e.g. UTM 4640 73255 and 4642 73265). These bodies may be tectonically disrupted fragments of a larger horizon and also includes larger concordant lenses at both Stolpfjellet (UTM 4627 73285), Tverrfjellet (UTM 4600 73250) and Gråfjell (e.g. UTM 4635 73225, 4610 73220, 4585 73217 and 4570 73217).

Figure 8: Amphibolite with angular xenoliths of a felsic rock.
Locality: Grønfjellet (UTM 456360 7330320).

Figure 9: Strongly deformed amphibolite with a cm-scale banding between amphibole and feldspar-rich laminae. Lenses of quartz (white) and calcite (yellow-brownish) is also seen.
Locality: Okstindtjønna (UTM 462680 7321400).

The amphibolites may be very important in prospecting for new ore deposits. It is probably not a coincidence that the most extensive amphibolite horizon is found in the footwall of the Bleikvassli deposit. The amphibolites are also to a large degree found at, or close to the contact between garnet-mica schist and calcareous mica schist. The amphibolites are often more deformed than the mica schists, due to its lower competency.

The amphibolites typically consist of 35-40 % plagioclase, 40-50 % green hornblende and variable amounts of biotite and epidote. Quartz and sphene are common subordinate phases, whereas rutile, carbonate, garnet and apatite are common accessory phases. Later influx of oxidizing fluids resulted in formation of epidote and locally also hematite. High content of biotite is usually a result of shear deformation, and sometimes amphibolite is totally replaced by a plagioclase-biotite schist. Heavy shearing also results in a lamination between feldspar-rich and amphibole-rich laminae at a cm-scale, or if rich in epidote, between feldspar + epidote and amphibole-rich laminae (fig.9).

Marbles

Thin lenses of both relatively pure and impure calcite marble are present at many places within the Kongsfjell Group, but are especially abundant at Kongsfjellet and north of Kjennsvatnet, at Kjennsvassfjellet. Dolomite marble seems to be absent in this group, as opposed to the Anders Larsa Group and equivalent units, where dolomite marbles are dominant (see above). The only thicker and continuous horizon of marble within the Kongsfjell Group extends from Gråfjell (UTM 4623 73217 to north of Kjennsvatnet (UTM 4707 73323), although it is missing for a couple of kilometers in Leirskardalen. The marble horizon is consisting of both relatively pure and impure calcite marble, and also have horizons of calcareous mica schists. North of Leirskardalen intercalations of garnet-mica schists are common.

The marble is well crystallized with grain-size up to 2-3 mm. It is typically displaying an irregular banding with impurities of muscovite and/or black carbonaceous material. Locally, irregular lenses of pyrite are also present. The regional amphibolite facies metamorphism has produced contact skarn with very coarse grained actinolite, epidote and locally diopside, especially at the contact to garnet-mica schist.

Quartz-feldspathic schists

Quartz-feldspathic schists are the field term designated for white schists with a high content of quartz, feldspar and mica (primarily muscovite). These schists are associated with the Bleikvassli deposit and with numerous small lead-zinc occurrences at Kongsfjellet. A large unit similar to the Kongsfjellet schists have also been found at Stolpfjellet, west of Kjennsvatnet (UTM 4603 73291 to 4641 73275).

Thick units of quartz-feldspathic schists are also found in the area between Leirskardalen (UTM 4550 73275 and Kjennsvassfjellet (UTM 468 7332), and structurally underlying garnet-mica schists typical of the Kongsfjell Group. These schists, which are the main lithologies of the Målvatnet unit, are however, much more diverse and heterogeneous than the schists at Kongsfjellet and Stolpfjellet, which suggest that they have a different origin (see below).

The quartz-feldspathic schists are best developed at Kongsfjellet where intense folding in the area cause repetition of the beds. The schists can be followed southwards to Halvarddalen, where they are folded around the hinge zone of one of the large recumbent folds and can be followed to the north to Bleikvatnet.

Similar to the quartz-feldspathic schists on Kongsfjellet, the unit on Stolpfjellet is sandwiched between a garnet-mica schist, structurally below, and a calcareous mica schist. Also resembling Kongsfjellet, is the presence of thin discontinuous marble and amphibolite horizons at the contact between garnet-mica schist and quartz-feldspathic schist. The unit wedge out toward the east and west and reach a maximum thickness of approximately 200 meters in the central parts. Although, the unit is named a quartz-feldspathic schist, it is in reality comprising psammites, kyanite schists, graphitic schists, conformable orthogneisses and tourmalinites, in addition to the quartz-feldspathic schists. The kyanite schist is up to 50 m thick and contain 20-50 vol% white kyanite. Its field appearance is indistinguishable from the kyanite schist found in the hanging wall rocks of the Bleikvassli deposit. The tourmalinite occur as a 10-30 cm thick layer that can be followed for a few meters before it disappears under a snow fan.

The Kongsfjell and the Stolpfjellet schists contain 30-50 % quartz, 0-45 % alkalifeldspar, 5-40 % muscovite, 5-15% plagioclase and 5-20 % biotite. Carbonate, garnet, epidote/ clinozoisite and apatite are the most common accessories. The variations in the content of quartz, alkalifeldspar and muscovite are due to veinlets of quartz and muscovite overprinting an earlier formed assemblage of quartz, alkalifeldspar, plagioclase and muscovite. The veinlets have suffered folding and are either the result of later retrograde metamorphism (see below) or alteration related to the hydrothermal activity in the area.

Coticules

At one locality at Kongsfjellet (UTM 4519 73090) one of the quartz-feldspathic schist beds contain small lenses consisting of mainly quartz, very fine-grained pink garnet and magnetite. Some calcite which are nearly opaque, because of inclusions of iron-hydroxides, are present in small amounts.

Figure 10
a): Weathering resistant lens of quartz-garnet-magnetite rock intercalated in quartz-feldspathic schist, seen in the center of photo and extending to the top. The length of the lens is 6 m.

b): Close-up of the lens in photo 10 a, showing the delicate mm-scale banding between pink garnet, magnetite and quartz. Locality: Kongsfjellet (UTM 451900 7309030).

The quartz-garnet-magnetite lenses are quite evenly distributed in the schist, and are between one and ten cm in thickness and between one cm and six meters in length (fig.10 a). The thicker lenses have a mm-scale lamination with sharp boundaries between quartz and garnet laminae (fig.10 b). The extent of this schist unit is difficult to decide because of the intense folding, but is at least 200 meters.

Microprobe has been utilized on one sample, and the analyses show that the garnets have a grossular-spessartine-almandine composition ($gros_{12-17}$ $spess_{28-30}$ $alm_{45-50}$). The calcite contains up to 4% MnO and the inclusions in the calcite are Fe-Mn hydroxides. The mineralogy of the lenses, the high content of Mn in the minerals and the very fine lamination strongly suggest an exhalative origin, which probably is related to the lead-zinc mineralizations in the area. Exhalative Fe-Mn cherts are termed coticules (Renard 1878) and are regardes as distal facies of sulfide deposits formed at the seafloor (e.g. Spry 1990). Similar laminated garnet-quartz rocks have also been found related to the Bleikvassli deposit (Skauli 1992).

Orthogneisses

Orthogneiss is a field term used for schistose and partly gneissic quartz-feldspathic rocks with a presumed intrusive origin. Small bodies are present in the Kongsfjell Group at Tverrfjellet (UTM 4636 73255), Skardhaugen (UTM 4565 73242) and at Gråfjell (UTM 4603 73215).

The rocks typically consists of 30-50 % quartz and 30-45 % feldspar and the rest mainly being muscovite. The feldspar can be dominantly plagioclase, as is the case for the horizon at Gråfjell (UTM 4603 73215), but usually it is alkalifeldspar. The most typical subordinate phases are carbonate, biotite and epidote, while garnet and kyanite have been found as common accessories.

The rocks locally show a heteroblastic texture, but a recrystallized, granoblastic texture is more typical. The samples with heteroblastic texture have some larger grains of feldspar in a fine grained matrix of quartz and feldspar. These grains may represent relict fenocrysts. A more gneissic texture is shown by coarse grained leucosomes of quartz and feldspar in a more fine-grained matrix. Occurrence of porphyroblastic muscovite and epidote is probably a result of later retrograde metamorphism (see below). The grains of muscovite and biotite are parallel oriented, forming the schistosity in the rocks. The quartz-feldspar leucosomes are parallel to this schistosity.

The bodies are relatively homogeneous, but locally a diffuse banding occur, which might be due to deformation and metamorphism. At one locality, Tverrfjellet (UTM 4636 73255), the felsic gneiss is crosscutting the surrounding garnet-mica schist, but has at least been folded during $D_3$ (fig.11, see below, for structural geology). If the other orthogneisses are of the same age, but have formed as sills, it might indicate that these rocks are intrusives of a younger age than the sedimentary rocks in the area. This could be compared to the result that the microcline gneiss in the Bleikvassli area has been shown to have formed more than 100 Ma later than at least the Anders Larsa/Lifjell Unit (see below). Dating of these rocks are crucial for interpretation of the tectonic evolution of the area.

Figure 11: Body of orthogneiss deformed and folded during the $D_3$ phase. The body is also shown to intrude the surrounding garnet-mica schist (dark rock in the background). Hammer shaft 35 cm, photo towards the North. Locality: Tverrfjellet (UTM 463600 7325500).

<u>Graphitic schists</u>

Graphite rich mica schist occur as relatively thin but laterally persistent intercalations, primarily in the garnet-mica schists, but also at the contact between quartz-feldspathic schist and garnet-mica schist in the Kongsfjellet area, across Stormyra and at Halvardåsen. Typically, they vary in thickness between 5 and 30 meters and, normally, they can be followed for kilometers along strike. The contact toward the quartz-feldspathic schist is sharp and well defined, whereas the transition toward garnet-mica schist is gradational and characterized by progressively declining concentrations of garnet and an increase in the content of white mica. Due to a few percent of pyrrhotite and pyrite, the graphitic schists crop out with a brown weathering crust which is visible from long distances. The graphite contents vary from less than a percent to several tens of percent in examples from the south slopes of Artfjellet and the valley between Nordtuva and Grønfjell, immediately south of Okstindene.

The microcline gneiss

Originally this field name was applied to a massive light, grayish rock type occurring mainly in the foot wall of the Bleikvassli deposit (e.g. Skauli, 1992). We have now extended this term to include similar rock types in the Halvardåsen area and on Kongsfjellet, which were discovered during regional mapping, as well as additional examples observed in drill cores from the northern end of the Bleikvassli deposit, and from detailed mapping along Bleikvassforsen, south of the mine. All these examples occur in the uppermost part of the Kongsfjell Group, approximately at the same stratigraphic level as the amphibolites and in close proximity to the massive sulphide occurrences. At the type locality for the microcline gneiss, adjacent to the Bleikvassli deposit, it is composed of white microcline, phengitic mica, biotite, subordinate amounts of plagioclase and quartz and accessory clinozoisite with allanite cores, sphene, zircon and calcite. White microcline occur as monomineralic aggregates giving the rock a spotted appearance, that at first glance seems to be porphyroblasts. Microcline also represents more than 85 percent of the matrix. Biotite and phengite are lepidoblastic along the sheared margins of the gneiss but have a random orientation in the interior of the gneiss. Whole rock chemistry and electron microprobe analysis of individual minerals are presented elsewhere (Larsen et al. *in review*). U/Pb geochronology on abraded and unabraded zircon concentrates gave a uniform concordant age of 481 ±2 Ma. This age documents that the microcline gneiss at Bleikvassli formed more than 100 Ma later than the synsedimentary Bleikvassli deposit. This fact together with the chemistry and other features of the gneiss (Larsen et al., *in review*), show that the microcline gneiss at Bleikvassli is not a metamorphosed alteration zone (Skauli, 1992), but rather should be interpreted as an alkaline syenite with agpaitic to miascitic affinities. Although quite similar in field appearance, the microcline gneiss in the Halvardåsen area is truly porphyroblastic, having coarse-grained eyes of single, white feldspar crystals. Also, as opposed to the microcline gneiss at Bleikvassli deposit, it has the morphology of a sill, tapering toward pointed ends from a maximum thickness in the central part of ca. 20 meters. Results from chemical and petrographic analyses are expected medium 1996.

**Målvatnet Unit**

The Målvatnet unit comprises mainly garnet-mica schists and quartz-feldspathic schists. Subordinate are amphibolites, bodies of ultramafic rocks, calcareous mica schists and calcite marble.

Quartz-feldspathic schists

The quartz-feldspathic schists of the Målvatnet Unit are very variable, in both appearance and mineralogy. The schists can be divided into dark biotite-amphibole schists, light quartz-feldspar schists, locally rich in carbonate, quartz-rich garnet-mica schists, biotite-muscovite schists, quartzitic schists and quartzites. The variations are on different scales, from less than one meter to several tens of meters (fig.12, 13). Light muscovite-rich quartz-feldspathic schists, however, dominate and appear

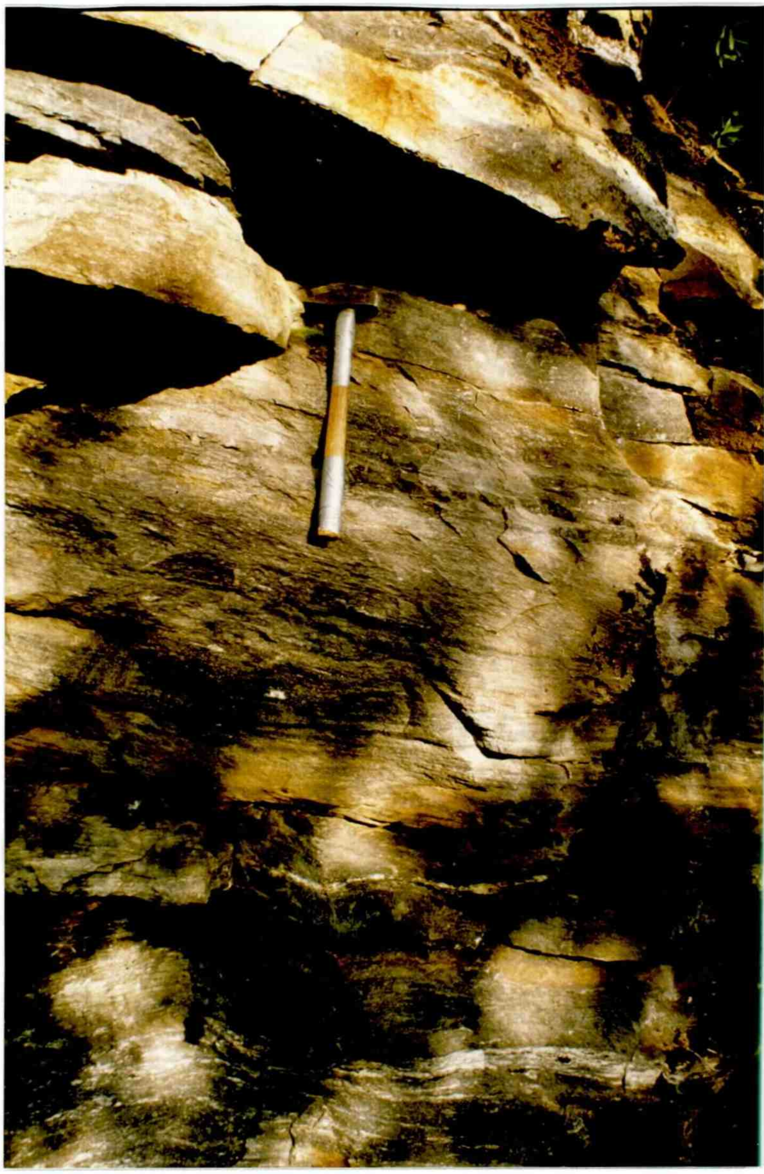

Fig.12
a): Quartz-feldspathic schists of the Målvatnet Unit, showing a dm-scale banding with a smaller scale diffuse lamination, due to variations in the content of biotite and quartz + feldspar.

b): close-up of similar schist, from same locality, showing that banding is partly due to folding and shearing. Locality: Leirskardalen (UTM 454910 7328270). Length of hammer shaft is 35 cm.

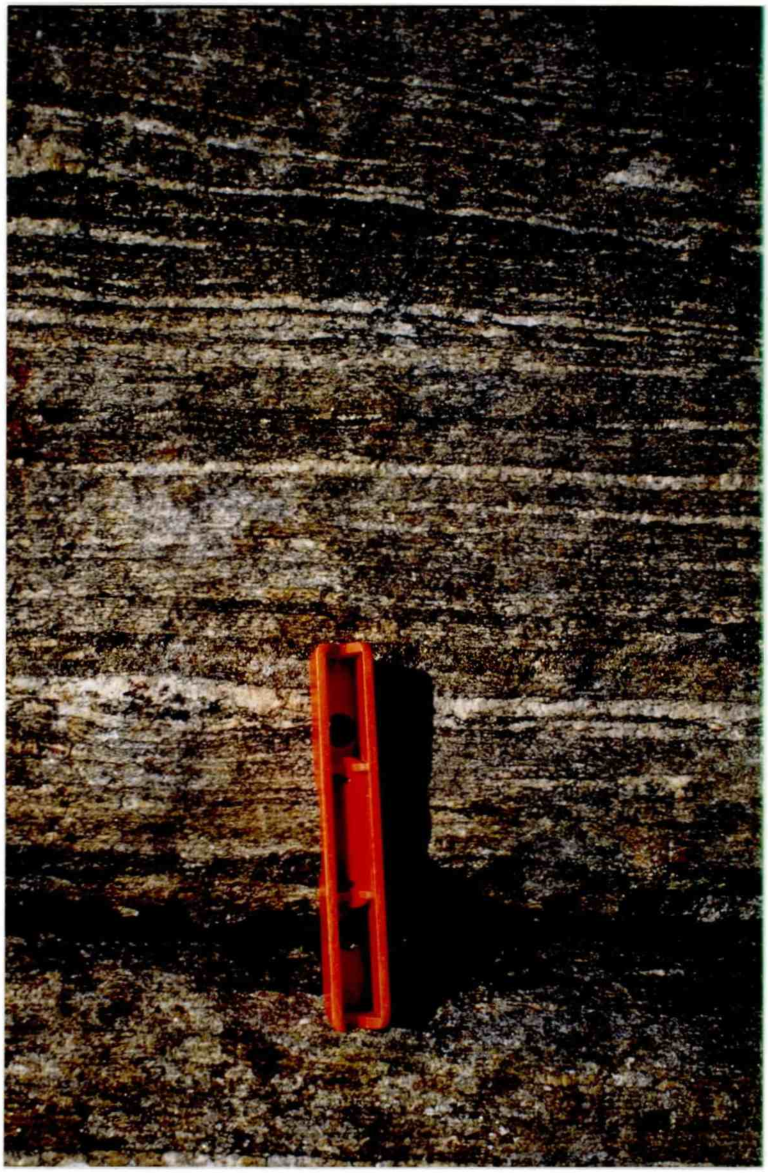

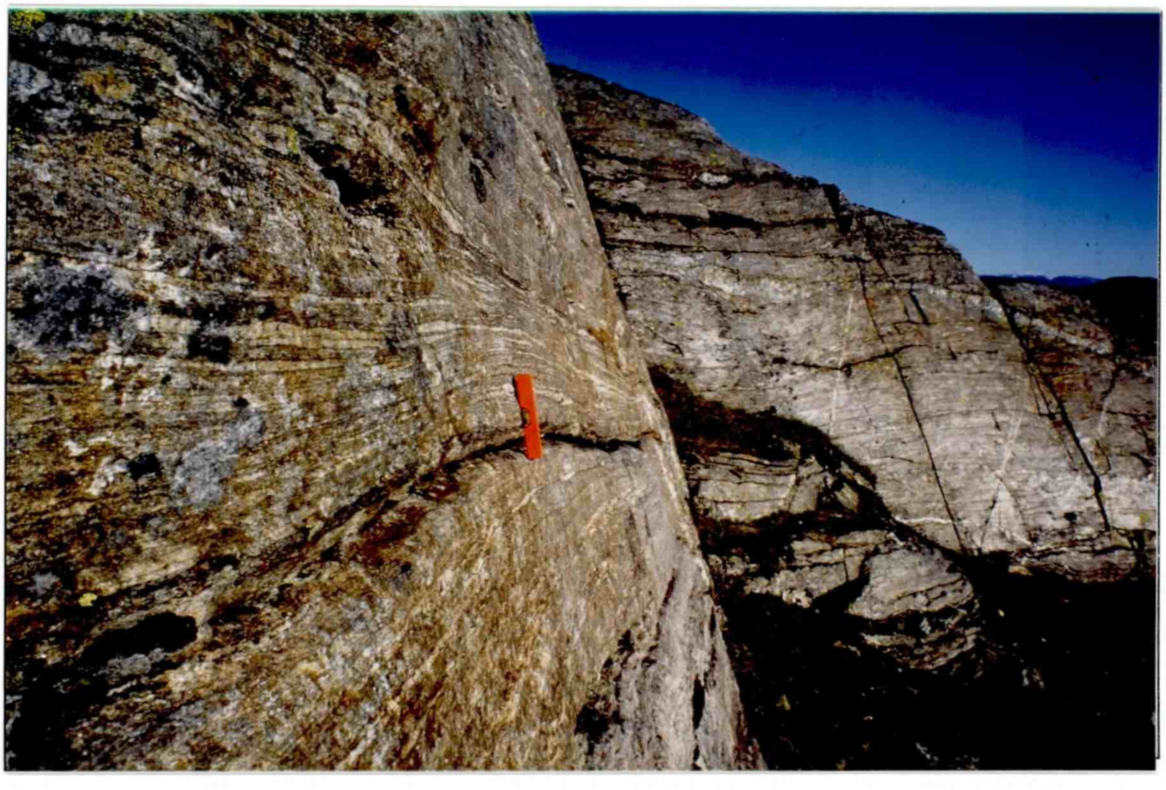

Fig.13 a,b: Overview and close-up of massive laminated and banded biotite-rich quartz-feldspathic schist of the Målvatnet Unit, where the banding is due to variations in the content of biotite and quartz + feldspar. Lenses of quartz are also present. Locality: North of Måltinden (UTM 461980 7335050). Length of ruler is 15 cm.

similar to the quartz-feldspathic schists of the Kongsfjell Group. Common to all these schists are a pronounced planar schistosity. The strong heterogeneity have led to use of the collective term quartz-feldspathic schists and they have also been mapped as one unit (mapping out the different lithologies is not possible or necessary within the frames of this project).

The variations in the schists can be described by a 250 m long but only about 25 m thick section in the northern end of Kjennsvatnet (UTM 4650 73305, fig.14). The profile shows that generally there are variations between biotite and muscovite-rich schists and variations in grain-size. Intercalations of thin units of marble are common. Some lithologies also have a gneissose banding with leucosomes of coarse-grained quartz and feldspar. Typically, the biotite-rich schists have a higher content of garnet and in places also contain lenses of amphibolite. A nearby muscovite schist (UTM 465160 7330630) is very rich in kyanite.

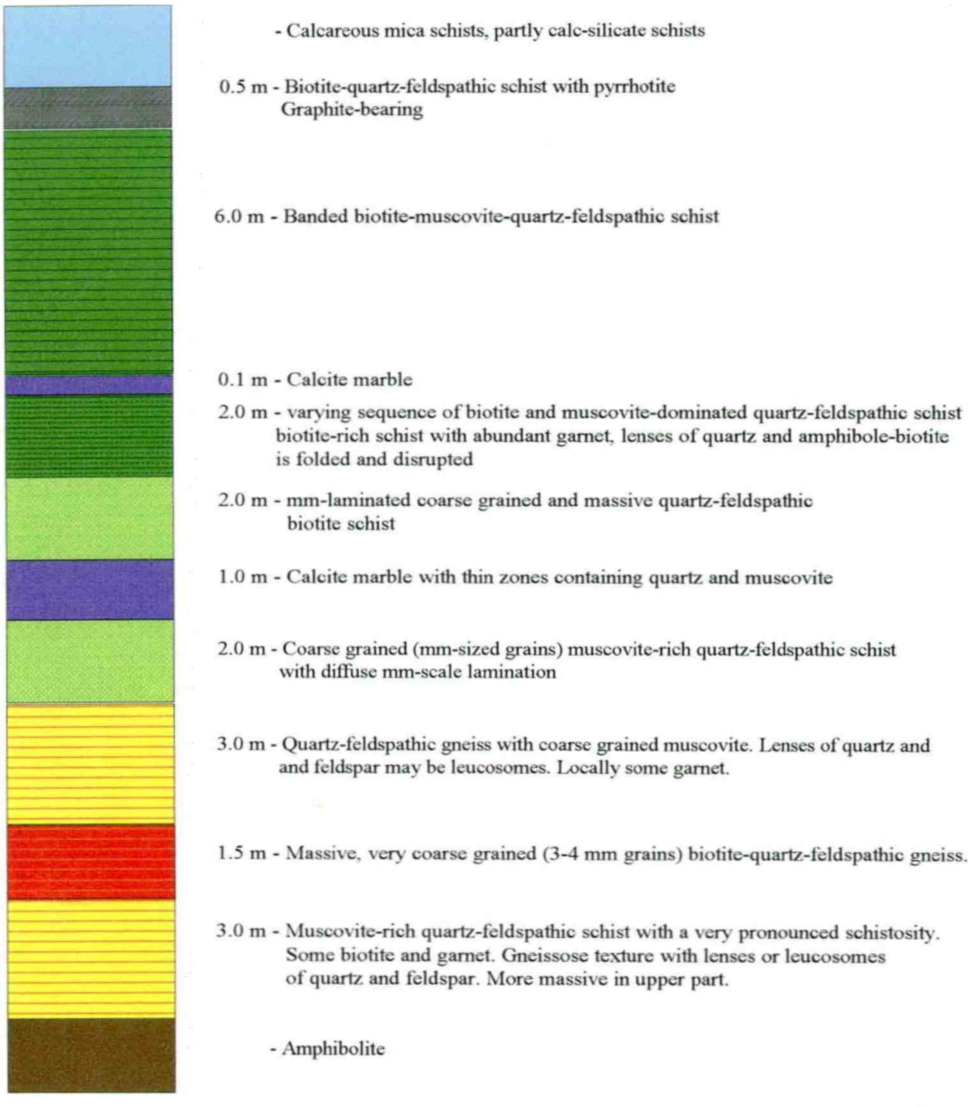


Figure 14: Profile through a representative section of the quartz-feldspathic schists in the Målvatnet Unit. Locality: Northern shore of Kjennsvatnet (UTM 464900 7330500).

Close to Kjelbekken and at the southern banks of Målvatnet (UTM 458650 7330760), there is a conspicuous coarse-grained, light grey, quartz-rich schist with ellipsoidal lenses of quartz and feldspar in biotite-rich matrix (fig.15). The lenses are from 1 mm to 4 cm in size (long axis) and are separated from each other by only thin folia of biotite and muscovite. The long axis is about 2-4 times longer than the short axis. The thickness of the schist is more than 20 meters and it grades into light grey quartz-rich quartz-feldspathic schists with muscovite. The unit can be followed for about 200 m along strike. The texture is probably a result of strong deformation of an originally banded quartz-feldspathic schist.

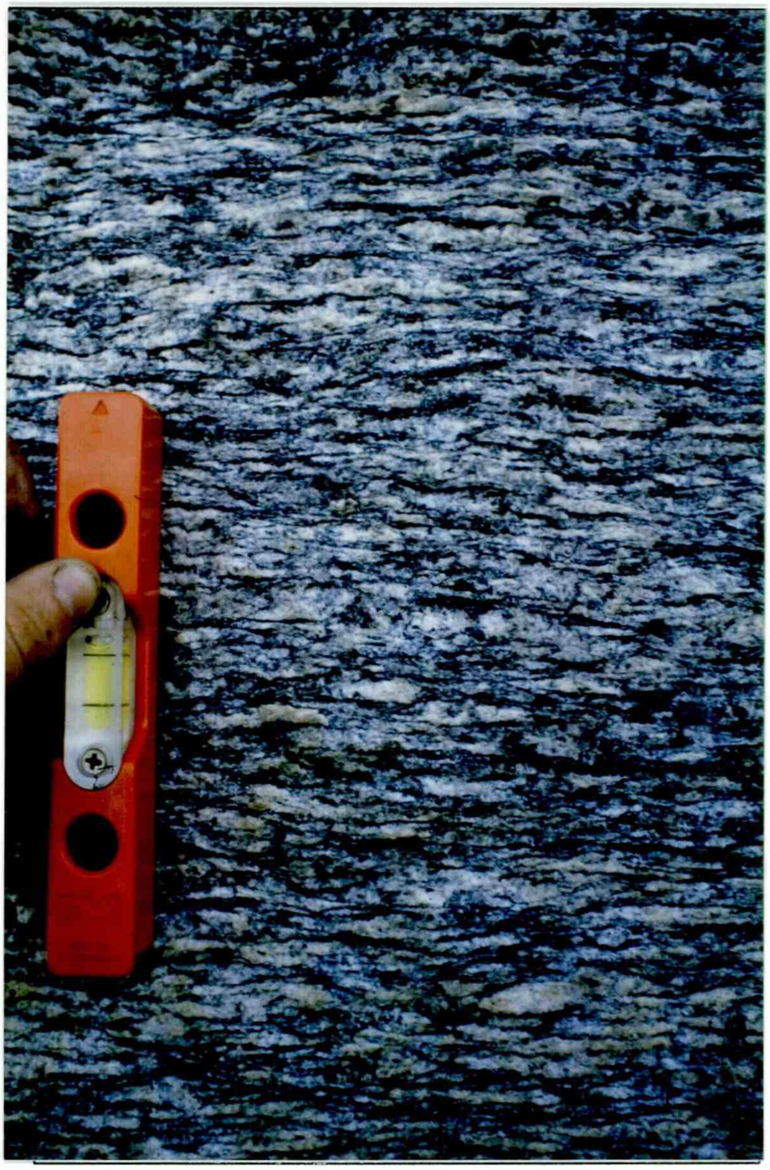

Figure 15: Coarse-grained quartz-feldspathic schist of the Målvatnet Unit with a pseudoconglomeratic texture. The ellipsoidal lenses consist of quartz + alkalifeldspar and is surrounded by biotite-rich matrix. Locality: Shore of Målvatnet (UTM 458650 7330760). Length of ruler is 15 cm.

The mineralogy of the quartz-feldspathic schists is generally simple, consisting of variable amounts of quartz, muscovite, biotite, alkalifeldspar and plagioclase. A diffuse banding is due to variation in the content of micas and the content of feldspar plus quartz. Subordinate phases can be zoisite, epidote and sphene, while pyrite, apatite, garnet, tourmaline and carbonate have been found in accessory amounts. The texture is generally heteroblastic to granoblastic, with lepidoblastic parallel-oriented micas giving the rock a discrete to zonal cleavage. Epidote and zoisite are typically occurring as poikiloblasts.

At Kviturdfjellet east of Målvatnet (UTM 453830 7333720) a conspicuous quartz-fuchsite schist has been found within the quartz-feldspar schists, containing a rich impregnation of pyrite. The pyrite grains have inclusions of arsenopyrite. Gold is known to be associated with arsenopyrite at a number of mineralizations within the Uppermost Allochthon. The fuchsite is enriched in a number of 10-20 cm thick zones over a total thickness of a few meters. The lateral extent of the zones is uncertain.

The garnet-mica schists which are included in the lithology of quartz-feldspathic schists, are coarse-grained, rich in quartz and muscovite and typically contain irregular lenses of quartz, green amphibole and iron-rich carbonate. They are also kyanite-bearing. Locally lenses and bands of amphibolite are present (e.g. UTM 464080 7333160).

The garnet-mica schists of the Målvatnet Unit are in general quite similar to the schists in the Kongsfjell Group. There are several thin units and one conspicuous thick kyanite-rich unit. The latter which occur north of Målvatnet contain both muscovite and biotite. Numerous lenses containing quartz together with coarse grained hornblende are typical of these schists.

Figure 16: One of the isolated ultramafic bodies (middle of this picture) with typical almond or ellipsoidal shape. It is underlain by an amphibolite horizon and overlain by a thick unit of garnet-mica schist. In the background (upper right) is quartz-feldspathic schists at Stolpfjellet. Locality: Stolpfjellkråa (UTM 461480 7330100). Photo towards the east.

Ultramafic rocks

Numerous isolated ultramafic bodies occur associated with a thin unit of garnet-mica schist, close to the contact with the Kongsfjell Group. The bodies typically have an ellipsoidal or almond shape (fig.16), which also is a typical morphology for such isolated bodies elsewhere in the Caledonides (Qvale & Stigh 1985). The smallest bodies are only a couple of meters in diameter, while the largest, which have the names Falkestolen and Svarthammaren, have a long-axis of up to 200 m. These bodies consist generally of tremolite, talc, clinopyroxene and magnesite. A couple of the bodies contain weak, irregular impregnation of chromite. Tremolite typically occur in star-shaped aggregates of up two cm long, greenish needles, while magnesite occur in up to one cm large, yellowish crystals. Talc is more irregularly distributed and in some cases seems to be concentrated in veinlets and high-strain zones, close to or at the contact to the surrounding rocks. Tremolite is always seen to overgrow pyroxene and talc, and is occasionally occurring in cross-cutting veins and veinlets where the mineral is asbestose.

Marbles

Like the Kongsfjell Group, only thin calcite marble beds have been found in the Målvatnet Unit. Several 1-10 meter thick beds occur intercalated in quartz-feldspathic schists in the area between Målvatnet and Kjennsvatnet. Despite their very limited thickness, the beds are very persistent and can be followed for several kilometers. A laterally extensive bed also marks the contact between the Målvatn unit and the Kongsfjell Group in the area (see below). The marbles are very similar to the Kongsfjell calcite marbles, with diffuse banding of graphite and with a similar grain size of 2-3 mm.

## GEOCHEMISTRY

A total of 209 whole-rock XRF and ICP-MS analyses were carried out in 1994 (appendix). Most analyses are from various lithologies in the Kongsfjell Group, whereas the other units are only represented by a few samples. A similar amount of analyses of samples from 1995 are underway. The average and range of the preliminary results from the different lithologies are presented in table form in this report. A complete list of the analyses is presented in the appendix.

Mica schists

The garnet-mica schists, calcareous mica schists and graphite schists are all of sedimentary origin and it is therefore natural to compare these rock types. The average, standard deviation (not for graphite schists, because of few samples) and range in chemistry are displayed in table 1. All schist types vary strongly in composition, such as a range of 51-75 % in $SiO_2$, 12.2-22.6 % in $Al_2O_3$,

## Table 1: Mica schists - average data

| | Graphite schists (n=6) | | | Garnet-mica schists (n=26) | | | | Calcareous mica schists (n=13) | | | |
|---|---|---|---|---|---|---|---|---|---|---|---|
| | average | min. | max. | average | Stdev. | min. | max. | average | Stdev. | min. | max. |
| SiO2 | 59.88 | 46.46 | 84.61 | 60.04 | 5.95 | 51.58 | 75.29 | 58.73 | 4.91 | 53.55 | 71.46 |
| Al2O3 | 14.77 | 6.39 | 21.02 | 16.86 | 2.50 | 12.18 | 22.56 | 13.81 | 1.85 | 10.95 | 16.21 |
| Fe2O3 | 6.39 | 0.70 | 10.60 | 8.11 | 2.55 | 1.03 | 16.90 | 6.65 | 1.19 | 4.91 | 9.14 |
| TiO2 | 0.77 | 0.31 | 1.30 | 0.91 | 0.25 | 0.11 | 1.70 | 0.82 | 0.17 | 0.58 | 1.18 |
| MgO | 3.34 | 0.73 | 8.03 | 3.52 | 1.16 | 1.36 | 6.05 | 4.34 | 0.85 | 2.46 | 5.66 |
| CaO | 4.04 | 0.15 | 10.13 | 2.91 | 2.35 | 0.44 | 8.30 | 6.88 | 2.64 | 2.54 | 10.01 |
| Na2O | 1.53 | 0.42 | 3.02 | 1.14 | 1.19 | 0.26 | 4.50 | 1.76 | 0.55 | 0.74 | 2.85 |
| K2O | 3.20 | 1.33 | 6.02 | 3.37 | 1.18 | 0.45 | 5.54 | 2.56 | 0.75 | 0.87 | 3.62 |
| MnO | 0.07 | 0.03 | 0.15 | 0.14 | 0.08 | 0.01 | 0.27 | 0.08 | 0.03 | 0.04 | 0.16 |
| P2O5 | 0.20 | 0.02 | 0.45 | 0.17 | 0.05 | 0.02 | 0.25 | 0.20 | 0.03 | 0.12 | 0.24 |
| LOI | 4.00 | 1.88 | 7.94 | 1.76 | 1.69 | -2.38 | 7.79 | 2.78 | 1.81 | 0.92 | 6.17 |
| SUM | 98.19 | 97.39 | 98.59 | 98.93 | 0.52 | 97.89 | 100.17 | 98.62 | 0.29 | 98.13 | 99.08 |
| Ba | 927 | 291 | 1477 | 807 | 1388 | 226 | 7535 | 403 | 152 | 192 | 805 |
| Sb | n.d. | <10 | <10 | n.d. | - | <10 | <10 | n.d. | - | <10 | <10 |
| Sn | n.d. | <10 | <10 | n.d. | - | <10 | 12 | n.d. | - | <10 | <10 |
| Cd | n.d. | <10 | <10 | n.d. | - | <10 | <10 | n.d. | - | <10 | <10 |
| Ag | n.d. | <10 | <10 | n.d. | - | <10 | <10 | n.d. | - | <10 | <10 |
| Ga | 17 | <10 | 25 | 20 | 4 | 14 | 29 | 16 | 3 | 11 | 19 |
| Zn | 144 | 6 | 464 | 99 | 23 | 57 | 136 | 86 | 15 | 53 | 106 |
| Cu | 62 | <5 | 147 | 26 | 25 | <5 | 110 | 36 | 19 | 10 | 86 |
| Ni | 18 | <5 | 37 | 37 | 16 | <5 | 65 | 63 | 19 | 35 | 85 |
| Yb | n.d. | <10 | <10 | n.d. | - | <10 | <10 | n.d. | - | <10 | <10 |
| Co | 20 | <10 | 44 | 20 | 9 | <10 | 34 | 19 | 7 | 11 | 33 |
| Ce | 41 | <10 | 103 | 72 | 42 | <10 | 138 | 54 | 21 | <10 | 85 |
| La | 25 | <10 | 61 | 41 | 25 | <10 | 102 | 34 | 10 | 12 | 46 |
| Nd | 19 | <10 | 39 | 30 | 18 | <10 | 69 | 25 | 7 | <10 | 35 |
| W | n.d. | <30 | <30 | n.d. | - | <30 | <30 | n.d. | - | <30 | <30 |
| Mo | n.d. | <5 | 51 | n.d. | - | <5 | <5 | n.d. | - | <5 | 7 |
| Nb | 11 | <5 | 19 | 16 | 6 | <5 | 33 | 12 | 3 | 6 | 15 |
| Zr | 131 | 53 | 225 | 193 | 50 | 50 | 302 | 182 | 29 | 144 | 250 |
| Y | 31 | 12 | 45 | 29 | 8 | 16 | 48 | 31 | 6 | 16 | 38 |
| Sr | 198 | 41 | 329 | 140 | 117 | 48 | 490 | 190 | 53 | 88 | 262 |
| Rb | 98 | 23 | 251 | 149 | 68 | 6 | 359 | 100 | 31 | 21 | 139 |
| U | n.d. | <10 | 19 | n.d. | - | <10 | 18 | 10 | 5 | <10 | 21 |
| Th | 12 | <10 | 24 | 16 | 17 | <10 | 92 | 10 | 5 | <10 | 17 |
| Pb | 28 | <10 | 82 | 25 | 15 | <10 | 59 | 20 | 5 | 14 | 29 |
| Cr | 56 | <5 | 111 | 90 | 34 | 5 | 155 | 124 | 25 | 73 | 158 |
| V | 223 | 88 | 477 | 130 | 46 | 10 | 266 | 121 | 28 | 82 | 190 |
| As | n.d. | <10 | <10 | n.d. | - | <10 | <10 | n.d. | - | <10 | <10 |
| Sc | 17 | <10 | 27 | 21 | 6 | <10 | 32 | 18 | 3 | 13 | 24 |
| S | 2.39 | 0.10 | 5.01 | n.d. | - | <0.10 | 1.56 | n.d. | - | <0.10 | 0.67 |
| Cl | n.d. | <0.10 | <0.10 | n.d. | - | <0.10 | <0.10 | n.d. | - | <0.10 | <0.10 |
| F | 0.14 | <0.10 | 0.21 | n.d. | - | <0.10 | 0.21 | 0.09 | 0.04 | <0.10 | 0.15 |

n.d. - not determined, because of few data above detection limits
n = 13, 13 samples analyzed

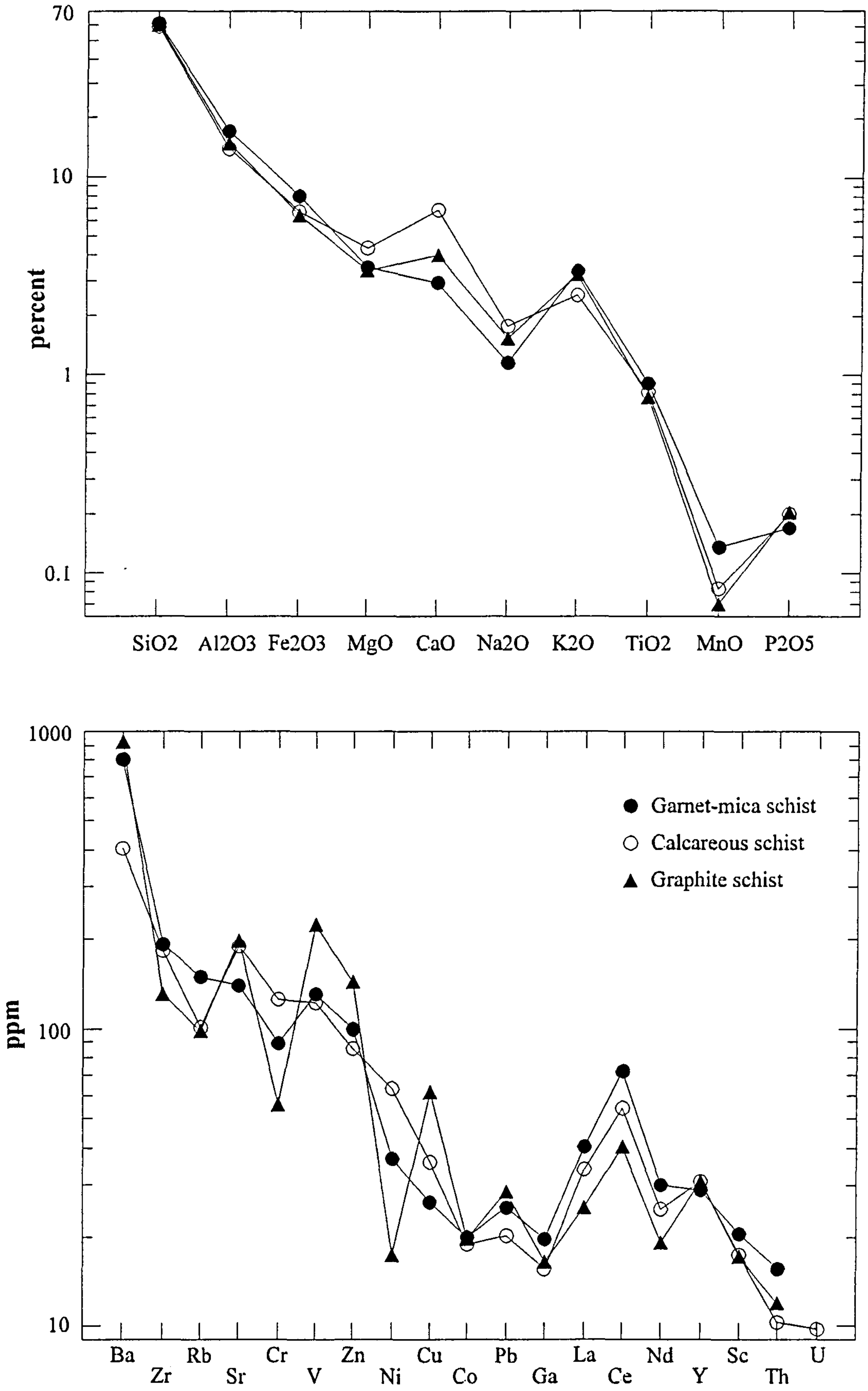


Fig.17: Spider diagram showing the variation in major, minor and trace elements of the garnet-mica schists, calcareous mica schists and graphite schists of the Kongsfjell Group.

1.0-16.9 % in $Fe_2O_{3(t)}$ and 0.45-5.54 % in $K_2O$ for the garnet-mica schists. Most trace elements show similar large variations.

The average of the data are displayed in fig.17. As the diagrams show, the calcareous mica schists and the garnet-mica schists have a very similar pattern or trend. The only exceptions are Ca, Ba, Sr, Rb, Ni.and Cr. This indicates that the rock types have the same origin as sediments. The sharp contacts observed between the two rock types must however be explained (fig.6). The graphite schists follow a different trend than the other schist types, having a high content of Cu, Zn, Pb, due to the presence of small amounts of sulfides, which are typical for rocks with a reducing capacity. Also typical, the graphite schists have a relatively high content of Ba and V.

Regarding the garnet-mica schists, the chemical variations corresponds to the mineralogy. The content of Al, K, Fe, Rb and Cr are higher in the central areas around and north of Okstindene, compared for instance to the garnet-mica schists at Kongsfjell. This is in agreement with the higher content of muscovite and the occurrence of large amounts of kyanite in these areas. A high content of alumina and potassium indicate that these sediments originally had a higher content of clay minerals.

Helicopter borne radiometric surveys also support a high potassium content, because the schists around Okstindene are characterized by a strong positive K-anomaly.

The content of CaO in the calcareous mica schists directly reflect the variations of carbonates in the rocks, which is shown by the fact that there is a weak negative correlation between Ca and Al. (Correlation coefficient = -0.39). Some dolomite must be present because there is strong positive correlation between Mg and Ca (correlation coefficient = 0.74). Sr is incorporated in the carbonates as shown by a high degree of correlation to Ca (correlation coefficient = 0.68). Trace elements like Co, Zn, Rb, Ba, Cr, V, Ni, Ga, and Sc are apparently incorporated in muscovite and biotite, as seen by correlation coefficients in the range 0.75-0.9 with Al, K and partly Fe (for biotite).

Amphibolites

At present whole-rock analyses have been carried out on 19 samples from the Kongsfjell Group, 4 samples from the Anders Larsa and Lifjell Groups and one sample from the Målvatn Unit. The average of the analyses are presented in table 2, and are also compared to analyses from the Mofjellet Group (Paul Reitan´s data). More analyses, and especially from the Anders Larsa and Målvatn Unit, are underway.

With the limited number of analyses in mind, the amphibolites from the different units turn out to have the same range in composition. The amphibolites in the Kongsfjell Group are metabasalts ranging from olivine-normative tholeiites to andesites with a $SiO_2$-content between 44 and 58 %, a $Fe_2O_{3(tot)}$-content between 7.3 and 15.3 %, a MgO-content between 2.9 and 12.0 % and a CaO-content between 6.2 and 11.8 %. The 4 samples from Anders Larsa/Lifjell Unit and the one from the Målvatnet Unit are with respect to most elements, within the range of the Kongsfjell samples. However, the Anders Larsa amphibolites have a larger range in $K_2O$ and Ba and a higher content of Ce, Nd, Zr and Y.

The Mofjellet Group basalts are very similar to the basalts from the Okstindene area, with respect to most major and trace elements. The average content of alumina is higher, but the range is greater than for the Okstindene samples. Another, perhaps more important feature is a markedly lower content of yttrium (range 7-35, compared to 16-65 ppm) and titanium (range 0.22-2.29 vs. 0.57-2.48 ppm).

The samples have been plotted in various diagrams, preferably including elements with restricted mobility, in order to further classify the rocks and to reveal their possible (premetamorphic and pretectonic) origin. The amphibolites range from alkaline basalts to andesites in the `Winchester-diagram'- $SiO_2$ vs. $Zr/TiO_2$ (fig.18), which is also shown in the (less reliable) total alkali vs. silica diagram (fig.19). There are virtually no differences between the basalts from the different groups.

The average minor and trace element data from the amphibolites have been normalized against N-MORB and E-MORB composition and plotted in spider-diagrams (fig.20 a, b). The plots show the general similarity between the different amphibolites. Normalized to N-MORB, the general pattern is enrichment of LIL elements and Ce and depletion of Zr, Ti and Y, a pattern which is typical for island arc basalts, as found in the Western Pacific. The contents of Rb and Ba in especially the Mofjellet Group and Ba in the Anders Larsa/Lifjell Unit are, however, much higher than typical ensimatic arcs, whereas for the HFS elements, the contents are similar. Compared to E-MORB, there is still an enrichment of LILE, while the content of the other elements are similar to this MORB type.

In the V vs. Ti diagram (fig.21) the Mofjellet samples seem to have a stronger affinity to an arc composition than the other groups, which is also shown by the Cr vs. Ti, the Ti-Zr-Sr and the TiO2-MnO-P2O5 diagram (fig.22, 23, 25). The Ti-Zr-Y diagram (fig.25) gives a rather "indiscriminate" picture, but the Mofjellet samples show somewhat greater affinity to OFB and WPB. A WPB character is also shown for the Mofjellet basalts in the Zr/Y vs. Zr diagram (fig.26), while the Okstindene basalts have a MORB to IAT affinity. The $TiO_2$ vs. $FeO_t/MgO$-diagram (fig.27) show a weak IAT fractionation trend for the Mofjellet basalts and a similarly weak MORB trend for the Okstindene basalts.

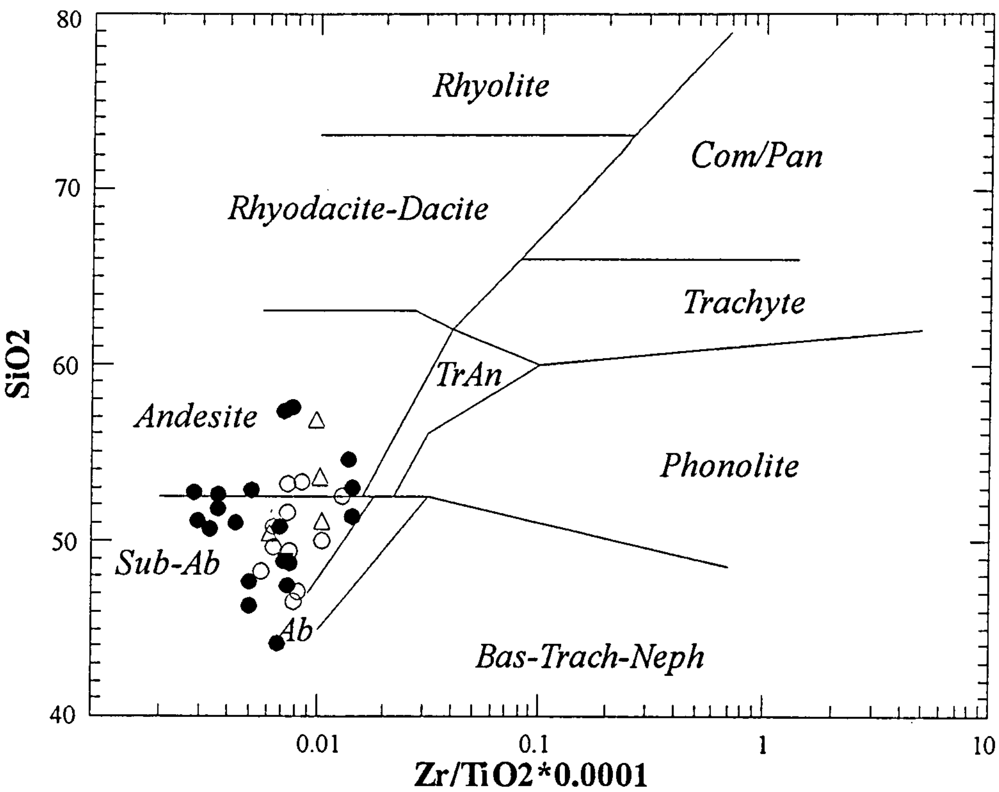


Figure 18: Classification of the amphibolites in the Okstindene Area, including samples (provided by Paul Reitan) from the Mofjell Group. Diagram redrawn from Winchester & Floyd 1977. Filled circles - Kongsfjell Group, open circles - Mofjell Group, open triangle - Anders Larsa Group, Filled triangle - Målvatnet Unit.

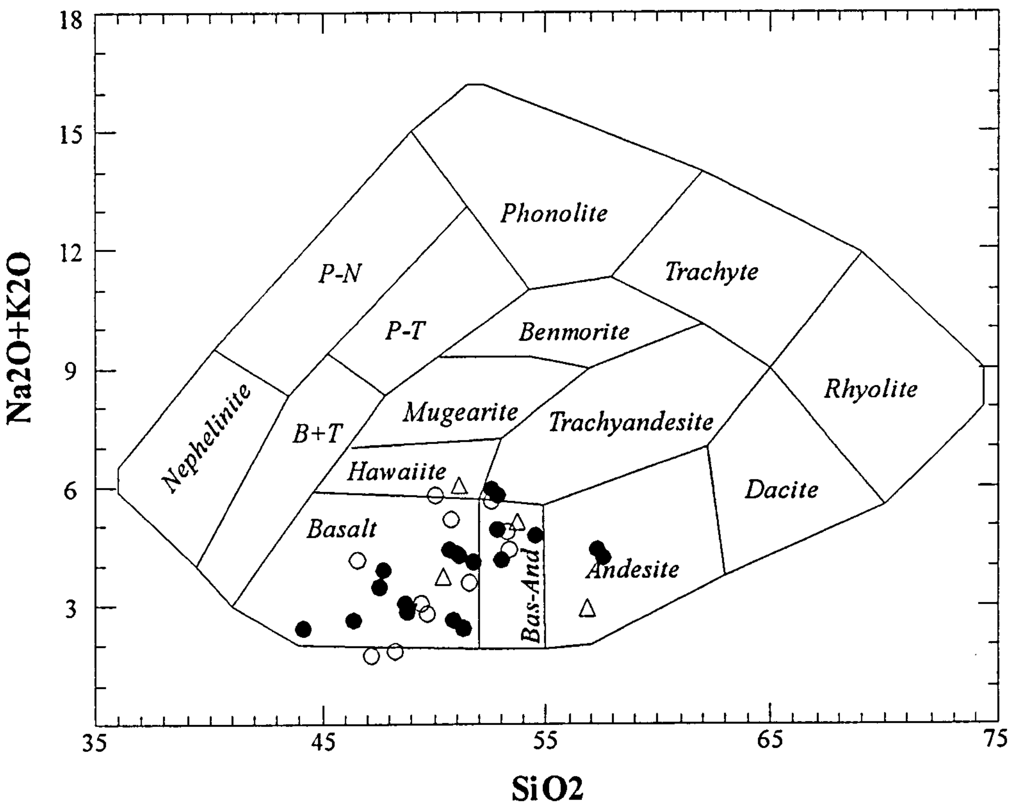


Figure 19: Classification of the amphibolites by the total alkali vs. Silica diagram, from Cox et al. (1979). Samples and legend as in fig.18.

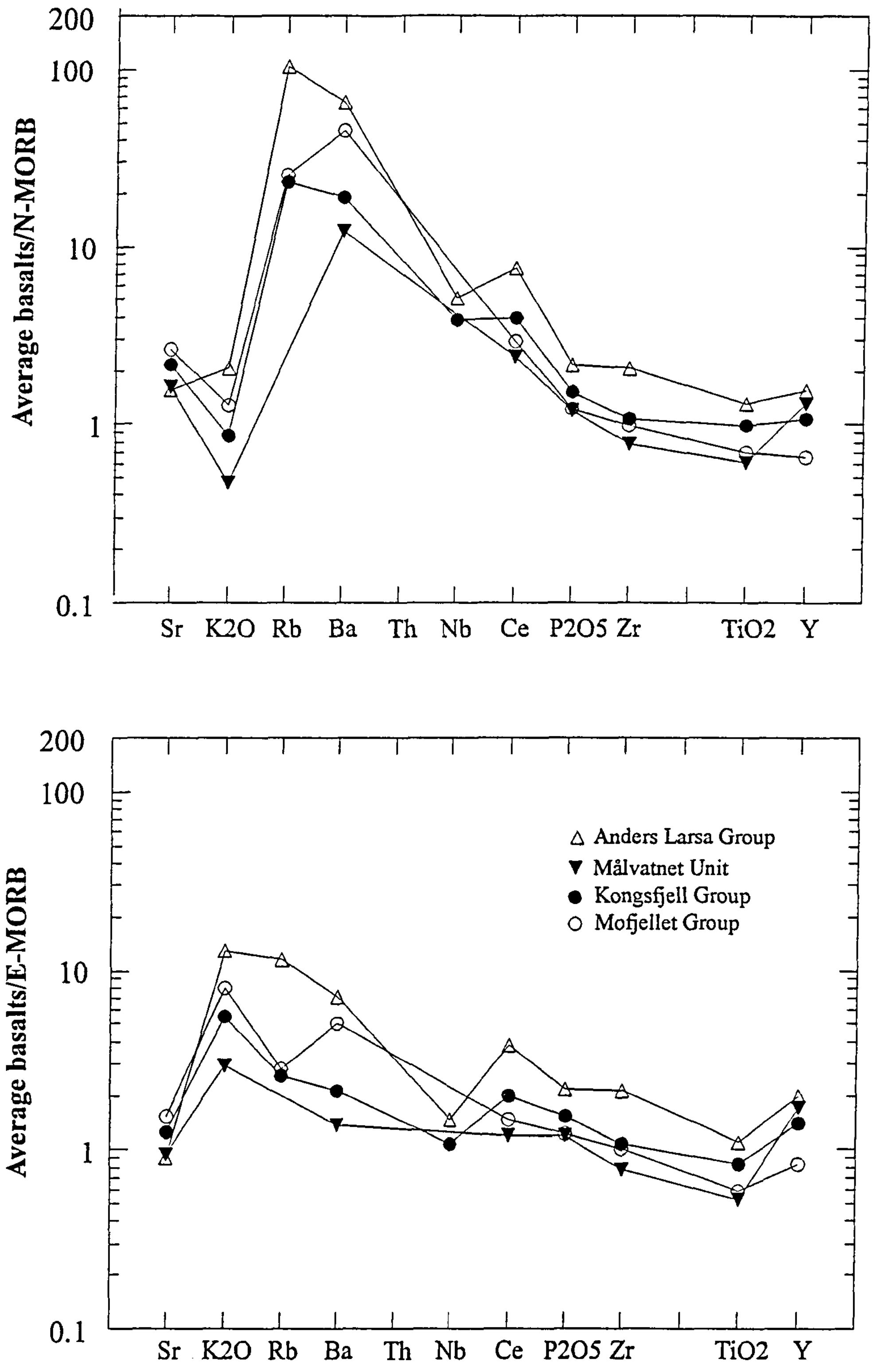


Figure 20 a, b: Amphibolites from the Okstindene Area and Mofjellet normalized against N-MORB and E-MORB, respectively. MORB data from Sun & McDonough (1989).

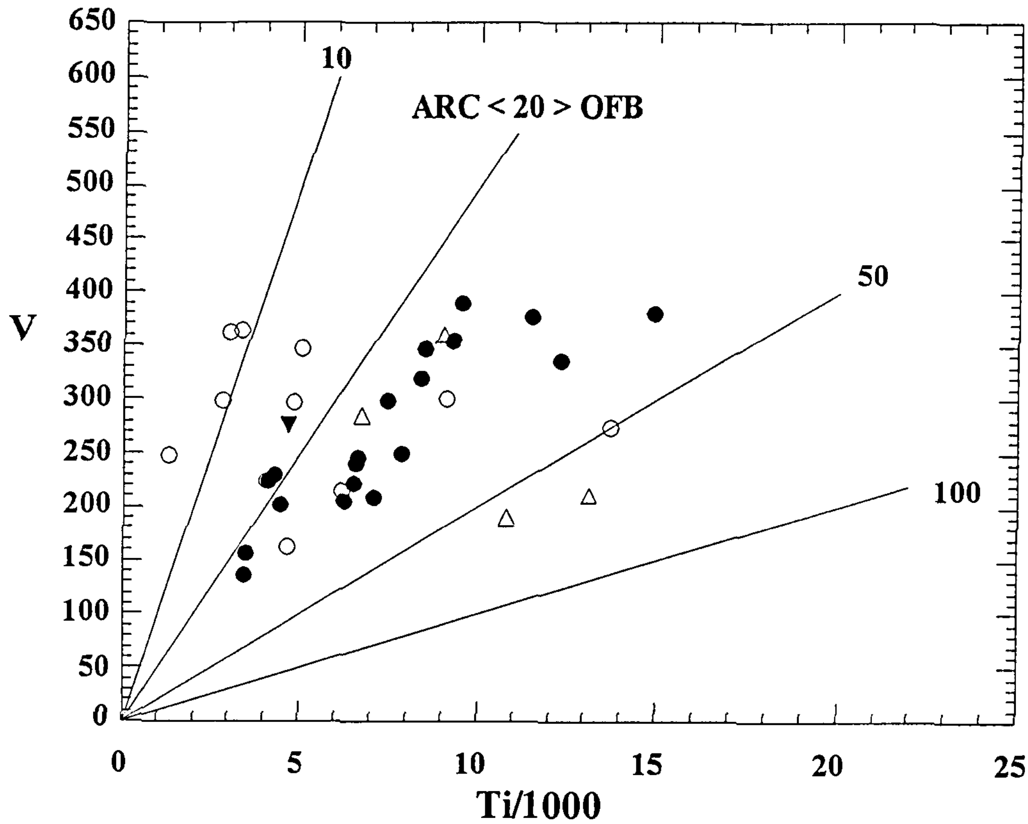


*Figure 21: Okstindene and Mofjell amphibolites plotted in the Ti-V discriminant diagram, by Shervais 1982. Filled circles - Kongsfjell Group, open circles - Mofjell Group, open triangle - Anders Larsa Group, Filled triangle - Målvatnet Unit.*

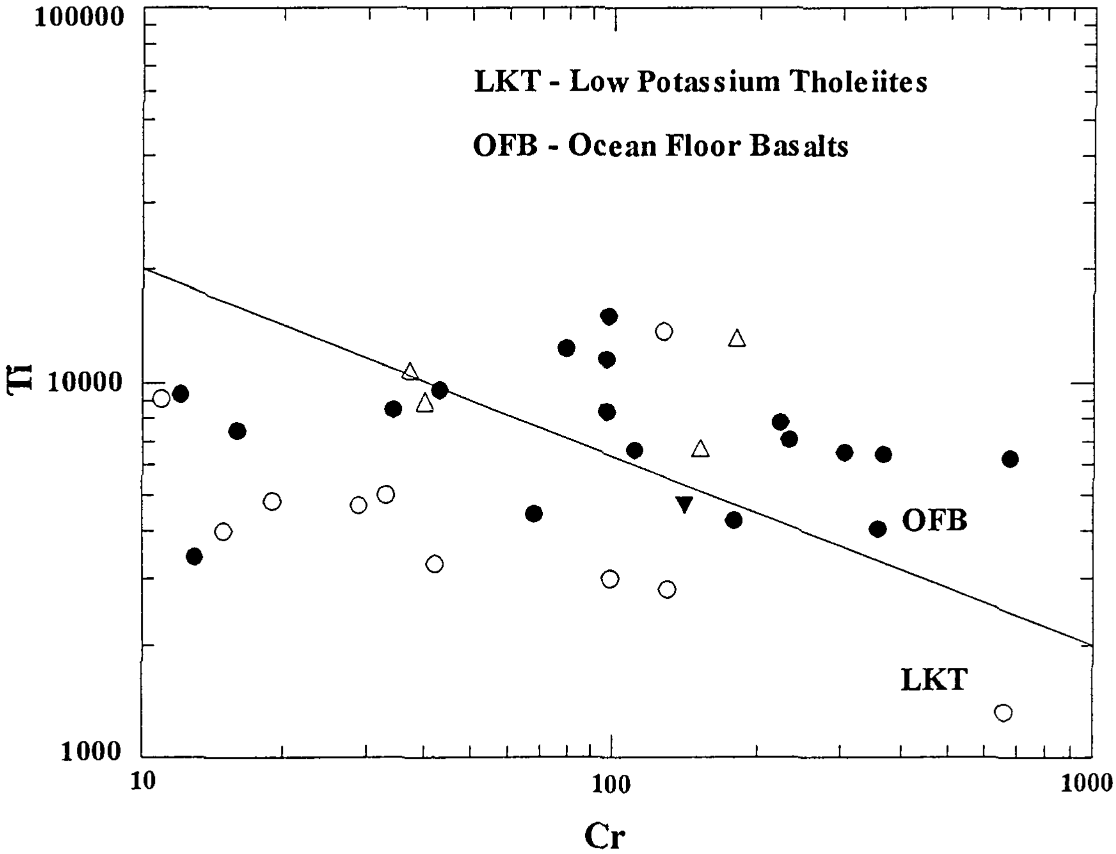


Figure 22: Okstindene and Mofjell amphibolites plotted in the Ti-Cr discriminant diagram, by Pearce (1975). Legend as in fig.21.

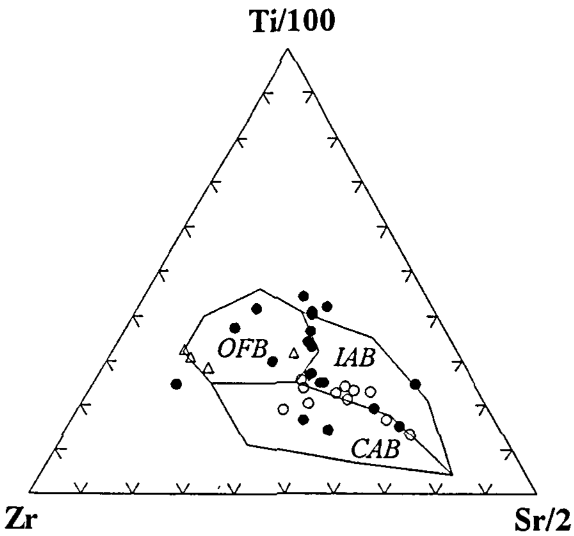


Fig.23: Okstindene and Mofjell amphibolites plotted in the Ti/100-Zr-Sr/2 discriminant diagram, by Pearce & Cann (1973). Filled circles - Kongsfjell Group, open circles - Mofjell Group, open triangle - Anders Larsa Group, Filled triangle - Målvatnet Unit.

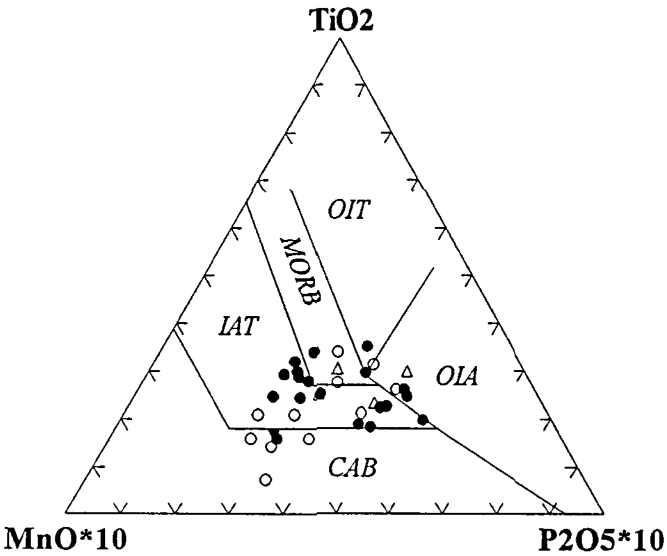


Fig.24: Okstindene and Mofjell amphibolites plotted in the $TiO_2$-MnO*10-$P_2O_5$*10 discriminant diagram, by Mullen (1983). Legend as in fig.23.

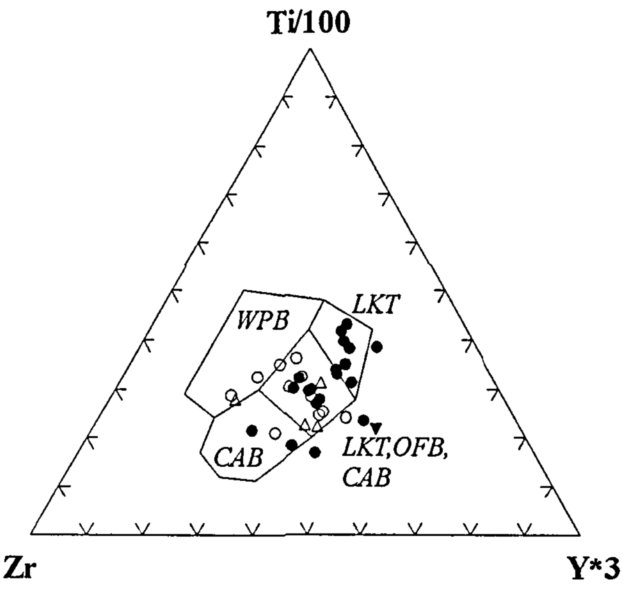


Fig.25: Okstindene and Mofjell amphibolites plotted in the Ti/100-Zr-Y*3 discriminant diagram, by Pearce & Cann (1973). Legend as in fig.23.

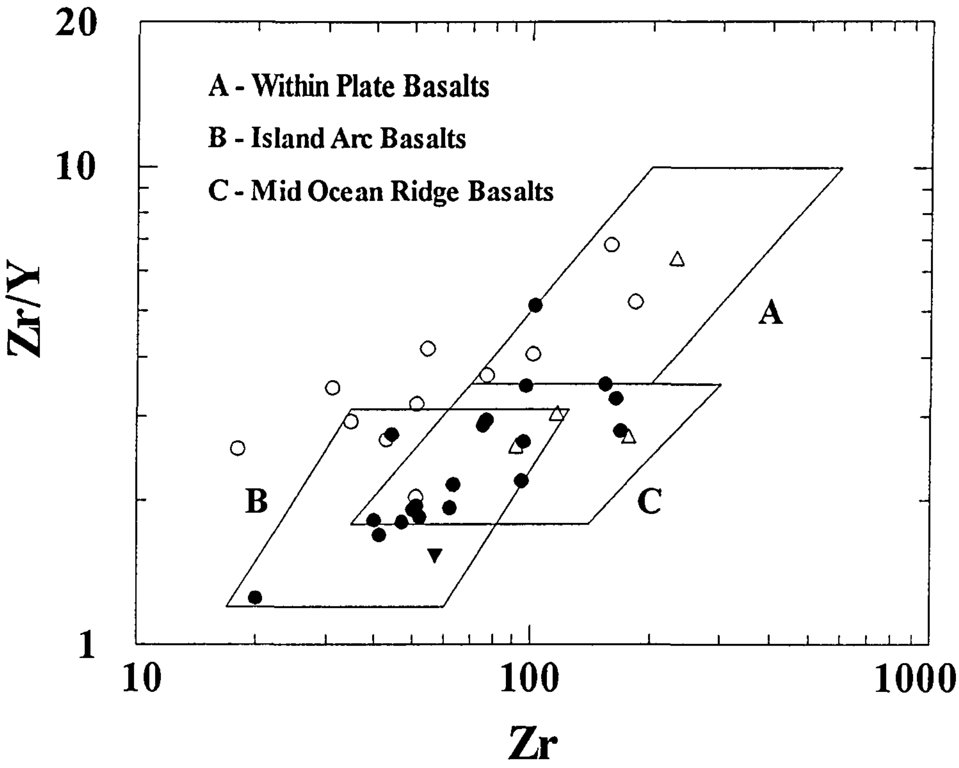


Fig.26: Okstindene and Mofjell amphibolites plotted in the Zr/Y vs. Zr discriminant diagram, by Pearce & Norry (1979). Filled circles - Kongsfjell Group, open circles - Mofjell Group, open triangle - Anders Larsa Group, Filled triangle - Målvatnet Unit.

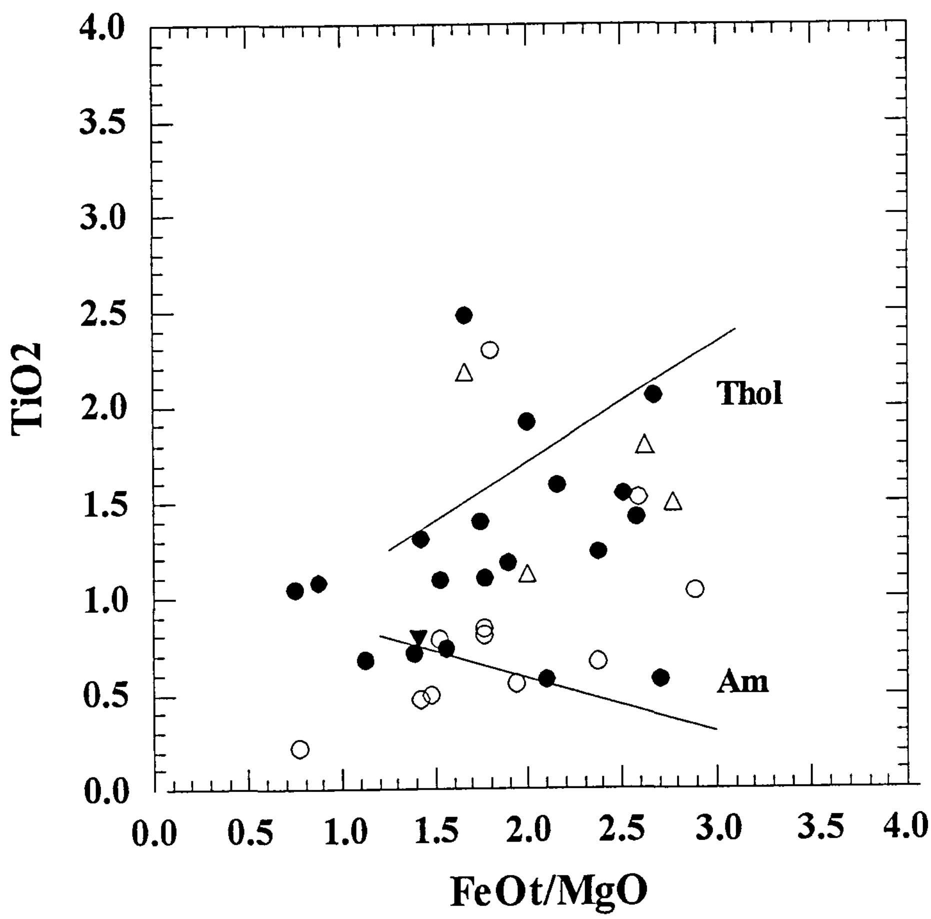


Fig.27: Okstindene and Mofjell amphibolites plotted in the TiO2 vs. $FeO_t$/MgO trend diagram, by Miayshiro (1974). Legend as in fig. 26.

# Table 2: Amphibolites -average data

| | Mofjell | n =11 | | | Kongsfjell | n=19 | | | Anders Larsa | n=4 | | | Målvatn |
|---|---|---|---|---|---|---|---|---|---|---|---|---|---|
| | average | std | max | min | average | std | max | min | average | std | max | min | |
| SiO2 | 50.23 | 2.20 | 53.33 | 46.54 | 51.08 | 3.43 | 57.59 | 44.11 | 53.03 | 2.91 | 56.86 | 50.44 | 48.89 |
| Al2O3 | 17.27 | 2.66 | 19.83 | 11.00 | 15.72 | 1.44 | 19.43 | 13.84 | 13.85 | 1.38 | 15.11 | 12.17 | 13.11 |
| Fe2O3 | 11.23 | 1.98 | 14.27 | 7.62 | 11.51 | 2.55 | 15.25 | 7.30 | 12.92 | 0.99 | 13.93 | 11.55 | 12.45 |
| TiO2 | 0.88 | 0.59 | 2.29 | 0.22 | 1.25 | 0.51 | 2.48 | 0.57 | 1.65 | 0.45 | 2.18 | 1.12 | 0.78 |
| MgO | 6.11 | 2.53 | 11.78 | 2.38 | 6.11 | 1.97 | 11.95 | 2.85 | 5.30 | 0.93 | 6.27 | 4.48 | 7.95 |
| CaO | 9.29 | 2.89 | 16.41 | 5.07 | 8.74 | 1.94 | 11.83 | 6.24 | 6.84 | 1.35 | 8.73 | 5.61 | 11.54 |
| Na2O | 2.99 | 1.09 | 4.63 | 1.25 | 3.29 | 1.16 | 5.67 | 1.62 | 2.98 | 0.36 | 3.50 | 2.74 | 2.52 |
| K2O | 0.92 | 0.70 | 2.17 | 0.27 | 0.63 | 0.51 | 2.11 | 0.26 | 1.48 | 1.36 | 3.32 | 0.18 | 0.34 |
| MnO | 0.16 | 0.04 | 0.23 | 0.10 | 0.17 | 0.05 | 0.25 | 0.09 | 0.19 | 0.04 | 0.24 | 0.16 | 0.25 |
| P2O5 | 0.14 | 0.08 | 0.30 | 0.06 | 0.18 | 0.07 | 0.39 | 0.09 | 0.26 | 0.11 | 0.35 | 0.15 | 0.14 |
| LOI | 0.56 | 0.22 | 0.95 | 0.30 | 0.56 | 0.20 | 1.06 | 0.24 | 0.67 | 0.23 | 0.93 | 0.39 | 1.02 |
| Sum | 99.78 | 0.33 | 100.08 | 99.18 | 99.24 | 0.55 | 99.90 | 98.18 | 99.15 | 0.41 | 99.75 | 98.87 | 98.98 |
| Ba | 288 | 269 | 958 | 39 | 120 | 91 | 318 | 36 | 411 | 425 | 1014 | 31 | 78 |
| Sb | nd | - | <10 | <10 | nd | - | <10 | <10 | nd | - | <10 | <10 | <10 |
| Sn | nd | - | <10 | <10 | nd | - | <10 | <10 | nd | - | <10 | <10 | <10 |
| Cd | nd | - | <10 | <10 | nd | - | <10 | <10 | nd | - | <10 | <10 | <10 |
| Ag | nd | - | <10 | <10 | nd | - | <10 | <10 | nd | - | <10 | <10 | <10 |
| Ga | 16 | 3 | 20 | 12 | 17 | 3 | 26 | 13 | 20 | 4 | 23 | 14 | 13 |
| Zn | 94 | 18 | 118 | 61 | 85 | 31 | 172 | 36 | 114 | 4 | 118 | 110 | 113 |
| Cu | 70 | 100 | 317 | <5 | 67 | 52 | 184 | <5 | 29 | 30 | 61 | <5 | 88 |
| Ni | 31 | 46 | 153 | <5 | 63 | 74 | 327 | <5 | 41 | 25 | 73 | 20 | 74 |
| Yb | nd | - | <10 | <10 | nd | - | <10 | <10 | nd | - | <10 | <10 | <10 |
| Co | 41 | 11 | 56 | 23 | 39 | 10 | 59 | 18 | 41 | 3 | 45 | 37 | 50 |
| Ce | 22 | 20 | 58 | <10 | 30 | 16 | 57 | <10 | 57 | 26 | 78 | 19 | 18 |
| La | nd | - | 22 | <10 | 11 | 7 | 27 | <10 | 18 | 13 | 35 | <10 | 12 |
| Nd | nd | - | 16 | <10 | nd | - | 18 | <10 | nd | - | 37 | <10 | <10 |
| W | nd | - | <30 | <30 | nd | - | <30 | <30 | nd | - | <30 | <30 | <30 |
| Mo | nd | - | <5 | <5 | nd | - | <5 | <5 | nd | - | <5 | <5 | <5 |
| Nb | nd | - | 14 | <5 | 9 | 10 | 37 | <5 | 12 | 14 | 32 | <5 | <5 |
| Zr | 73 | 55 | 182 | 18 | 79 | 43 | 168 | 20 | 154 | 63 | 231 | 92 | 57 |
| Y | 18 | 9 | 35 | 7 | 30 | 12 | 60 | 16 | 44 | 14 | 65 | 35 | 37 |
| Sr | 236 | 109 | 439 | 105 | 194 | 63 | 295 | 95 | 140 | 67 | 204 | 71 | 148 |
| Rb | 14 | 17 | 53 | <5 | 13 | 27 | 116 | <5 | 58 | 65 | 139 | <5 | <5 |
| U | nd | - | 11 | <10 | nd | - | 13 | <10 | nd | - | <10 | <10 | <10 |
| Th | nd | - | <10 | <10 | nd | - | <10 | <10 | nd | - | <10 | <10 | <10 |
| Pb | nd | - | 13 | <10 | nd | - | 25 | <10 | nd | - | 23 | <10 | <10 |
| Cr | 106 | 198 | 653 | <5 | 158 | 170 | 671 | <5 | 102 | 75 | 180 | 37 | 141 |
| V | 280 | 62 | 363 | 162 | 269 | 78 | 389 | 136 | 262 | 77 | 359 | 191 | 275 |
| As | nd | - | <10 | <10 | nd | - | <10 | <10 | nd | - | <10 | <10 | <10 |
| Sc | 36 | 9 | 46 | 19 | 38 | 9 | 56 | 19 | 37 | 10 | 47 | 24 | 43 |
| S | nd | - | 0.11 | 0.11 | nd | - | <0.10 | <0.10 | nd | - | <0.10 | <0.10 | <0.10 |
| Cl | nd | - | <0.10 | <0.10 | nd | - | <0.10 | <0.10 | nd | - | <0.10 | <0.10 | <0.10 |
| F | nd | - | 0.15 | <0.10 | nd | - | 0.19 | <0.10 | 0.14 | 0.03 | 0.19 | 0.12 | 0.18 |

n.d. - not determined, because of few data above detection limits
n=11, 11 samples analyzed

## Marbles

The average whole rock data for the calcite and dolomite marbles are tabulated in table 3. From the raw data (see appendix), but also when looking at the range in major elements of the dolomite and calcite marbles in the table, the marbles are either consisting of calcite or dolomite and none of the samples have intermediate compositions with both dolomite and calcite. This is also (as noted above), shown by the fact that there is a sharp boundary between the marbles in the field.

Both the calcite and dolomite marbles can be quite pure, as the analyses show. The content of silicates, as represented by $SiO_2$, $Al_2O_3$, $K_2O$ and $Na_2O$, are if added together, in the range of 1.79-3.13 % for the calcite marbles and 0.29-2.81 for the dolomite marbles. The content of $SiO_2$ is practically the same in the two marble types, while the content of $K_2O$ and $Al_2O_3$ is higher in the calcite marble, showing that muscovite is present in the calcite marbles, while quartz is the main impurity in the dolomite marbles. Apatite is present in both marble types, but higher in the calcite marbles, as shown by the $P_2O_5$ content. Also, the content of fluorine is higher in the calcite marble. With respect to trace elements, the contents of all elements are higher in the calcite marbles. This is especially notable for Sr, which has a range in average contents between 1100 and 2000 ppm in the calcite marbles, compared to 56 and 116 ppm in the dolomite marbles.

## Strontium isotopes

There are only small differences between the marbles in the different lithological units, with respect to both major and trace elements. The Anders Larsa dolomite marble is the most pure, while the Dunderlandsdalen calcite marble has the highest content of Ba. To investigate further possible correlations between the units, Sr-isotope analyses of the marbles were undertaken. The results have also been used to provide ages of the marbles and to assess the reason for the sharp boundary between calcite and dolomite marbles. Only the purest marbles were used for Sr-isotope analysis.

The analyses are shown in table 4 and displayed in fig. 28. The $^{87}Rb/^{86}Sr$-ratios are in general so low, that the $^{87}Sr/^{86}Sr$-ratios are not significantly affected unless the marbles are older than about 1000 Ma, an age for which there is no evidence in the area. Thus the $^{87}Sr/^{86}Sr$-ratios measured in the marbles today are regarded to be very close to the initial ratios.

The first notable feature is that there is a relatively large spread in the data, but that the dolomite marbles have higher $^{87}Sr/^{86}Sr$-ratios than the calcite marbles of the same lithological unit. The dolomite data from each unit also show a wider range than the calcite data. As shown above, the dolomite marbles have a much lower content of Sr, compared to the calcite marbles. Thus the $^{87}Sr/^{86}Sr$-ratios in the dolomite marbles could have been changed to a larger degree than the calcite marbles because of their lower Sr content, with influence from other sources of strontium. Because the main lithologies in the area are continental metasediments, a shift to higher $^{87}Sr/^{86}Sr$-ratios would

# Table 3: Marbles - average data

| | Anders Larsa Group | | | Anders Larsa Group | | | Dunderlandsdalen | | | Dunderlandsdalen | | | Kongsfjell group | | | Stor-Akersvatn | | | Stor-Akersvatn | | | Plurdal group | |
|---|---|---|---|---|---|---|---|---|---|---|---|---|---|---|---|---|---|---|---|---|---|---|---|---|
| | calcite marble | | | dolomite marble | | | calcite marble | | | dolomite marble | | | calcite marble | | | calcite marble | | | dolomite marble | | | calcite | dolomite |
| | Average | min. | max. | Average | min. | max. | Average | min. | max. | Average | min. | max. | Average | min. | max. | Average | min. | max. | Average | min. | max. | | |
| SiO2 | 2.38 | 1.14 | 3.09 | 0.20 | 0.11 | 0.29 | 2.24 | 0.34 | 4.14 | 2.66 | 0.35 | 8.57 | 2.57 | 1.03 | 4.17 | 1.42 | 0.07 | 2.82 | 2.04 | 0.25 | 7.17 | 2.58 | 1.23 |
| Al2O3 | 0.45 | 0.16 | 0.58 | 0.06 | 0.01 | 0.10 | 0.46 | 0.05 | 0.87 | 0.14 | 0.04 | 0.24 | 0.25 | 0.05 | 0.46 | 0.19 | 0.04 | 0.46 | 0.05 | 0.01 | 0.09 | 0.31 | 0.06 |
| Fe2O3 | 0.18 | 0.08 | 0.31 | 0.08 | 0.04 | 0.13 | 0.27 | 0.12 | 0.42 | 0.12 | 0.05 | 0.22 | 0.23 | 0.13 | 0.46 | 0.13 | 0.07 | 0.23 | 0.08 | 0.04 | 0.13 | 0.19 | 0.35 |
| TiO2 | 0.03 | 0.02 | 0.05 | 0.01 | 0.01 | 0.01 | 0.04 | 0.01 | 0.06 | 0.01 | 0.01 | 0.01 | 0.02 | 0.01 | 0.03 | 0.02 | 0.01 | 0.03 | 0.03 | 0.02 | 0.03 | 0.02 | < -4 |
| MgO | 2.05 | 0.35 | 7.62 | 22.59 | 21.91 | 22.99 | 0.93 | 0.49 | 1.37 | 21.62 | 20.30 | 22.40 | 0.70 | 0.27 | 1.29 | 1.07 | 0.11 | 2.80 | 21.83 | 21.26 | 22.21 | 0.62 | 20.97 |
| CaO | 51.53 | 47.17 | 53.17 | 30.70 | 30.44 | 30.99 | 52.77 | 50.61 | 54.92 | 30.04 | 28.39 | 30.80 | 52.90 | 50.61 | 54.71 | 53.36 | 51.79 | 54.63 | 30.36 | 29.56 | 31.08 | 52.94 | 30.23 |
| Na2O | 0.17 | 0.15 | 0.18 | n.d. | - | - | n.d. | - | - | n.d. | - | - | n.d. | - | - | 0.12 | 0.12 | 0.12 | n.d. | - | - | <0.10 | <0.10 |
| K2O | 0.13 | 0.05 | 0.16 | 0.03 | 0.01 | 0.06 | 0.10 | 0.00 | 0.19 | 0.01 | 0.01 | 0.01 | 0.08 | 0.02 | 0.14 | 0.06 | 0.01 | 0.16 | 0.01 | 0.01 | 0.01 | 0.08 | < -3 |
| MnO | 0.01 | 0.00 | 0.01 | n.d. | - | - | 0.01 | 0.00 | 0.01 | 0.01 | 0.00 | 0.02 | 0.02 | 0.01 | 0.02 | 0.00 | 0.00 | 0.01 | n.d. | - | - | 0.01 | 0.13 |
| P2O5 | 0.20 | 0.12 | 0.28 | 0.12 | 0.04 | 0.18 | 0.18 | 0.14 | 0.22 | 0.13 | 0.12 | 0.16 | 0.24 | 0.16 | 0.28 | 0.25 | 0.19 | 0.33 | 0.17 | 0.12 | 0.26 | 0.33 | 0.31 |
| Ba | 44 | 36 | 55 | 21 | 18 | 24 | 80 | 63 | 96 | 24 | 20 | 27 | 46 | 35 | 74 | 39 | 28 | 48 | 22 | 19 | 26 | 54 | 23 |
| Sb | n.d. | - | - | n.d. | - | - | n.d. | - | - | n.d. | - | - | n.d. | - | - | n.d. | - | - | n.d. | - | - | <10 | <10 |
| Sn | n.d. | - | - | n.d. | - | - | n.d. | - | - | n.d. | - | - | n.d. | - | - | n.d. | - | - | n.d. | - | - | <10 | <10 |
| Cd | n.d. | - | - | n.d. | - | - | n.d. | - | - | n.d. | - | - | n.d. | - | - | n.d. | - | - | n.d. | - | - | <10 | <10 |
| Ag | n.d. | - | - | n.d. | - | - | n.d. | - | - | n.d. | - | - | n.d. | - | - | n.d. | - | - | n.d. | - | - | <10 | <10 |
| Ga | n.d. | - | - | n.d. | - | - | n.d. | - | - | n.d. | - | - | n.d. | - | - | n.d. | - | - | n.d. | - | - | <10 | <10 |
| Zn | n.d. | - | - | n.d. | - | - | n.d. | - | - | n.d. | - | - | 8 | 6 | 10 | n.d. | - | - | n.d. | - | - | <5 | <5 |
| Cu | 5 | 5 | 5 | n.d. | - | - | 6 | 6 | 6 | n.d. | - | - | 7 | 6 | 8 | n.d. | - | - | n.d. | - | - | <5 | <5 |
| Ni | 6 | 5 | 6 | n.d. | - | - | 7 | 7 | 7 | n.d. | - | - | n.d. | - | - | 5 | 5 | 5 | 6 | 6 | 6 | <5 | <5 |
| Yb | 14 | 12 | 16 | n.d. | - | - | 12 | 12 | 12 | n.d. | - | - | 12 | 10 | 16 | 14 | 11 | 19 | n.d. | - | - | <10 | <10 |
| Co | n.d. | 0 | 0 | n.d. | - | - | n.d. | 0 | 0 | n.d. | - | - | n.d. | - | - | n.d. | - | - | n.d. | - | - | <10 | <10 |
| Ce | n.d. | 0 | 0 | n.d. | - | - | n.d. | 0 | 0 | n.d. | - | - | n.d. | - | - | n.d. | - | - | n.d. | - | - | <10 | <10 |
| La | n.d. | 0 | 0 | n.d. | - | - | n.d. | 0 | 0 | n.d. | - | - | n.d. | - | - | n.d. | - | - | n.d. | - | - | <10 | <10 |
| Nd | n.d. | 0 | 0 | n.d. | - | - | n.d. | 0 | 0 | n.d. | - | - | n.d. | - | - | n.d. | - | - | n.d. | - | - | <10 | <10 |
| W | n.d. | 0 | 0 | n.d. | - | - | n.d. | 0 | 0 | n.d. | - | - | n.d. | - | - | n.d. | - | - | n.d. | - | - | <30 | <30 |
| Mo | n.d. | 0 | 0 | n.d. | - | - | n.d. | 0 | 0 | n.d. | - | - | 6 | 6 | 6 | n.d. | - | - | n.d. | - | - | <5 | <5 |
| Nb | n.d. | 0 | 0 | n.d. | - | - | n.d. | 0 | 0 | n.d. | - | - | n.d. | - | - | n.d. | - | - | n.d. | - | - | <5 | <5 |
| Zr | 26 | 18 | 32 | 0 | 0 | 0 | 37 | 33 | 40 | n.d. | - | - | 14 | 8 | 22 | 20 | 12 | 34 | n.d. | - | - | 26 | 0 |
| Y | 11 | 11 | 11 | 6 | 6 | 6 | 5 | 5 | 5 | 6 | 6 | 6 | 13 | 7 | 17 | 11 | 8 | 15 | 7 | 5 | 9 | 7 | 5 |
| Sr | 1134.7 | 342.3 | 1563.3 | 62.9 | 52.9 | 76.6 | 1960.0 | 1614.9 | 2305.1 | 116.2 | 85.8 | 130.6 | 621.3 | 13.3 | 1001.2 | 1348.9 | 826.1 | 2136.1 | 55.8 | 45.0 | 69.6 | 1151.1 | 81.9 |
| Rb | 0.56 | 0.28 | 0.85 | 0.81 | 0.02 | 2.43 | 0.20 | 0.02 | 0.38 | 0.22 | 0.01 | 0.83 | 0.11 | 0.03 | 0.13 | 0.13 | 0.01 | 0.48 | 0.05 | 0.01 | 0.14 | 0.48 | 0.04 |
| U | 48 | 28 | 65 | 38 | 33 | 46 | 79 | 49 | 108 | 37 | 30 | 49 | 48 | 22 | 65 | 66 | 18 | 109 | 34 | 18 | 48 | 36 | 47 |
| Th | n.d. | - | - | 11 | 11 | 11 | n.d. | - | - | n.d. | - | - | n.d. | - | - | 11 | 11 | 11 | 13 | 13 | 13 | <10 | <10 |
| Pb | n.d. | - | - | n.d. | - | - | n.d. | - | - | n.d. | - | - | 35 | 11 | 74 | n.d. | - | - | n.d. | - | - | <10 | <10 |
| Cr | n.d. | - | - | n.d. | - | - | n.d. | - | - | n.d. | - | - | n.d. | - | - | n.d. | - | - | n.d. | - | - | <5 | <5 |
| V | 15 | 13 | 17 | 10 | 7 | 12 | 14 | 11 | 17 | 9 | 7 | 11 | 15 | 13 | 17 | 15 | 12 | 20 | 9 | 7 | 11 | 18 | 8 |
| As | n.d. | - | - | n.d. | - | - | n.d. | - | - | n.d. | - | - | n.d. | - | - | n.d. | - | - | n.d. | - | - | <10 | <10 |
| Sc | n.d. | - | - | n.d. | - | - | n.d. | - | - | 10 | 10 | 10 | n.d. | - | - | n.d. | - | - | 10 | 10 | 10 | <10 | <10 |
| S | n.d. | - | - | n.d. | - | - | n.d. | - | - | n.d. | - | - | n.d. | - | - | n.d. | - | - | n.d. | - | - | <0.10 | <0.10 |
| CL | n.d. | - | - | n.d. | - | - | n.d. | - | - | n.d. | - | - | n.d. | - | - | n.d. | - | - | n.d. | - | - | <0.10 | <0.10 |
| F | 0.75 | 0.69 | 0.79 | 0.45 | 0.42 | 0.47 | 0.77 | 0.72 | 0.82 | 0.46 | 0.44 | 0.48 | 0.77 | 0.73 | 0.80 | 0.76 | 0.70 | 0.80 | 0.47 | 0.43 | 0.51 | 0.78 | 0.50 |
| no.samples | | 5 | | | 5 | | | 2 | | | 4 | | | 5 | | | 8 | | | 6 | | 1 | 1 |

n.d. - not determined, because of few data above detection limits be expected. An other possibility is that the differences are due to the process of dolomitization. These two alternatives are discussed further below.

Considering the differences between the units, the dolomite marbles are excluded because of the large range and because of the shift in the isotope values. With exception of the Kongsfjell marbles, the other calcite marble units seem to give a narrow well defined range in their isotope values (Table 4 and Fig. 28). The calcite marbles in the Anders Larsa Group and Lifjell Unit (from Storakersvatnet) fall in a narrow range and give both a value around 0.7074. Only two samples of calcite marbles have been sampled from the Plurdalen Group s.s. These two show quite a spread, but fall on a trend toward a dolomite marble. The lower value of 0.7078 is therefore preferred. The Dunderlandsdalen calcite marbles are also represented by only two samples, also with some spread. The lowermost have the same value, 0.7069, as the lowermost of the corresponding dolomite marbles, and is preferred.

The Kongsfjell marbles have lower $^{87}Sr/^{86}Sr$ -ratios than the others and show a considerable spread. There is, however, a notable decrease in the isotope ratios with increase in the Sr-content. The lower value of 0.7057 which is given by two of the samples is indeed lower than the other samples, while the higher value of 0.7069, also given by two samples, is similar to the Dunderlandsdalen marble. The similar isotope ratios obtained for the marbles in the Lifjell Unit, the Anders Larsa Group and also the Plurdalen Group support the correlation between these units.

The isotope values of the marbles can be used to give an age estimate of the different lithological units. This is because marine carbonates are known to reflect the Sr isotopic composition of seawater at the time of formation, and the Sr isotopic composition of seawater has varied considerably through time (Burke et al. 1982, Faure 1986, Kaufman et al. 1993). Plotting the different carbonates on the seawater Sr isotopic curve (fig.29), suggest that the Anders Larsa, Dunderlandsdalen, Plurdalen and Lifjell unit marbles were formed at ages ranging from 590-600 Ma. The data is not of such precision that any The lower value of the Kongsfjell marbles does intersect the curve in Middle Proterozoic (1400 Ma), which is highly unlikely, while the higher Sr-isotope value gives an age of 590 Ma, which is similar to the Dunderlandsdalen marbles.

To investigate the strong differences between the Sr-isotope ratios in the dolomite marbles and calcite marbles, the $^{87}Sr/^{86}Sr$ -ratios have been plotted against the Sr content in the samples (fig.30). Such a diagram can be used to investigate if the differences are the result of mixing between two sources. If this is the case, the samples should follow a hyperbolic trend in the diagram. The dolomite marbles follow a continuous, straight trend, with consistently low Sr-content and strongly varying isotope ratios. The calcite marbles on the other hand seem to spread out considerably, both in isotope ratios and content of Sr. However, there is a more consistent picture, if each unit is

## Table 4: Marbles - Sr isotopes

| Unit | Rocktype | Sample-no. | 87Rb/86Sr | Se | 87Sr/86Sr | Sr (ppm) | Rb (ppm) |
|---|---|---|---|---|---|---|---|
| Anders Larsa | calcite marble | 296 | 0.00052 | 0.00001 | 0.70721 | 1563.28 | 0.28 |
| Anders Larsa | calcite marble | 298 | 0.00098 | 0.00001 | 0.70738 | 1063.94 | 0.36 |
| Anders Larsa | calcite marble | 295 | 0.00114 | 0.00001 | 0.70717 | 1569.30 | 0.73 |
| Anders Larsa | calcite marble | 299 | 0.00718 | 0.00007 | 0.70741 | 342.31 | 0.85 |
| Anders Larsa | dolomite marble | 292 | 0.13293 | 0.00133 | 0.70967 | 52.90 | 2.43 |
| Anders Larsa | dolomite marble | 293 | 0.02684 | 0.00027 | 0.70956 | 76.56 | 0.71 |
| Anders Larsa | dolomite marble | 294 | 0.00338 | 0.00003 | 0.70895 | 68.47 | 0.08 |
| Anders Larsa | dolomite marble | 300 | 0.00108 | 0.00001 | 0.70801 | 53.63 | 0.02 |
| Dunderlandsdalen | calcite marble | 284 | 0.00068 | 0.00001 | 0.70724 | 1614.89 | 0.38 |
| Dunderlandsdalen | calcite marble | 285 | 0.00003 | 0.00000 | 0.70685 | 2305.13 | 0.02 |
| Dunderlandsdalen | dolomite marble | 280 | 0.00023 | 0.00000 | 0.70707 | 125.66 | 0.01 |
| Dunderlandsdalen | dolomite marble | 281 | 0.00044 | 0.00000 | 0.70710 | 130.59 | 0.02 |
| Dunderlandsdalen | dolomite marble | 282 | 0.00026 | 0.00000 | 0.70692 | 122.52 | 0.01 |
| Dunderlandsdalen | dolomite marble | 283 | 0.02798 | 0.00028 | 0.70778 | 85.81 | 0.83 |
| Grasvatnet | calcite marble | 252 | 0.00041 | 0.00000 | 0.70852 | 2136.09 | 0.30 |
| Grasvatnet | calcite marble | 253 | 0.00005 | 0.00000 | 0.70864 | 1758.62 | 0.03 |
| Grasvatnet | dolomite marble | 247 | 0.00257 | 0.00003 | 0.70779 | 44.99 | 0.04 |
| Grasvatnet | dolomite marble | 248 | 0.00582 | 0.00006 | 0.70790 | 69.64 | 0.14 |
| Kongsfjell | calcite marble | 243 | 0.01743 | 0.00017 | 0.70690 | 13.28 | 0.08 |
| Kongsfjell | calcite marble | 244 | 0.00069 | 0.00001 | 0.70564 | 833.53 | 0.20 |
| Kongsfjell | calcite marble | 254 | 0.00009 | 0.00000 | 0.70570 | 1001.15 | 0.03 |
| Kongsfjell | calcite marble | 255 | 0.00056 | 0.00001 | 0.70694 | 464.48 | 0.09 |
| Kongsfjell | calcite marble | 256 | 0.00047 | 0.00000 | 0.70669 | 794.22 | 0.13 |
| Plurdal | calcite marble | 288 | 0.00024 | 0.00000 | 0.70782 | 1569.52 | 0.13 |
| Plurdal | calcite marble | 286 | 0.00324 | 0.00003 | 0.70825 | 732.62 | 0.82 |
| Plurdal | dolomite marble | 287 | 0.00141 | 0.00001 | 0.70870 | 81.89 | 0.04 |
| Stor-Akersvatnet | calcite marble | 265 | 0.00121 | 0.00001 | 0.70745 | 1145.56 | 0.48 |
| Stor-Akersvatnet | calcite marble | 267 | 0.00007 | 0.00000 | 0.70740 | 826.09 | 0.02 |
| Stor-Akersvatnet | calcite marble | 268 | 0.00007 | 0.00000 | 0.70735 | 1956.58 | 0.05 |
| Stor-Akersvatnet | calcite marble | 276 | 0.00012 | 0.00000 | 0.70739 | 935.35 | 0.04 |
| Stor-Akersvatnet | calcite marble | 277 | 0.00003 | 0.00000 | 0.70737 | 888.70 | 0.01 |
| Stor-Akersvatnet | calcite marble | 275 | 0.00023 | 0.00000 | 0.70737 | 1143.80 | 0.09 |
| Stor-Akersvatnet | dolomite marble | 269 | 0.00058 | 0.00001 | 0.70902 | 50.21 | 0.01 |
| Stor-Akersvatnet | dolomite marble | 270 | 0.00217 | 0.00002 | 0.70818 | 53.28 | 0.04 |
| Stor-Akersvatnet | dolomite marble | 278 | 0.00104 | 0.00001 | 0.70781 | 55.81 | 0.02 |
| Stor-Akersvatnet | dolomite marble | 279 | 0.00095 | 0.00001 | 0.70815 | 61.11 | 0.02 |

1 sigma confidence level (Se) for 87/86Sr is 0.000030

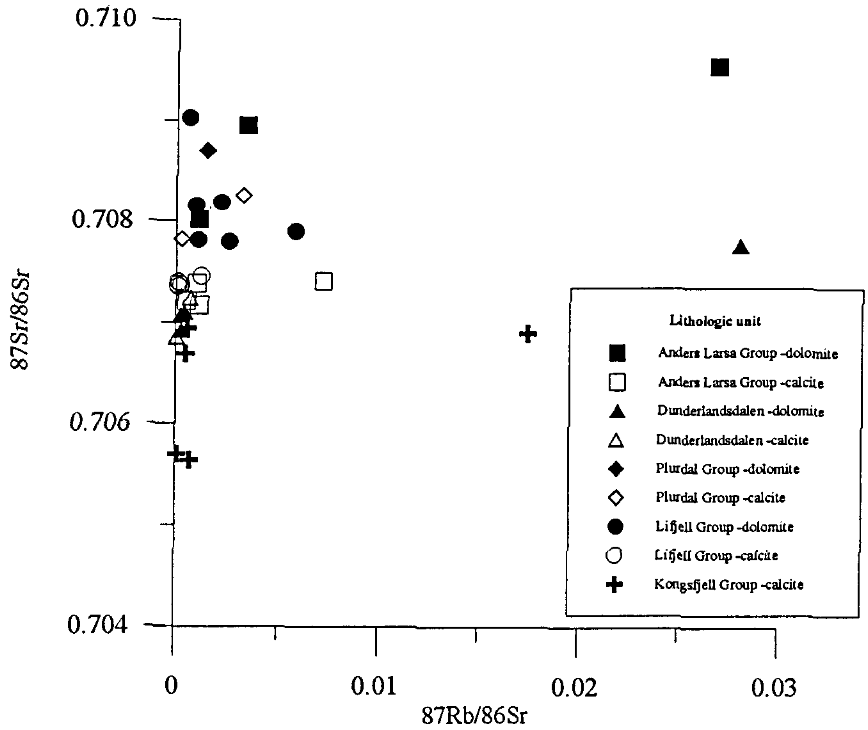


Figure 28: Plot of the Rb-Sr isotopic data from the marbles in the Rödingsfjäll Nappe Complex in $^{87}Sr/^{86}Sr$ vs. $^{87}Rb/^{86}Sr$ diagram. Filled symbols are dolomite marbles and open symbols calcite marbles.

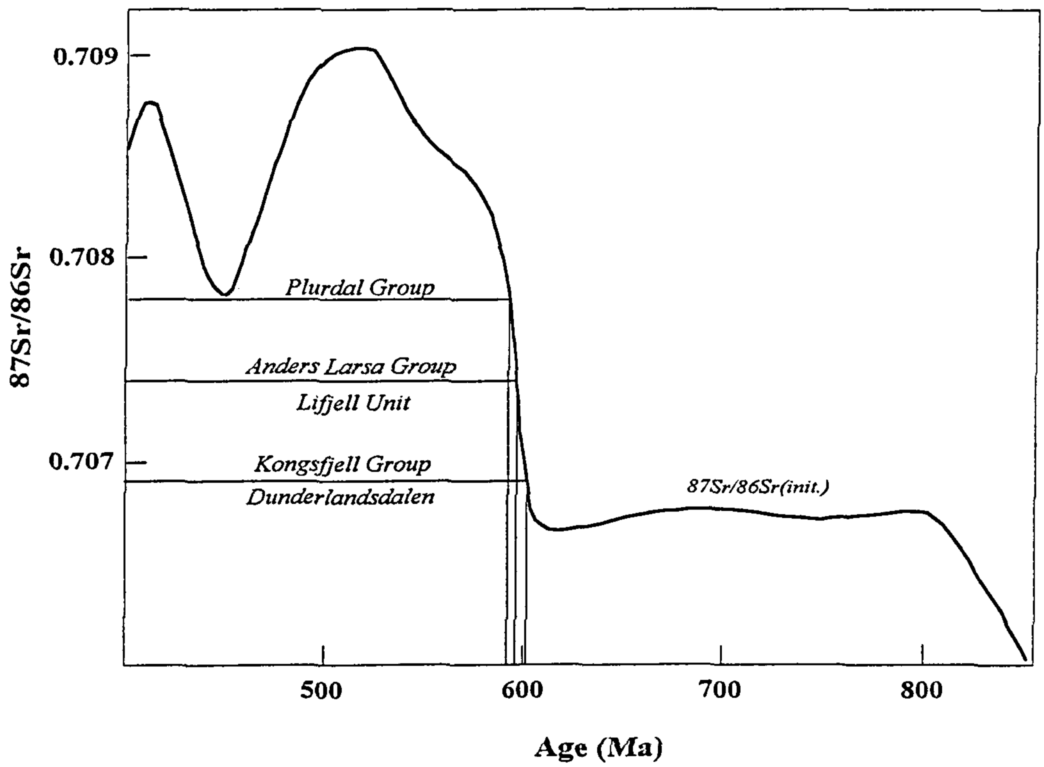


Figure 29: A diagram showing the marbles in the Rödingsfjäll Nappe Complex in relation to the Sr-isotopic composition of seawater through time. Seawater curve from Trønnes & Sundvoll (1995).

considered separately. Most data are from the thick marble units in the Anders Larsa Group and from the Lifjell Unit around Storakersvatnet. The combined dolomite and calcite data from these units plot on a nearly perfect hyperbolic trend, showing that mixing has taken place. The end members are probably seawater and sedimentary rocks. The favored process for formation of dolomite is diagenesis, with Mg coming from seawater. During diagenesis, the original seawater, which is trapped as porewater in the sediments will be expected to change because of reaction with the sediments. If the sediments have a high content of clay minerals, the Sr-isotopes of the water will be shifted to higher values and approaching the values of the sediments.

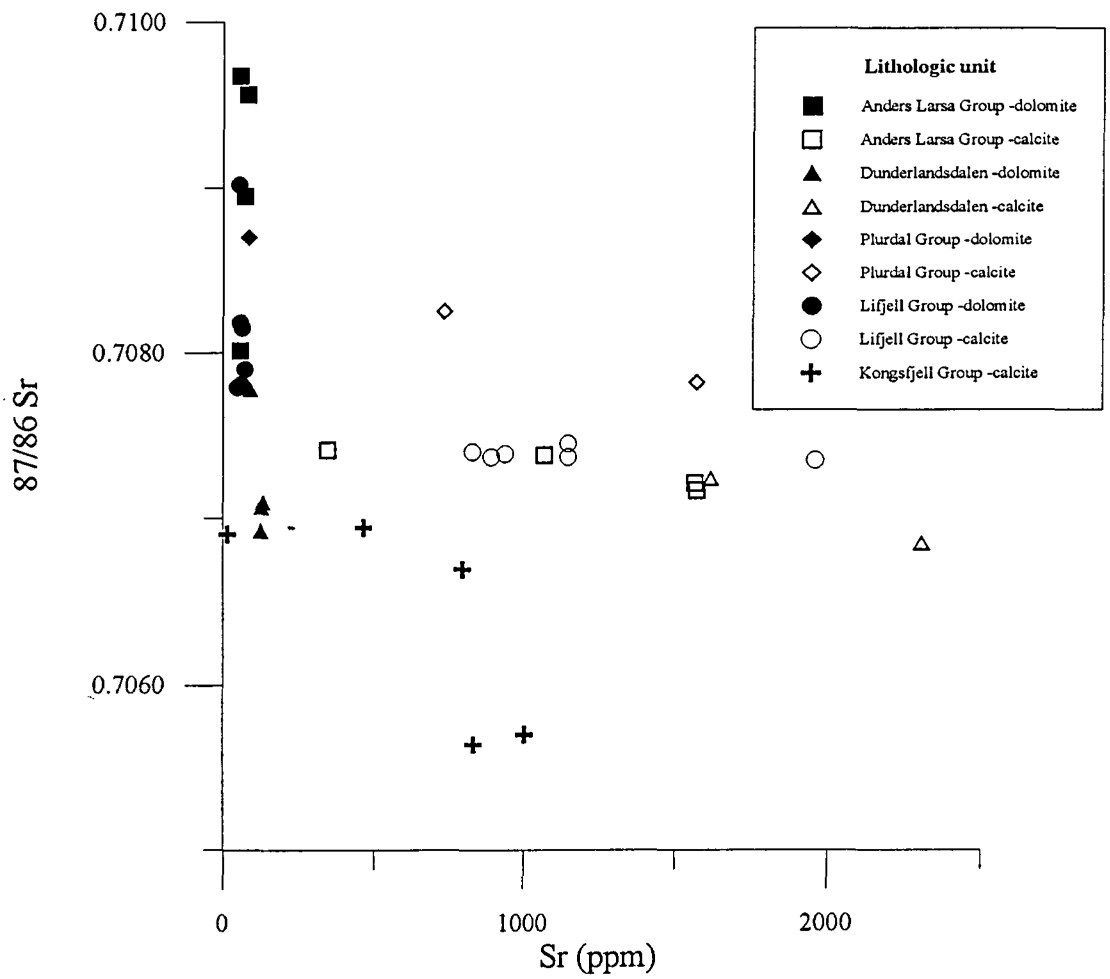


Figure 30: Plot of the $^{87}Sr/^{86}Sr$ isotopic ratios against the Sr-content for the marbles in the Rödingsfjäll Nappe Complex. Filled symbols are dolomite marbles and open symbols calcite marbles.

Quartz-feldspathic schists and orthogneisses.

It seems reasonable to compare the different felsic schists in the Okstindene area to reveal similarities and differences between them and to try to find out which rocks are of igneous and which of sedimentary origin. All of the rocks contain quartz, alkali feldspar and/or plagioclase, biotite and muscovite as major phases (see above) and thus are quartz-feldspathic schists.

The average composition of the schists are shown in table 5, and for comparison, grey gneisses and so-called acid metavolcanics from the Mofjellet area have been included (data from Paul Reitan). All the rocks have a comparable high $SiO_2$ content (70-79 %), and a total alkali content of 5-7.4%, which classify the rocks as rhyodacite to rhyolites, if an igneous origin is presumed. The $K_2O/Na_2O+CaO$-ratio vary from 0.59 to 1.90, showing that both alkali feldspar and plagioclase can be the dominant feldspar, which has also been shown by the microscope work (see above).

Considering the minor and trace elements, there are some important differences between the units. The orthogneisses and quartz-feldspathic schists of the Kongsfjell Group have a low content of $Fe_2O_{3(t)}$, $TiO_2$, $P_2O_5$, Zr, V and Cr compared to the Målvatnet quartz-feldspathic schists, and the range is also smaller. The Målvatnet schists are similar to the Mofjellet grey gneisses, whereas the other felsic rocks of the Okstindene Area seems to be more similar to the acid metavolcanics from Mofjellet.

Plotting some of the more immobile elements against each other, confirm these comparisons, and also shed some light on the origin of the rocks (fig.31). There is a rather consistent picture in all the four plots, Zr vs. $Al_2O_3$, $TiO_2$ and Y and $TiO_2$ vs. $Al_2O_3$, in that the orthogneisses and the Kongsfjell quartz-feldspathic schists lie along trends which project through origin (especially in the Zr-plots), whereas the Målvatnet schists plot randomly. The Stolpfjellet quartz-feldspathic schists follow trends which do not project through origin in Zr-plots and plot randomly in the Al-Ti plot. The Mofjellet grey gneisses also plot rather randomly in the different diagrams, while the acid metavolcanics fall on a trend toward the origin.

Trends which project through origin appearing when incompatible and immobile elements are plotted against each other, are strong indications of igneous rocks. From this, it appears that the Kongsfjell quartz-feldspathic schists and the orthogneisses are both of igneous origin, representing metamorphosed and deformed rhyodacites and rhyolites (fig.32). They are also similar to the acid metavolcanics in the Mofjellet Area.

The Målvatnet schists and the Stolpfjellet quartz-feldspathic schists, on the other hand, seem to be of sedimentary origin, since they plot randomly in plots of incompatible and

# Table 5: Felsic schists and gneisses

| Unit | Kongsfjell Group | | | Kongsfjell Group | | | | Lifjell | | Mofjell Group | | |
|---|---|---|---|---|---|---|---|---|---|---|---|---|
| Rocktype | orthogneiss | | n=4 | qz-fsp schist | | n=13 | | orthogneiss | | acid metavolcanics | | n=3 |
| | average | min. | max. | average | st.dev. | min. | max. | sample 1 | sample 2 | average | min. | max. |
| SiO2 | 77.43 | 76.80 | 78.01 | 72.48 | 3.06 | 66.69 | 78.60 | 71.99 | 77.06 | 79.14 | 75.71 | 85.88 |
| Al2O3 | 12.95 | 12.28 | 14.22 | 13.70 | 1.54 | 11.61 | 15.82 | 15.09 | 11.94 | 9.95 | 5.53 | 13.05 |
| Fe2O3 | 1.00 | 0.65 | 1.24 | 2.05 | 0.82 | 0.87 | 3.96 | 2.34 | 0.28 | 1.17 | 1.09 | 1.23 |
| TiO2 | 0.07 | 0.05 | 0.08 | 0.14 | 0.07 | 0.08 | 0.36 | 0.11 | 0.06 | 0.07 | 0.02 | 0.15 |
| MgO | 0.26 | 0.16 | 0.48 | 1.69 | 1.21 | 0.51 | 4.33 | 0.15 | 0.17 | 0.40 | 0.09 | 0.99 |
| CaO | 0.39 | 0.12 | 0.93 | 1.14 | 0.71 | 0.20 | 2.81 | 1.12 | 1.01 | 1.16 | 0.04 | 2.07 |
| Na2O | 3.29 | 0.43 | 5.97 | 1.53 | 1.43 | <0.10 | 4.26 | 3.70 | 2.39 | 1.13 | 0.34 | 1.73 |
| K2O | 2.42 | 1.50 | 3.75 | 4.42 | 1.91 | 2.19 | 7.84 | 3.73 | 4.19 | 4.37 | 3.47 | 5.74 |
| MnO | 0.03 | <0.01 | 0.06 | 0.04 | 0.02 | 0.01 | 0.07 | 0.04 | 0.01 | 0.02 | <0.01 | 0.02 |
| P2O5 | 0.02 | 0.01 | 0.03 | 0.03 | 0.02 | 0.01 | 0.11 | 0.04 | 0.01 | 0.03 | <0.01 | 0.05 |
| LOI | 1.09 | 0.42 | 1.96 | 1.52 | 0.52 | 0.63 | 2.32 | 1.23 | 1.30 | 0.90 | 0.72 | 1.18 |
| SUM | 98.94 | 98.48 | 99.48 | 98.73 | 0.46 | 98.08 | 99.60 | 99.54 | 98.43 | 98.33 | 97.71 | 99.08 |
| Ba | 358 | 55 | 528 | 475 | 367 | 51 | 1039 | 479 | 593 | 2600 | 711 | 5798 |
| Sb | n.d. | <10 | <10 | n.d. | - | <10 | <10 | <10 | <10 | n.d. | <10 | <10 |
| Sn | n.d. | <10 | <10 | n.d. | - | <10 | <10 | <10 | <10 | n.d. | <10 | <10 |
| Cd | n.d. | <10 | 12 | n.d. | - | <10 | <10 | <10 | <10 | n.d. | <10 | <10 |
| Ag | n.d. | <10 | <10 | n.d. | - | <10 | <10 | <10 | <10 | n.d. | <10 | <10 |
| Ga | n.d. | <10 | 13 | 15 | 3 | 12 | 21 | 15 | <10 | n.d. | <10 | <10 |
| Zn | 28 | 13 | 33 | 63 | 43 | 27 | 194 | 71 | 5 | 23 | <5 | 47 |
| Cu | n.d. | <5 | 18 | 6 | 3 | <5 | 14 | 5 | <5 | n.d. | <5 | <5 |
| Ni | n.d. | <5 | <5 | n.d. | - | <5 | 13 | <5 | <5 | n.d. | <5 | <5 |
| Yb | n.d. | <10 | <10 | n.d. | - | <10 | <10 | <10 | <10 | 12 | 11 | 13 |
| Co | n.d. | <10 | <10 | n.d. | - | <10 | <10 | <10 | <10 | n.d. | <10 | <10 |
| Ce | 25 | <10 | 40 | 80 | 39 | 18 | 169 | 73 | 44 | 24 | <10 | 46 |
| La | 20 | <10 | 39 | 50 | 22 | 15 | 90 | 44 | 36 | n.d. | <10 | 18 |
| Nd | 16 | <10 | 24 | 45 | 22 | 13 | 85 | 38 | 28 | n.d. | <10 | 25 |
| W | n.d. | <30 | 32 | n.d. | - | <30 | 32 | <30 | <30 | n.d. | <30 | <30 |
| Mo | n.d. | <5 | <5 | n.d. | - | <5 | 6 | <5 | <5 | n.d. | <5 | 26 |
| Nb | 13 | 6 | 24 | 25 | 7 | 15 | 38 | 16 | 9 | n.d. | <5 | 14 |
| Zr | 89 | 72 | 107 | 180 | 31 | 118 | 220 | 141 | 69 | 83 | 43 | 130 |
| Y | 23 | 6 | 36 | 41 | 9 | 29 | 62 | 9 | 19 | 16 | 6 | 28 |
| Sr | 59 | 25 | 98 | 84 | 78 | 24 | 304 | 128 | 71 | 56 | 22 | 101 |
| Rb | 100 | 56 | 125 | 143 | 43 | 82 | 197 | 139 | 140 | 84 | 63 | 104 |
| U | n.d. | <10 | <10 | n.d. | - | <10 | 18 | <10 | <10 | 11 | <10 | 14 |
| Th | 16 | <10 | 29 | 49 | 28 | 18 | 97 | <10 | 19 | 10 | <10 | 13 |
| Pb | 44 | 14 | 124 | 36 | 20 | 14 | 77 | 21 | 33 | 13 | <10 | 19 |
| Cr | n.d. | <5 | <5 | n.d. | - | <5 | 31 | 11 | 13 | n.d. | <5 | 11 |
| V | 6 | <5 | 9 | 10 | 12 | <5 | 50 | 6 | 6 | 11 | 9 | 14 |
| As | n.d. | <10 | <10 | n.d. | - | <10 | <10 | <10 | <10 | 17 | <10 | 30 |
| Sc | n.d. | <10 | <10 | n.d. | - | <10 | 13 | <10 | <10 | n.d. | <10 | <10 |
| S | n.d | <0.10 | <0.10 | n.d. | - | <0.10 | <0.10 | <0.10 | <0.10 | 0 | 0 | 1 |
| CL | n.d. | <0.10 | <0.10 | n.d. | - | <0.10 | <0.10 | <0.10 | <0.10 | n.d. | <0.10 | <0.10 |
| F | n.d. | <0.10 | <0.10 | n.d. | - | <0.10 | <0.10 | <0.10 | <0.10 | n.d. | <0.10 | <0.10 |

| Unit | Mofjell Group | | | | Målvatn | | | | Stolpfjell | | |
|---|---|---|---|---|---|---|---|---|---|---|---|
| Rocktype | grey gneiss | | | n=9 | qz-fsp schist | | | n=7 | qz-fsp schist | | n=4 |
| | average | st.dev. | min. | max. | average | st.dev. | min. | max. | average | min. | max. |
| SiO2 | 70.06 | 3.48 | 65.54 | 75.63 | 70.64 | 5.35 | 60.00 | 76.27 | 74.06 | 69.65 | 77.09 |
| Al2O3 | 14.41 | 1.60 | 11.56 | 16.08 | 13.16 | 2.62 | 11.06 | 18.56 | 13.74 | 11.56 | 17.32 |
| Fe2O3 | 4.08 | 1.64 | 1.07 | 6.04 | 4.84 | 2.42 | 1.41 | 8.54 | 1.60 | 1.17 | 2.52 |
| TiO2 | 0.30 | 0.13 | 0.07 | 0.47 | 0.79 | 0.43 | 0.08 | 1.29 | 0.16 | 0.10 | 0.28 |
| MgO | 1.65 | 1.33 | 0.13 | 4.10 | 1.64 | 0.82 | 0.58 | 2.71 | 0.85 | 0.40 | 1.22 |
| CaO | 1.93 | 0.96 | 0.57 | 3.55 | 1.20 | 0.92 | 0.29 | 2.96 | 1.65 | 0.20 | 3.54 |
| Na2O | 3.30 | 1.44 | 0.82 | 4.54 | 1.40 | 0.75 | 0.21 | 2.29 | 2.56 | 1.15 | 4.18 |
| K2O | 3.09 | 2.45 | 1.30 | 8.71 | 3.57 | 0.97 | 2.46 | 5.19 | 3.23 | 2.15 | 4.87 |
| MnO | 0.08 | 0.06 | 0.02 | 0.17 | 0.06 | 0.04 | 0.01 | 0.14 | 0.04 | 0.01 | 0.09 |
| P2O5 | 0.06 | 0.04 | <0.01 | 0.12 | 0.10 | 0.06 | 0.02 | 0.21 | 0.05 | 0.01 | 0.13 |
| LOI | 0.56 | 0.19 | 0.25 | 0.87 | 1.35 | 0.48 | 0.78 | 2.08 | 1.07 | 0.79 | 1.62 |
| SUM | 99.54 | 0.53 | 98.70 | 100.14 | 98.76 | 0.28 | 98.39 | 99.19 | 99.00 | 98.66 | 99.52 |
| Ba | 393 | 244 | 37 | 888 | 585 | 221 | 139 | 840 | 1182 | 594 | 2410 |
| Sb | n.d. | - | <10 | <10 | n.d. | - | <10 | <10 | n.d. | <10 | <10 |
| Sn | n.d. | - | <10 | <10 | n.d. | - | <10 | 69 | n.d. | <10 | <10 |
| Cd | n.d. | - | <10 | <10 | n.d. | - | <10 | <10 | n.d. | <10 | <10 |
| Ag | n.d. | - | <10 | <10 | n.d. | - | <10 | <10 | n.d. | <10 | <10 |
| Ga | 13 | 4 | <10 | 19 | 17 | 3 | 13 | 21 | 15 | 11 | 19 |
| Zn | 82 | 29 | 16 | 116 | 43 | 37 | <5 | 107 | 63 | 49 | 78 |
| Cu | n.d. | - | <5 | 17 | 15 | 13 | <5 | 38 | n.d. | <5 | <5 |
| Ni | n.d. | - | <5 | 6 | 11 | 6 | <5 | 20 | n.d. | <5 | <5 |
| Yb | n.d. | - | <10 | 12 | n.d. | - | <10 | <10 | n.d. | <10 | <10 |
| Co | n.d. | - | <10 | <10 | n.d. | - | <10 | 12 | n.d. | <10 | <10 |
| Ce | 57 | 50 | <10 | 143 | 46 | 27 | <10 | 91 | 57 | 28 | 82 |
| La | 24 | 27 | <10 | 76 | 19 | 15 | <10 | 39 | 34 | 16 | 49 |
| Nd | 23 | 24 | <10 | 72 | 23 | 14 | <10 | 43 | 32 | 17 | 46 |
| W | n.d. | - | <30 | <30 | n.d. | - | <30 | <30 | n.d. | <30 | <30 |
| Mo | n.d. | - | <5 | <5 | n.d. | - | <5 | 5 | n.d. | <5 | <5 |
| Nb | 17 | 23 | <5 | 58 | 16 | 3 | 13 | 21 | 15 | 10 | 24 |
| Zr | 175 | 133 | 80 | 431 | 368 | 213 | 99 | 686 | 141 | 136 | 148 |
| Y | 34 | 16 | 19 | 69 | 31 | 5 | 21 | 37 | 30 | 22 | 39 |
| Sr | 97 | 41 | 49 | 158 | 75 | 45 | 21 | 132 | 221 | 136 | 375 |
| Rb | 69 | 52 | <10 | 154 | 162 | 60 | 106 | 285 | 135 | 66 | 182 |
| U | n.d. | - | <10 | 13 | n.d. | - | <10 | <10 | n.d. | <10 | <10 |
| Th | n.d. | - | <10 | 32 | 25 | 29 | <10 | 87 | n.d. | <10 | 24 |
| Pb | 10 | 7 | <10 | 27 | 16 | 9 | <10 | 27 | 25 | 17 | 36 |
| Cr | n.d. | - | <5 | 7 | 42 | 33 | <5 | 102 | n.d. | <5 | <5 |
| V | 22 | 14 | 7 | 50 | 77 | 49 | <5 | 137 | 10 | 9 | 11 |
| As | n.d. | - | <10 | <10 | n.d. | - | <10 | <10 | n.d. | <10 | <10 |
| Sc | 10 | 5 | <10 | 18 | 13 | 6 | <10 | 21 | n.d. | <10 | 10 |
| S | n.d. | - | <0.10 | <0.10 | n.d. | - | <0.10 | <0.10 | n.d | <0.10 | <0.10 |
| CL | n.d. | - | <0.10 | <0.10 | n.d. | - | <0.10 | <0.10 | n.d. | <0.10 | <0.10 |
| F | n.d. | - | <0.10 | <0.10 | n.d. | - | <0.10 | <0.10 | n.d. | <0.10 | <0.10 |

n.d. - not determined, because of few data above detection limit

n=4, 4 samples analyzed

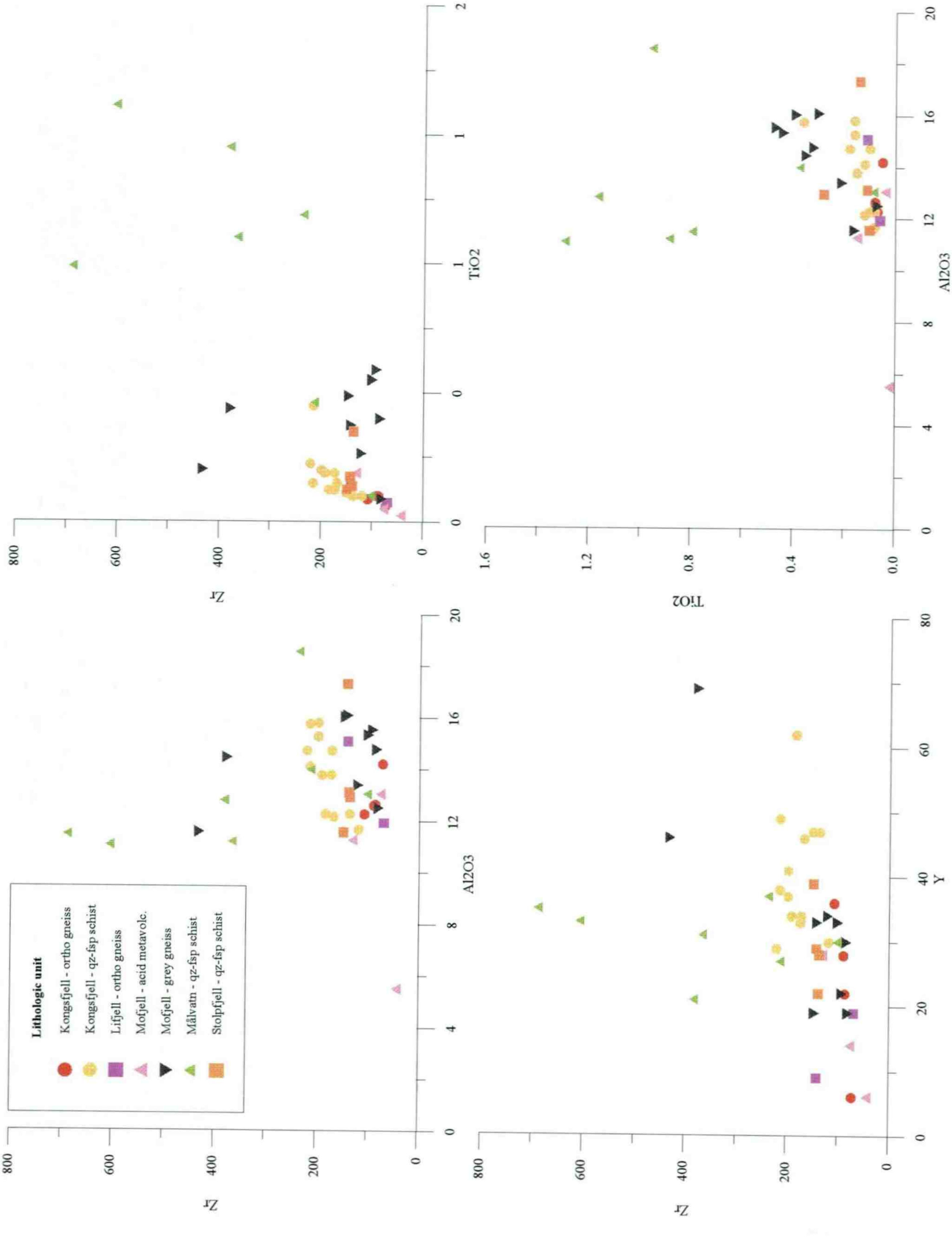


Figure 31: Plots of Zr vs. $Al_2O_3$, Zr vs. Y, Zr vs. $TiO_2$ and $TiO_2$ vs. $Al_2O_3$ of the felsic rocks in the Okstindene area, including acid metavolcanics and gray gneisses from the Mofjell Group. Rocks which fall on trends projecting through the origin are probably of igneous origin. Mofjell data provided by Paul Reitan (pers.comm.).

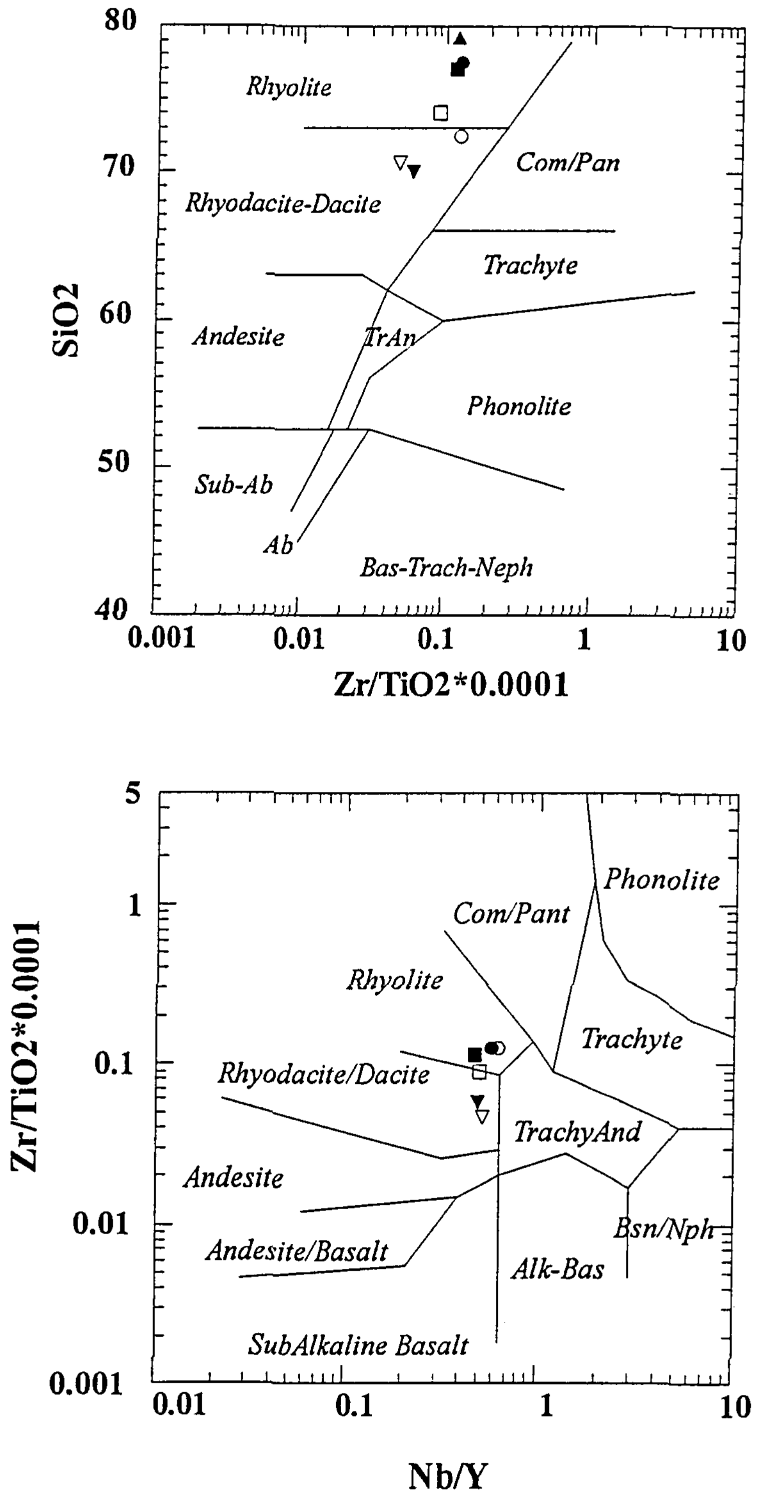


Figure 32: Discrimination diagrams of felsic rocks in the Okstindene Area, including grey gneisses and acid metavolcanics from the Mofjell Area. Legend: Filled circles - Kongsfjell orthogneisses, Open circles - Kongsfjell quartz-feldspar schists, Filled square - Lifjell orthogneisses, Upright triangle - Mofjell acid metavolcanics, Inverted, filled triangle - Mofjell grey gneisses, Inverted, open triangle - Målvatn quartz-feldspar schists, Open square - *Stolpfjellet quartz-feldspar schists. Diagrams redrawn from Winchester & Floyd (1977).*

immobile elements. This is also supported by high contents of elements such as P, Zr, Ti, Cr, V, which partly will be incorporated in heavy minerals. The high content of feldspar in these rocks and rather low content ofsilica in comparison to the other schists, indicate that they must be rather immature, e.g. graywackes or arkoses.

## STRUCTURAL GEOLOGY

The area has a complex structural history, including structures probably resulting from both Caledonian and pre-Caledonian events. Five major phases of deformation have been recognized in the area.

### $D_1$ and $D_2$

The first two phases led to transversal isoclinal folding and repetition of lithologies at all scales. These two phases can not be easily unraveled in the field, unless detailed mapping and structural analysis are applied as it has been done by S.B. Olesen (1984) at Kongsfjellet and P.H. Larsen at Simafjell (1984), immediately north of Bleikvatnet. It is beyond the scope of this project to separate these two phases, although it would have been possible to do so on Stolpfjellet-Tverrfjellet, where there are good exposures and large lithological variations. Some mesoscale examples have been seen during this work, and an example from Grasfjellet is shown in fig.33 a, b. These two phases are responsible for the regional foliation and schistosity in the area.

### $D_3$

The $D_3$ phase folded the units into large-scale recumbent folds, with flat-lying axial planes and SSW to WNW trending fold axes with shallow plunges (fig.34 a,b).

As argued above, the Anders Larsa Group and the Lifjell Unit have very similar lithologies, both containing thick units of calcite and dolomite marbles and with similar Sr-isotope ratios. This indicate that the units could be correlated with each other. South of Halvarddalen, the two units are only separated by less than 2 km of Kongsfjell Group lithologies, and they may merge beneath the Helgeland Nappe Complex further south. Correlation of these two units, which are lying structurally beneath (Lifjell Unit) and above (Anders Larsa Group) the Kongsfjell Group, implies presence of a megascale recumbent and generally south to southeast-facing $F_3$-fold in the Okstindene area. Since the fold is bounded by thrusts, both underneath and above, it may be justified to use the term fold nappe, for this large scale structure.

The core of this $F_3$-structure is probably the Målvatnet unit, but some more work is needed in the northern part of the area to confirm this. The Kongsfjell Group disappears north of

Fig.33 a, b: Overview and close-up photos of an older gneissic banding in kyanite-rich garnet-mica schist probably formed under D1, which have been isoclinally folded during D2 with formation of an axial plane schistosity. Locality: Grasfjellet (UTM 473620 7331950).

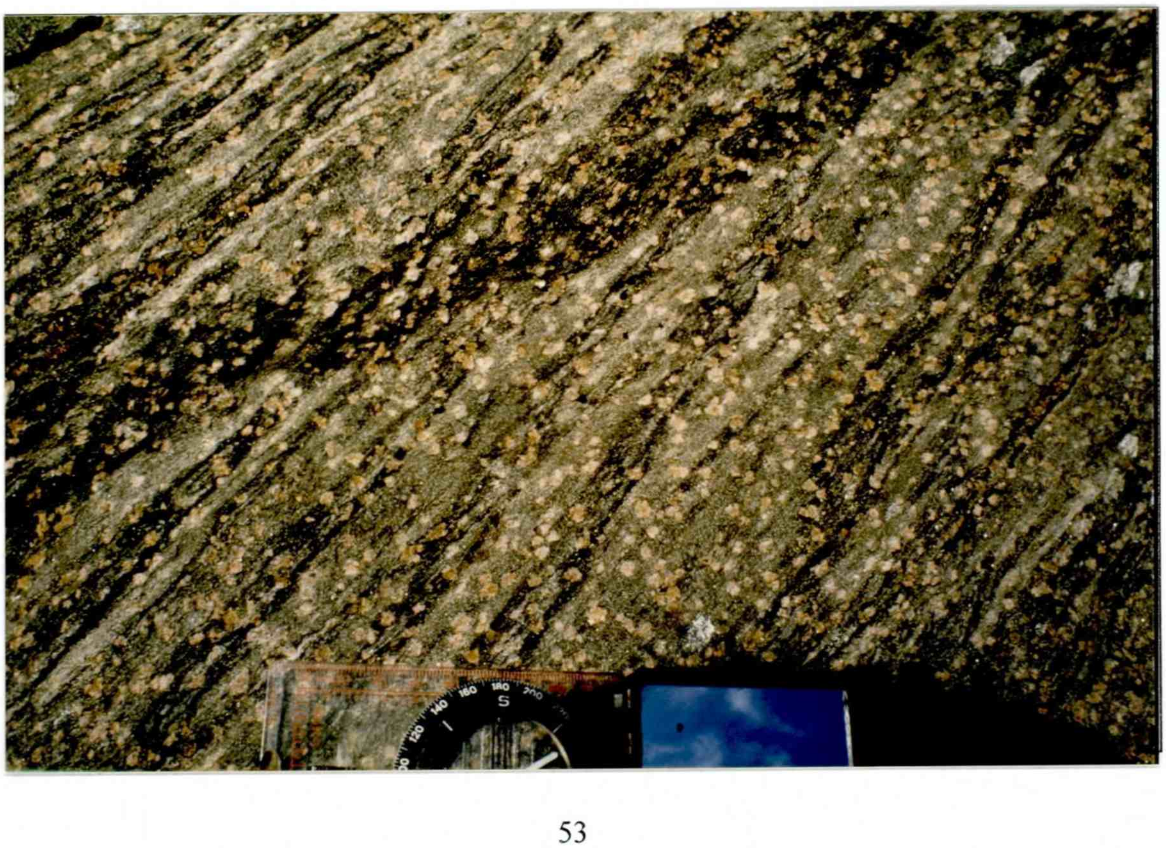

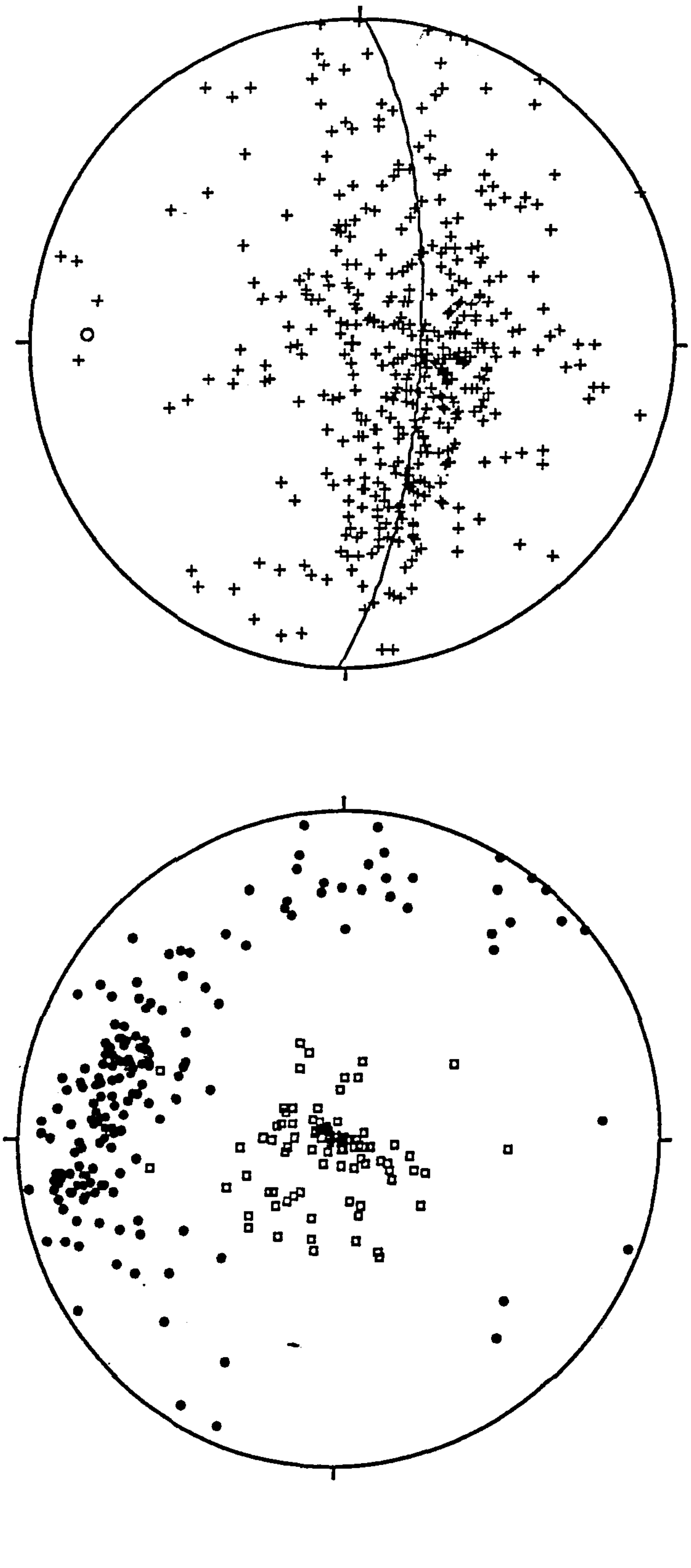

Figure 34 a: Plots of $S_2$-foliations from the area between Kongsfjellet and Artfjellet, defining a regional $F_3$-fold structure. b): Plots of $F_3$-fold axes (filled circles) and axial planes (open squares) from the Okstindene Area, defining a large scale $F_4$-structure. In both plots equal area projection and lower hemisphere are used. For planar data the poles are plotted.

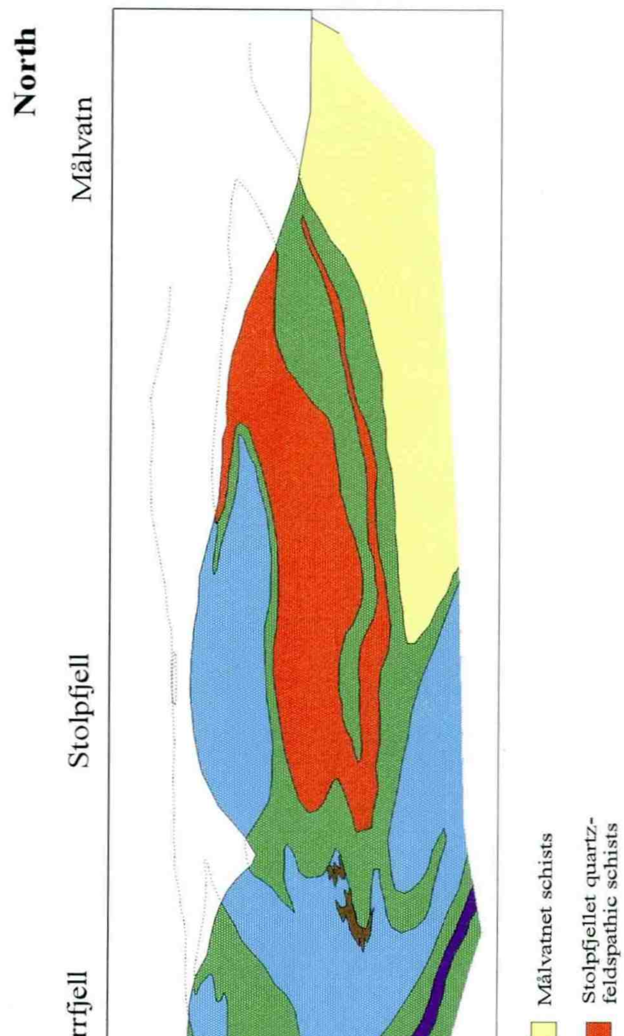


Figure 35: Vertical profile from Gråfjell in the southeast to Målvatnet in the northwest, showing the major $F_3$ recumbent fold structure.

Fig.36 a: Intense, small scale $F_3$-folds in gneissose garnet-mica schist. Fold-axis 223/44. Locality: Kjennsvasshammaren (UTM 467884 7325668), photo taken westwards.

b): Very intense, close to isoclinal, small scale folding of quartz-feldspathic schist. Ruler 15 cm. Photo taken westwards. Locality: West of Kjennsvatnet (UTM 464350 7327450). Both these localities are in the hinge-zone of a major $F_3$-structure.

Figure 37 a, b: F3-folds refolding F1-F2-structures in kyanite-rich garnet-mica schist (kyanite particularly abundant in photo b). Locality: Western shore of Grasvatnet (UTM 469840 7328460). Length of ruler is 15 cm.

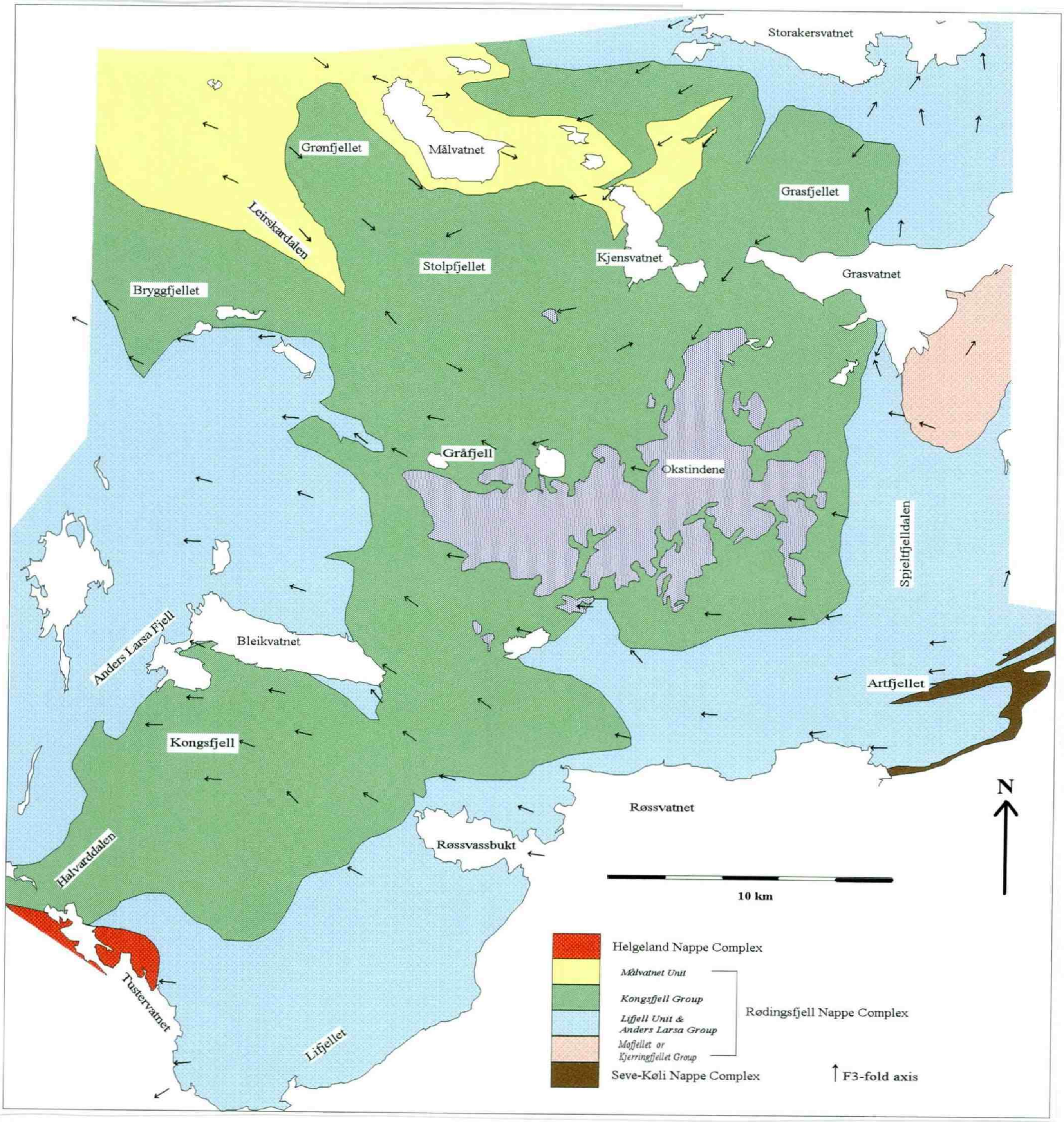


Figure 38: Regional geological map of the Okstindene Area, showing the orientations of the measured F3-folds in the field.

Målvatnet, but a part seems to continue structurally beneath the Målvatnet unit, forming the lower limb of the fold (see fig.2). In the core of the fold, such as in the Stolpfjellet-Tverrfjellet area, smaller scale $D_3$ folding of this structure is very intense and complex. Particularly the amphibolites, as good marker horizons, demonstrate the nature and complexity of the $D_3$ folding in this area. A NW-SE profile through the area show that these amphibolites might be parts of one larger horizon, which were disrupted during $D_3$ deformation (fig.35). The folding also explain the enhanced thickness of calcareous mica schists in Leirskardalen, formed as a result of refolding of $F_1$-$F_2$ structures. However, more detailed work is necessary to confirm this.

At the mega- to mesoscale, $D_3$ caused vertical compression and folded the $S_1/S_2$ foliation into large scale recumbent folds with fold-axes varying from SSW to WNW. This episode formed open to tight folds at all scales, except in the most competent varieties of the garnet-mica schist. Close to the hinge zones of the larger structures, intense small scale folding (crenulation folds) is typically found (fig.36 a, b). Mineral lineations have been developed parallel to the trend of the fold axes, as quartz rods especially in garnet-mica schists and quartz-feldspathic schists, and as parallel growth of amphibole in amphibolite and the garnet-mica schists on Lifjell.

$D_3$ folding from mega- to microscale are particularly well developed in the Bleikvassli - Kongsfjell area, where the Kongsfjell and Anders Larsa Group lithologies have been folded in several SW trending and alternating kilometerscale NW and SE facing recumbent folds at a scale of 2 km and more.

Mesoscale $F_3$-folds refolding $F_1$-$F_2$ structures are found at various localities. Particularly well exposed examples appear at the western shores of Grasvatnet, where kyanite rich layers in garnet-mica schists make the structural patterns very apparent (fig.37 a, b).

**$D_4$**

The $D_4$ phase led to formation of gentle to open folds or undulations, typically with interlimb angles of 150 degrees or more. The axial planes of this phase are steeply dipping, 70-90 degrees and the fold axes are generally flatlying and trending E-W. Deformation increases northwards and in mesoscale becomes distinguishable north of Leirskardalen, especially on the limbs of the $F_3$-folds, where the lithologies are flatlying and leading to a complex outcrop pattern.

Plotting up the axes of the $D_3$-phase on a regional map (fig.38), show that they vary in a systematic way, with S to SSW trending axes in the Kjennsvatnet and Grasvatnet-Storakersvatnet areas to westward trending axes in the Gråfjell-Bleikvassli area and finally WNW trending axes at Bryggfjellet. Regionally, this is manifested by the rock units being folded into a megascale open fold. This is well illustrated by the Kongsfjell Group, which in the Kongsfjell Area have a NE trend, from Okstindene to Kjennsvatnet/Grasfjellet a N trend and finally a NW trend from Kjennsvatnet to Målvatnet. Thus the fold have a wave length of more than 20 km and an amplitude of more than 10 km.

That this systematic variation in the orientation of $F_3$-axes is due to overprinting of $D_4$, is confirmed when the axes is plotted in a stereonet (fig.34 b). The axes form a well defined girdle in the net, defining a plane with a strike of about 225 degrees and a dip of about 25 degrees towards the northwest.

### $D_5$

$D_5$ is the latest phase recognized in the area. It is a very open phase, with probably an east-west trending fold axis. It is only affecting the area north of the Okstindene Glacier, which because of interference with $D_4$, gives a pattern with gentle culminations and depressions. The best example is the northern part of Spjeltfjelldalen, where gneisses of possible Mofjellet Group or Ørtfjell Group lithologies are coming up in a culmination (fig.2). Lithologies of the Lifjell Unit is draping the gneisses in a circular structure. This culmination goes into a depression north of Grasvatnet, causing the Lifjell Unit to turn eastwards and disappear beneath Grasfjellet. The depression goes into a new large culmination north of Grasfjellet, causing the Lifjell marbles to be dominant around Storakersvatnet. This culmination also makes the hinge zone of a major $D_3$-fold axis outcrop and go up in the air at Kjensvassfjellet. Also the $D_3$ fold axes have been reoriented by the $D_5$ phase, and the foldaxes in the area have trends in north to western direction, as opposed to the general southwest trend.

Similarly, in the Stolpfjellet-Målvatnet area, the $D_3$ axes generally have a SSE trend, which does not fit with the overall pattern. Most likely, the $F_3$ axes in this area have been reoriented by the $D_5$ phase (see below).

### Contact relationships

The nature of the contact between the different units is very important for unraveling the architecture and the sequential history and evolution of the area.

The contacts between the Rödingsfjäll Nappe Complex and the adjacent Seve-Köli and Helgeland Nappe Complexes, are marked by shear zones and extensive development of mylonites.

Within the Rödingsfjäll Nappe Complex, the contacts between the different lithological units appear either to be inconformities or of tectonic origin. The contact between the Mofjellet or

Kjerringfjell Group and Lifjell Group, which is exposed south of Grasvatnet, most likely is tectonic, but more work is necessary to verify that.

The contact between the Lifjell Group and Kongsfjell Group has been established as tectonic, and imbrications and repetitions of units have been found in the southern part of Spjeltfjelldalen, while in the northern part of the valley, close to Grasvatnet, the contact seems to be sharp, but concordant without any signs of deformation. However, peak metamorphism (at least middle amphibolite facies) which was reached after the main nappe emplacement, has probably obliterated many structures. Further north, the contact is well exposed in the high mountain wall of Grasfjellet, and an amphibolite at the contact has a strongly developed schistosity. This is also the case for the immediately overlying garnet-mica schist. In a thin section of the amphibolite, a totally recrystallized texture is seen, but there is distinct banding between monomineralic amphibole and plagioclase-quartz lamina at mm scale. The banding has probably resulted from shear deformation.

The contact between the Anders Larsa and Kongsfjell Groups has been interpreted as both tectonic and primary - sedimentary. What seems to be clear is that lithologies in the Kongsfjell Group tend to wedge out against the contact and that there has been some movement at the contact, at least locally (e.g. Ramberg 1967). The contact has been followed in detail both at Gråfjell and at Bryggfjellet. At Gråfjell the contact is characterized by regional metamorphic skarn composed of mainly epidote and actinolite, whereas at Bryggfjellet about 3 km to the north, the contact is characterized by rusty schists with a very pronounced schistosity.

In the area between Bleikvatnet and Bryggfjelldalen, the contact between the Anders Larsa and Kongsfjell Groups is clearly discordant. Particularly in the area between Nordtuva and Tverrfjellet, immediately south of Okstindene, it is clear that a calcareous mica schist wedge out in the contact between the Anders Larsa marbles to the west and the Kongsfjell Group garnet-mica schist to the east. However, it is not possible to conclude if this discordance has a tectonic or a sedimentary origin.

The contact between the Kongsfjell Group and the Målvatnet Unit seems to be a sedimentary contact, probably also an unconformity. In the area between Kjennsvatnet and Målvatnet the contact is marked by a 25-75 cm thick calcite marble horizon (fig.39). This thin marble is followed for at least 3 km along the contact. Such a persistence of an incompetent marble is strongly in favor of a primary sedimentary contact. Following the contact from Leirskardalen to Målvatnet, the Målvatnet unit seems to cut through the Kongsfjell Group lithologies. For instance, the thick calcareous mica schist in Leirskardalen which is 500 m thick in the valley disappear at Grønfjellet, only 4 km to the north and the Målvatnet schists is instead in contact with garnet-mica schists. From this the contact seem to be a unconformity.

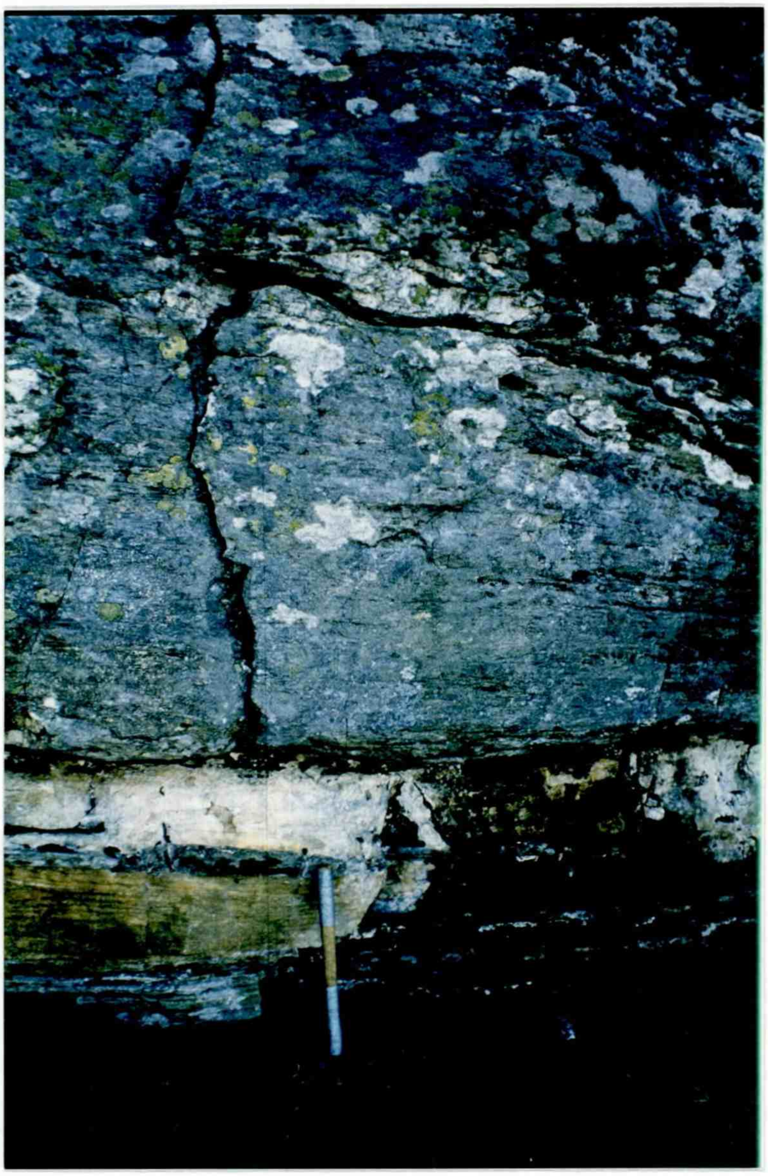

Figure 39: Thin marble unit (by the hammer), separating the Målvatn Unit from the Kongsfjell Group. The marble is overlain by Kongsfjell garnet-mica schist which is calcareous (upper two-third of photo). Hammershaft 35 cm. Locality: Foothills of Stolpfjellet (UTM 464300 7329950)

# DISCUSSION

## Origin of the lithologies

All the units in the area are dominated by lithologies of sedimentary origin, comprising mainly garnet-mica schists, calcareous mica schists, quartz-feldspathic schists and marbles. The schists are generally quartz-feldspar rich, but with variable contents of mica. The high content of feldspar show that the sediments are rather immature, and not transported too far from their sources.

The Anders Larsa Group and Lifjell Unit are characterized by thick layers of calcite and dolomite marbles, together with mica schists. The presence of the marbles implies a shallow marine environment, and the calcareous mica schists may represent metamorphosed marls.

The high contents of Al, K, Fe, Rb and Cr in the garnet-mica schists of the central part of the Kongsfjell Group, which also are kyanite rich, indicate that the sediments originally were more clay rich, and therefore deposited under low energy conditions. This, together with the limited presence of marbles, but high content of mica schists, imply that the Kongsfjell Group represents a deeper marine environment than the Anders Larsa Group / Lifjell Unit. The calcareous schists in the Kongsfjell Group could represent sediments which partly derived their carbonate content from the marbles in the Anders Larsa Group and that these carbonate rocks at a certain time were available for erosion. This would also explain that the calcareous schists only are found at the higher stratigraphic levels and close to the boundaries of the large sedimentary basin. Another possibility is that these schists could represent marly sediments.

The Målvatnet Unit is dominated by quartz-feldspathic schists and garnet-mica schists. Numerous intercalations of thin calcite marble horizons are found within the schist units, which together with a variable mineralogy and geochemistry, strongly indicate a sedimentary origin of the quartz-feldspathic schists. The high content of feldspar in most of these schists points to derivation from either gneissic basement rocks or felsic volcanics. Another possibility is waterlain felsic tuffs mixed up with clastic sediments.

Amphibolites are present in all the three major units in the area, but are more abundant in the Anders Larsa Group/Lifjell Unit and Kongsfjell Group than in the Målvatnet Unit. The large extent of the individual amphibolite horizons strongly indicate that they represent volcanic flows.

The geochemistry show that they are metabasalts to -andesites with a probable island arc to transitional MORB affinity. The Mofjellet amphibolites have a more typical island arc composition.

As mentioned above, the amphibolites are spatially associated with calcareous mica schists and are commonly present at the contact between calcareous mica schists and garnet-mica schists in the Kongsfjell Group. The calcareous mica schists in especially the Kongsfjell Group are found at specific stratigraphic levels, close to the Anders Larsa Group and Lifjell unit and as mentioned with a sharp contact to the garnet-mica schists. If the calcareous schists are erosional products from the marble units, faulting could have caused erosion of the marbles and could also be pathways for the volcanics. Faulting and subsequent erosion could also lead to formation of an unconformity between the garnet-mica schists and the calcareous schists.

The solitary ultramafic bodies found at one stratigraphic level in the Målvatnet Unit, represent an enigma. However, they are all found close to the contact to the Kongsfjell Group, which probably has been a zone of weakness in the crust.

The marbles indicate an age of the sedimentary rocks ranging from about 590-600 Ma. This age fits very well with the concordant U-Pb zircon age 576 +/- 7 Ma of the Umbukta Gabbro Complex (Senior & Andriessen 1990) which intrudes into the sedimentary Kjerringfjell Group east of Mofjellet, and an Rb/Sr whole-rock age of 572 +/- 32 Ma from the Dalselv metagranite (Marker 1983), also intruding metasediments of the Rödingsfjäll Nappe Complex. These ages give a minimum age of the sedimentary rocks in the area. The Sr-isotope ages of the marbles are also comparable with marbles of the overlying Helgeland Nappe Complex (Trønnes & Sundvold 1995).

In striking contrast to this is the concordant U-Pb zircon age of 481 +/- 2 Ma of the microcline gneiss associated with the Bleikvassli deposit (Larsen et. al. in prep.). As mentioned above, this gneiss is interpreted to be a metamorphosed alkali-syenite, which is probably not related to the mineralization at Bleikvassli. The intrusion probably ascended along a zone of weakness (the same as the mineralizing fluids ?) in the crust and might be related to late stages of the same tectonic and metamorphic event which formed eclogites in the Seve Nappes (Sm-Nd age of 505 Ma, Mørk et al. 1991).

The intrusive character of the microcline gneiss, has very important consequences for the exploitation of the Bleikvassli orebody. Typical exploration drill holes at the mine have been stopped after intersecting the microcline gneiss in the footwall of the deposit. The intrusion may very well have crosscut the orebody and ore might be present structurally below it.

### Palaeotectonic environment

Even though there are indications of tectonic contacts between some of the units in the Okstindene area, the movements along the individual contacts have probably been very limited, since no signs of extensive deformation have been found. This means that the different units have been close to each other in space and time. Taking into account the association of arc to MORB amphibolites with high amounts of continent-derived sediments, the most probable environment for formation of the Okstindene lithologies is in a spreading regime behind an ensialic arc. The Mofjellet volcanics could then be part of the island arc and the quartz-feldspathic schists of the Målvatnet Unit could have been derived from mainly felsic arc volcanics or maybe felsic tuffs intermixed with clastic material formed at the arc side of the backarc basin. The Kongsfjell Group could represent the deeper part of the backarc basin, while the Lifjell, Anders Larsa and the equivalent Plurdal Group could represent a shelf sequence on the adjacent continent.

## IMPLICATIONS FOR PROSPECTING

The indications of correlations between the Anders Larsa, Lifjell and Plurdal Groups are important for future prospecting in the area. The Bleikvassli deposit is found very close to the contact between the Anders Larsa and the Kongsfjell Groups. This contact probably represent or is at least very close to the marginal fault zone of the sedimentary basin, which is a very favorable conduit for hydrothermal solutions and volcanics. Therefore, the contact between the Kongsfjell and Lifjell Unit all the way from Tustervatnet to Artfjellet and further up through Spjeltfjelldalen to Grasvatnet is very interesting and should be investigated in more detail. The presence of a strong geochemical anomaly at Grasvatnet, close to this contact is interesting and indeed, there are known mineralizations in the northern part of Spjeltfjelldalen at this contact. Adding to this is the extensive amphibolite horizon in the area.

The central part of the area consists of massive kyanite-garnet-mica schists. These schists probably represent the deeper part of the basin, which could contain large distal deposits. However, the lack of any signs of such deposits, and the general inaccessibility due to the alpine terrane and the presence of glaciers complicates prospecting of this area. Therefore future efforts should be concentrated to other areas.

The quartz-feldspathic schists at Stolpfjellet are very interesting because there are many similarities to the schists associated with the Bleikvassli deposit. Particularly interesting are the occurrences of kyanite schists and tourmalinites, which strongly indicate that hydrothermal activity has been present in the area.

**Further work**

1) Processing of geochemical data: More than 200 samples from different lithologies have been collected during the summer 1995 and are at present analyzed by XRF and ICP. Especially have many samples been collected from the Målvatn Unit. REE analyses will also be done on the intrusive and volcanic rocks in the area. These analyses will further constrain the geological setting of the different units in the area.

2) Carbonates show that the sedimentary rocks in the area are 590-600 million years old. At least in one case, amphibolites have intruded the sedimentary rocks and also orthogneisses show crosscutting relationships with the sediments. Furthermore, the microcline gneiss associated with the Bleikvassli deposit has a magmatic age of 481 million years. From these relationships it is apparent that dating is fundamental for unraveling the relationships between the different units and the geological evolution of the Rödingsfjäll Nappe Complex.

Key lithologies for dating by the U-Pb zircon method are the quartz-feldspathic schists in the Kongsfjell Group at Kongsfjell which seems to be magmatic, the felsic orthogneisses in the Kongsfjell Group and Lifjell Unit/Anders Larsa Group and the acid metavolcanics in the Mofjell

Group. Some samples of amphibolites have been sent for Sm-Nd analyses and may give at least some time constraints on the metamorphism in the area.

3) More mapping is necessary in the northern part of the area, north of Kjennsvassfjellet and Målvatnet. This is a key area for understanding the exact structure of the major recumbent $F_3$-fold in the area and the structural/stratigraphic relationships between the Kongsfjell Group and the Målvatnet Unit.

4) The contact relationships between the supposed Mofjell Group and Lifjell Unit in the culmination in the northern part of Spjeltfjelldalen must be investigated. It is a possibility that it is not the Mofjell Group, but rather the Ørtfjell Group, which is present in the core of this structure.

5) Detailed mapping is necessary to sort out the reason for the strong geochemical anomaly in the northern part of Spjeltfjelldalen, close to Grasvatnet.

6) The extent of the quartz-fuchsite schist at Kviturdfjellet should be mapped, in order to assess whether it is associated with a larger mineralization, and the possible source of the high chromium content.

7) The occurrence of the coticule horizon at Kongsfjell is promising and it could be connected to a larger sulfide mineralization. The zone should be mapped in detail (scale > 1:5000) and sampled in regular intervals to try to reveal any zonation in the Fe/Mn-ratio and content of base metals, which can help in finding out where the eventual mineralization is. Susceptibility measurements can be a great aid in mapping the coticule horizon and reveal Fe/Mn zonation.

## REFERENCES

Burke, W.H., Denison, R.E., Hetherington, E.A., Koepnick, R.B., Nelson, H.F. & Otto, J.B., 1982: Variation of seawater $^{87}Sr/^{86}Sr$ throughout Phanerozoic time. Geology v.10, p.516-519.

Cox, K.G., Bell, J.D. & Pankhurst, R.J., 1979: The interpretation of igneous rocks. George Allen & Unwin, London, 450 pp.

Faure, G., 1986: Principles of isotope geology (2nd ed.). J. Wiley & Sons, New York, 589 pp.

Kaufman, A.J., Jacobsen, S.B. & Knoll, A.H., 1993: The Vendian record of Sr and C isotopic variations in seawater: Implications for tectonics and palaeoclimate. Earth & Planet. Sci. Lett. 120, p.409-430.

Larsen, P.H., 1984: Simafjell med tilgrænsende områder. En strukturel og petrografisk analyse i de centrale nordnorske kaledonider. Unpubl. Thesis, University of Copenhagen, 1984.

Marker, M., 1983: Caledonian and pre-Caledonian geology of the Mofjell area, Nordland, Norway. Unpubl. Ph.D thesis, University of Copenhagen, 1983.

Miayshiro, A., 1974: Volcanic rock series in island arcs and active continental margins. Am. Jour. Sci. 274, p.321-355.

Mullen, E.D., 1983: $MnO/TiO_2/P_2O_5$: a minor element discriminant for basaltic rocks of oceanic environments and its implications for petrogenesis. Earth & Planet. Sci. Lett. 62, p.53-62.

Mørk, M.B.E., Kullerud, K. & Stabel, A., 1991: Sm-Nd dating of Seve eclogites, Norrbotten, Sweden - evidence of early Caledonian (505 Ma) high-pressure metamorphism. Contrib. Min. Petr. 99, p.344-351.

Olsen, S.B., 1984: Kongsfjellet - En strukturel og metamorf analyse i den sydligste del af Rödingsfjäll Nappen, Norge. Unpubl. Thesis, University of Copenhagen, 1984.

Pearce, J.A. & Cann, J.R., 1973: Tectonic setting of basic volcanic rocks determined using trace element analyses. Earth & Planet. Sci. Lett. 19, p.290-300.

Pearce, J.A. & Norry, M.J., 1979: Petrogenetic implications of Ti, Zr, Y and Nb variations in volcanic rocks. Contrib. Min. Petr. 69, 33-47.

Pearce, J.A., 1975: Basalt geochemistry used to investigate past tectonic environments on Cyprus. Tectonophysics 25, p.41-67.

Qvale, H. & Stigh, J., 1985: Ultramafic rocks in the Scandinavian Caledonides. In Gee, D.G. & Sturt, B.A. (eds.): The Caledonide Orogen - Scandinavia and related areas. J.Wiley & Sons Ltd. 1985.

Ramberg, I., 1967: Kongsfjell-områdets geologi, en petrografisk og strukturell undersøkelse i Helgeland, Nord-Norge. Norges Geologiske Undersøkelse 240, 152 pp.

Renard, A., 1878: Sur la structure et la composition minèralogique du coticule et sur ses rapports avec le phyllade oligistifère. Mèmoire curronnès de l' Academie Royale Belge 41, 42 pp.

Senior, A. & Andriessen, P.A.M., 1990: U/Pb and K/Ar determinations in the Upper and Uppermost Allochthons, central Scandinavian Caledonides. Geonytt 1/90, p.99 (abstract).

Shervais, J.W., 1982: Ti-V plots and the petrogenesis of modern and ophiolitic lavas. Earth & Planet. Sci. Lett. 59, p.101-118.

Skauli, H., 1992: On the formation of Zn-Pb deposits; a case study of the Bleikvassli deposit, northern Norway. Unpubl. Dr.Scient.Thesis, Univ. of Oslo, 1992.

Spry, P.G., 1990: Geochemistry and origin of coticules (spessartine-quartz rocks) associated with metamorphosed massive sulfide deposits. In Spry, P.G. & Bryndzia, T. (Eds.): Regional metamorphism of ore deposits, p.49-75. VSP, Utrecht.

Sun, S.S. & McDonough, W.F., 1989: Chemical and isotopic systematics of oceanic basalts: implications for mantle composition and processes. In Magmatism in the ocean basins. Geol.Soc. London, spec. Publ. 42, p.313-345.

Trønnes, R. & Sundvold, B., 1995: Isotopic composition, deposition ages and environ ments of Central Norwegian Caledonian marbles. Norges geol. Unders. Bull. 427, p.44-47.

Winchester, J.A. & Floyd, P.A., 1977: Geochemical discrimination of different magma series and their differentiation products using immobile elements. Chem. Geol. 20, p.325-343.

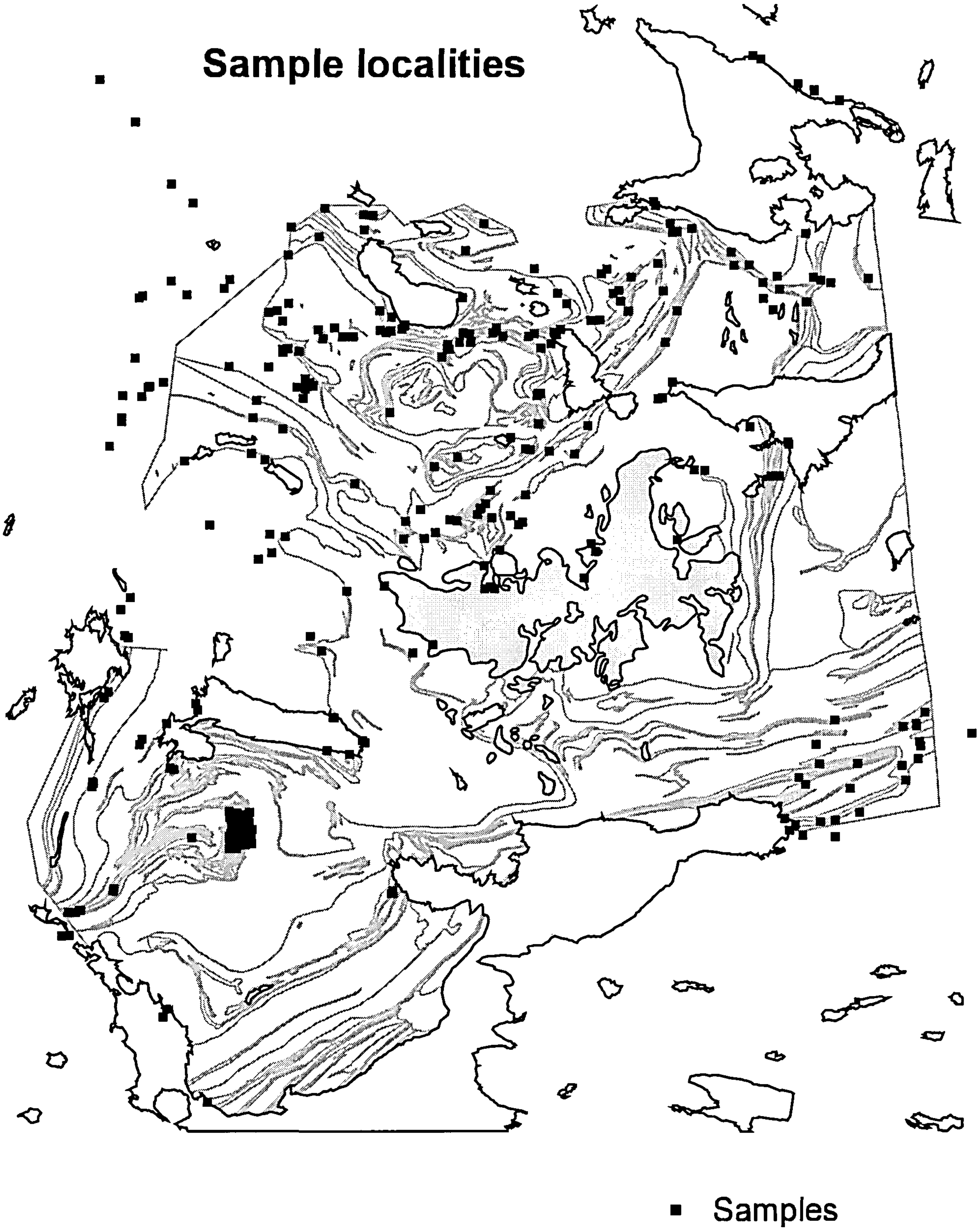
Sample localities
Samples

## XRF, major and minor elements

| Sample | Name | UTM-X | UTM-Y | SiO2 | Al2O3 | Fe2O3 | TiO2 | MgO | CaO | Na2O | K2O | MnO | P2O5 | Cl | F | Gl.tap | Sum |
|---|---|---|---|---|---|---|---|---|---|---|---|---|---|---|---|---|---|
| TB94019 | amphibolite | 452640 | 7321000 | 56.86 | 12.17 | 13.09 | 1.8 | 4.48 | 6.76 | 2.77 | 0.18 | 0.24 | 0.35 | <0.10 | 0.12 | 0.39 | 99.08 |
| TB94020 | amphibolite | 453200 | 7321280 | 71.66 | 13.73 | 5.69 | 0.86 | 1.88 | 0.91 | 0.4 | 2.89 | 0.05 | 0.11 | <0.10 | 0.16 | 1.44 | 99.62 |
| TB94024 | amphibolite | 460900 | 7322630 | 48.74 | 15.09 | 13.87 | 2.05 | 4.68 | 10.22 | 2.38 | 0.68 | 0.19 | 0.39 | <0.10 | 0.19 | 0.62 | 98.91 |
| TB94029 | amphibolite | 451410 | 7329080 | 56.64 | 17.99 | 9.12 | 1.08 | 3.88 | 2.83 | 1.1 | 4.2 | 0.15 | 0.21 | <0.10 | <0.10 | 1.44 | 98.65 |
| TB94031 | amphibolite | 462680 | 7321400 | 46.34 | 15.01 | 9.94 | 1.04 | 11.95 | 10.16 | 2.16 | 0.46 | 0.16 | 0.09 | <0.10 | 0.15 | 0.88 | 98.18 |
| TB94036 | amphibolite | 463930 | 7325610 | 50.84 | 15.96 | 9.74 | 1.09 | 5.76 | 11.47 | 2.12 | 0.52 | 0.15 | 0.23 | <0.10 | 0.14 | 0.64 | 98.51 |
| TB94039 | amphibolite | 459950 | 7324900 | 47.5 | 18.66 | 8.9 | 1.31 | 5.61 | 11.83 | 3.02 | 0.44 | 0.13 | 0.27 | <0.10 | 0.13 | 0.65 | 98.33 |
| TB94051 | amphibolite | 474160 | 7324530 | 50.44 | 15.11 | 13.93 | 1.5 | 4.52 | 8.73 | 2.89 | 0.82 | 0.17 | 0.17 | <0.10 | 0.19 | 0.6 | 98.87 |
| TB94057 | amphibolite | 458670 | 7321860 | 44.11 | 15.36 | 14.13 | 2.48 | 7.66 | 10.87 | 2.13 | 0.31 | 0.19 | 0.27 | <0.10 | 0.19 | 1.06 | 98.58 |
| TB94062 | amphibolite | 470020 | 7331440 | 52.96 | 13.84 | 12.49 | 1.18 | 5.94 | 7.24 | 2.03 | 2.11 | 0.19 | 0.16 | <0.10 | 0.17 | 0.54 | 98.68 |
| TB94066 | amphibolite | 470020 | 7334730 | 51.12 | 14.83 | 11.55 | 2.18 | 6.27 | 5.61 | 2.74 | 3.32 | 0.16 | 0.35 | <0.10 | 0.12 | 0.75 | 98.88 |
| TB94302 | amphibolite | 467680 | 7331820 | 48.89 | 13.11 | 12.45 | 0.78 | 7.95 | 11.54 | 2.52 | 0.34 | 0.25 | 0.14 | <0.10 | 0.18 | 1.02 | 98.98 |
| RBL94049a | amphibolite | 456320 | 7319680 | 50.99 | 14.7 | 14.05 | 1.42 | 4.9 | 8.65 | 3.75 | 0.54 | 0.21 | 0.14 | <0.10 | 0.11 | 0.24 | 99.59 |
| RBL94051 | amphibolite | 457000 | 7313390 | 51.09 | 14.29 | 14.27 | 1.59 | 5.97 | 7.59 | 3.96 | 0.27 | 0.21 | 0.13 | <0.10 | <0.10 | 0.42 | 99.79 |
| RBL94052 | amphibolite | 457000 | 7313390 | 52.8 | 14.98 | 13.22 | 1.24 | 5.02 | 6.99 | 4.63 | 0.27 | 0.25 | 0.13 | <0.10 | <0.10 | 0.24 | 99.77 |
| RBL94053 | amphibolite | 457090 | 7313310 | 51.78 | 14.72 | 12.45 | 1.4 | 6.42 | 7.99 | 3.82 | 0.28 | 0.2 | 0.13 | <0.10 | <0.10 | 0.34 | 99.54 |
| RBL94054 | amphibolite | 456470 | 7312820 | 52.79 | 15.51 | 10.47 | 0.71 | 6.77 | 6.86 | 5.47 | 0.29 | 0.13 | 0.09 | <0.10 | <0.10 | 0.59 | 99.69 |
| RBL94055 | amphibolite | 456470 | 7312820 | 52.57 | 15.21 | 11.69 | 1.1 | 5.94 | 6.24 | 5.67 | 0.28 | 0.11 | 0.15 | <0.10 | <0.10 | 0.48 | 99.45 |
| RBL94056 | amphibolite | 455520 | 7312980 | 47.7 | 14.96 | 15.25 | 1.91 | 6.87 | 8.03 | 3.62 | 0.26 | 0.21 | 0.16 | <0.10 | 0.11 | 0.55 | 99.52 |
| RBL94057 | amphibolite | 455520 | 7312980 | 50.71 | 14.69 | 15.12 | 1.55 | 5.41 | 6.96 | 4.12 | 0.29 | 0.23 | 0.17 | <0.10 | 0.12 | 0.34 | 99.58 |
| RBL94061 | amphibolite | 453110 | 7322060 | 53.68 | 13.3 | 13.12 | 1.12 | 5.92 | 6.24 | 3.5 | 1.6 | 0.18 | 0.15 | <0.10 | 0.14 | 0.93 | 99.75 |
| RBL94064 | amphibolite | 456560 | 7330320 | 57.59 | 16.89 | 8.58 | 0.57 | 2.85 | 7.56 | 3.35 | 0.86 | 0.19 | 0.11 | <0.10 | <0.10 | 0.71 | 99.25 |
| RBL94065 | amphibolite | 456360 | 7330320 | 57.28 | 16.65 | 9.48 | 0.58 | 4.07 | 6.57 | 3.35 | 1.04 | 0.11 | 0.15 | <0.10 | <0.10 | 0.48 | 99.78 |
| RBL94080 | amphibolite | 464280 | 7326700 | 48.81 | 16.91 | 8.47 | 1.08 | 8.73 | 11.63 | 2.37 | 0.48 | 0.14 | 0.23 | <0.10 | 0.11 | 0.58 | 99.41 |
| RBL94090 | amphibolite | 462750 | 7328630 | 54.55 | 19.43 | 7.3 | 0.74 | 4.21 | 8.05 | 3.03 | 1.71 | 0.09 | 0.21 | <0.10 | <0.10 | 0.58 | 99.9 |
| RBL94091 | amphibolite | 462750 | 7324630 | 51.31 | 15.77 | 9.24 | 0.68 | 7.36 | 11.24 | 1.62 | 0.81 | 0.13 | 0.16 | <0.10 | 0.13 | 0.7 | 99.02 |
| RBL94070 | calc silicate | 447720 | 7313230 | 52.99 | 10.13 | 5.84 | 0.66 | 8.25 | 15.97 | 2.55 | 0.47 | 0.12 | 0.19 | <0.10 | 0.16 | 1.19 | 98.36 |
| RBL94075 | calc silicate | 447640 | 7331920 | 51.15 | 12.27 | 8.42 | 1.3 | 6.03 | 14.39 | 3.14 | 0.84 | 0.13 | 0.34 | <0.10 | 0.18 | 0.86 | 98.87 |
| RBL94095 | calc silicate | 471430 | 7321460 | 52.49 | 13.87 | 15.14 | 3.32 | 5.9 | 5.93 | 0.38 | 0.75 | 0.29 | 0.55 | <0.10 | 0.13 | 0.93 | 99.55 |
| TB94014 | calc. schist | 462290 | 7319860 | 53.97 | 15.7 | 7.63 | 1.01 | 5.66 | 6.41 | 1.74 | 3.13 | 0.06 | 0.21 | <0.10 | 0.14 | 2.74 | 98.26 |
| TB94016 | calc. schist | 462040 | 7320740 | 53.55 | 16.16 | 7.72 | 0.87 | 5.5 | 5.8 | 1.61 | 3.62 | 0.07 | 0.2 | <0.10 | 0.12 | 3.5 | 98.6 |
| TB94022 | calc. schist | 458770 | 7322600 | 71.46 | 10.95 | 4.91 | 0.58 | 2.46 | 3.1 | 0.74 | 2.27 | 0.05 | 0.12 | <0.10 | <0.10 | 1.94 | 98.59 |
| TB94032 | calc. schist | 463750 | 7323720 | 54.06 | 15.87 | 7.55 | 0.92 | 5.25 | 6.48 | 1.99 | 3.19 | 0.08 | 0.24 | <0.10 | 0.11 | 3.16 | 98.79 |
| TB94038 | calc. schist | 460910 | 7325300 | 56.85 | 13.15 | 6.35 | 0.77 | 4.05 | 8.32 | 1.53 | 2.15 | 0.08 | 0.19 | <0.10 | 0.11 | 5.12 | 98.55 |
| TB94050 | calc. schist | 473970 | 7324520 | 63.28 | 11.56 | 5.06 | 0.65 | 4.03 | 9.8 | 2.45 | 0.87 | 0.09 | 0.22 | <0.10 | <0.10 | 1.08 | 99.08 |
| TB94058 | calc. schist | 459550 | 7321890 | 58.38 | 12.09 | 5.56 | 0.67 | 3.72 | 8.42 | 1.39 | 2.13 | 0.08 | 0.19 | <0.10 | 0.13 | 5.51 | 98.13 |
| TB94063 | calc. schist | 469200 | 7333410 | 56.96 | 14.09 | 6.88 | 0.8 | 4.94 | 9.43 | 1.53 | 2.84 | 0.09 | 0.22 | <0.10 | 0.15 | 0.92 | 98.7 |
| TB94064 | calc. schist | 469440 | 7332250 | 57.37 | 13.48 | 6.57 | 0.79 | 4.47 | 10.01 | 1.46 | 2.3 | 0.09 | 0.21 | <0.10 | 0.14 | 1.42 | 98.16 |
| TB94089 | calc. schist | 452570 | 7327660 | 59.59 | 16.21 | 6.74 | 0.94 | 3.88 | 2.54 | 2.85 | 3.53 | 0.04 | 0.18 | <0.10 | <0.10 | 2.22 | 98.72 |

*Major elements in %, minor in ppm*

| Sample | Name | UTM-X | UTM-Y | SiO2 | Al2O3 | Fe2O3 | TiO2 | MgO | CaO | Na2O | K2O | MnO | P2O5 | Cl | F | Gl.tap | Sum |
|---|---|---|---|---|---|---|---|---|---|---|---|---|---|---|---|---|---|
| TB94097 | calc. schist | 449570 | 7325130 | 63.4 | 13.23 | 6.72 | 0.85 | 4.04 | 3.58 | 2.22 | 2.96 | 0.11 | 0.2 | <0.10 | <0.10 | 1.34 | 98.64 |
| RBL94062 | calcareous mica s | 458110 | 7327170 | 57.78 | 15.05 | 9.14 | 1.18 | 4.35 | 5.88 | 2.05 | 2.17 | 0.16 | 0.18 | <0.10 | <0.10 | 1.06 | 98.99 |
| RBL94081 | calcareous schist | 463140 | 7326120 | 56.84 | 11.97 | 5.66 | 0.66 | 4.06 | 9.68 | 1.36 | 2.14 | 0.08 | 0.2 | <0.10 | <0.10 | 6.17 | 98.82 |
| TB94025 | calcite marble | 462080 | 7323350 | 14.59 | 1.85 | 0.39 | 0.087 | 2.09 | 43.81 | <0.10 | 0.687 | 0.029 | 0.22 | <0.10 | 0.68 | | 63.753 |
| TB94043 | calcite marble | 466340 | 7326610 | 4.17 | 0.46 | 0.46 | 0.032 | 1.29 | 50.61 | <0.10 | 0.142 | 0.019 | 0.23 | <0.10 | 0.77 | | 57.413 |
| TB94044 | calcite marble | 464740 | 7325550 | 1.81 | 0.28 | 0.13 | 0.017 | 0.71 | 53.22 | <0.10 | 0.082 | 0.012 | 0.28 | <0.10 | 0.78 | | 56.541 |
| TB94045 | calcite marble | 465780 | 7325410 | 20.15 | 5.32 | 1.83 | 0.264 | 1.57 | 37.97 | 0.2 | 1.128 | 0.059 | 0.15 | <0.10 | 0.58 | | 68.641 |
| TB94052 | calcite marble | 474290 | 7324530 | 2.41 | 0.34 | 0.16 | 0.033 | 0.29 | 53.84 | <0.10 | 0.091 | 0.008 | 0.26 | <0.10 | 0.76 | | 57.432 |
| TB94053 | calcite marble | 474320 | 7324520 | 1.57 | 0.18 | 0.09 | 0.026 | 0.36 | 53.7 | 0.12 | 0.025 | 0.008 | 0.19 | <0.10 | 0.78 | | 56.269 |
| TB94054 | calcite marble | 462360 | 7322760 | 1.03 | 0.05 | 0.14 | 0.008 | 0.76 | 54.71 | <0.10 | 0.021 | 0.016 | 0.16 | <0.10 | 0.73 | | 56.895 |
| TB94055 | calcite marble | 461870 | 7323130 | 3.91 | 0.21 | 0.26 | 0.011 | 0.27 | 52.58 | <0.10 | 0.068 | 0.023 | 0.27 | <0.10 | 0.77 | | 57.602 |
| TB94056 | calcite marble | 461870 | 7323130 | 1.93 | 0.27 | 0.14 | 0.019 | 0.49 | 53.36 | <0.10 | 0.081 | 0.019 | 0.28 | <0.10 | 0.8 | | 56.589 |
| TB94065 | calcite marble | 469830 | 7334700 | 2.82 | 0.46 | 0.23 | 0.03 | 1.73 | 51.79 | <0.10 | 0.164 | 0.004 | 0.24 | <0.10 | 0.7 | | 57.468 |
| TB94067 | calcite marble | 470630 | 7334860 | 0.71 | <0.01 | 0.07 | <0.004 | 2.8 | 52.04 | <0.10 | <0.003 | 0.004 | 0.24 | <0.10 | 0.8 | | 55.864 |
| TB94068 | calcite marble | 469730 | 7335060 | 0.22 | 0.05 | 0.11 | 0.006 | 1.5 | 53.4 | <0.10 | 0.011 | 0.003 | 0.33 | <0.10 | 0.76 | | 55.63 |
| TB94076 | calcite marble | 473500 | 7341920 | 1.13 | 0.13 | 0.09 | 0.01 | 0.46 | 54.63 | <0.10 | 0.042 | 0.003 | 0.19 | <0.10 | 0.8 | | 56.685 |
| TB94077 | calcite marble | 475050 | 7340900 | 0.07 | 0.04 | 0.09 | 0.005 | 1.34 | 53.83 | <0.10 | <0.003 | <0.002 | 0.3 | <0.10 | 0.77 | | 55.675 |
| TB94084 | calcite marble | 485140 | 7362660 | 4.14 | 0.87 | 0.42 | 0.057 | 1.37 | 50.61 | <0.10 | 0.185 | 0.006 | 0.22 | <0.10 | 0.72 | | 57.878 |
| TB94085 | calcite marble | 485110 | 7362510 | 0.34 | 0.05 | 0.12 | 0.007 | 0.49 | 54.92 | <0.10 | 0.004 | 0.003 | 0.14 | <0.10 | 0.82 | | 56.074 |
| TB94088 | calcite marble | 471110 | 7360730 | 2.58 | 0.31 | 0.19 | 0.018 | 0.62 | 52.94 | <0.10 | 0.076 | 0.012 | 0.33 | <0.10 | 0.78 | | 57.076 |
| TB94096 | calcite marble | 446920 | 7318900 | 3.09 | 0.57 | 0.31 | 0.048 | 0.83 | 51.72 | 0.18 | 0.149 | 0.006 | 0.17 | <0.10 | 0.78 | | 57.073 |
| TB94098 | calcite marble | 445790 | 7311600 | 1.88 | 0.41 | 0.16 | 0.023 | 0.44 | 53.17 | <0.10 | 0.134 | 0.005 | 0.28 | <0.10 | 0.76 | | 56.502 |
| TB94075 | calcite-dolomite m | 473150 | 7342070 | 2.45 | 0.1 | 0.19 | 0.006 | 0.11 | 53.66 | <0.10 | 0.022 | 0.004 | 0.28 | <0.10 | 0.73 | | 56.822 |
| TB94095 | calcite-dolomite m | 447100 | 7317810 | 3 | 0.55 | 0.13 | 0.032 | 1.02 | 52.61 | 0.15 | 0.163 | 0.008 | 0.2 | <0.10 | 0.79 | | 57.863 |
| TB94099 | calcite-dolomite m | 445750 | 7311670 | 1.14 | 0.16 | 0.08 | 0.018 | 7.62 | 47.17 | <0.10 | 0.054 | 0.004 | 0.23 | <0.10 | 0.69 | | 56.476 |
| TB94033 | chert | 463630 | 7322570 | 74.22 | 13.1 | 2.84 | 0.25 | 0.82 | 1.84 | 3.3 | 1.82 | 0.05 | 0.02 | <0.10 | <0.10 | 0.67 | 98.95 |
| TB94047 | dolomite marble | 474720 | 7325840 | 1.68 | 0.02 | 0.05 | <0.004 | 22.21 | 30.17 | <0.10 | <0.003 | <0.002 | 0.15 | <0.10 | 0.47 | | 54.28 |
| TB94048 | dolomite marble | 474660 | 7325950 | 0.5 | 0.09 | 0.13 | <0.004 | 22.15 | 30.7 | <0.10 | 0.014 | <0.002 | 0.26 | <0.10 | 0.48 | | 53.844 |
| TB94069 | dolomite marble | 469110 | 7335820 | 0.36 | 0.01 | 0.04 | <0.004 | 22.06 | 31.08 | <0.10 | <0.003 | <0.002 | 0.18 | <0.10 | 0.43 | | 53.73 |
| TB94070 | dolomite marble | 469030 | 7335990 | 0.25 | 0.09 | 0.09 | 0.018 | 21.9 | 30.94 | <0.10 | <0.003 | <0.002 | 0.2 | <0.10 | 0.46 | | 53.488 |
| TB94078 | dolomite marble | 475730 | 7340630 | 7.17 | <0.01 | 0.08 | <0.004 | 21.26 | 29.71 | <0.10 | <0.003 | <0.002 | 0.12 | <0.10 | 0.47 | | 58.34 |
| TB94079 | dolomite marble | 476780 | 7340260 | 2.25 | 0.04 | 0.06 | 0.031 | 21.39 | 29.56 | <0.10 | <0.003 | <0.002 | 0.13 | <0.10 | 0.51 | | 53.461 |
| TB94080 | dolomite marble | 477450 | 7366340 | 0.35 | 0.04 | 0.05 | 0.005 | 22.4 | 30.8 | <0.10 | <0.003 | 0.004 | 0.16 | <0.10 | 0.47 | | 53.809 |
| TB94081 | dolomite marble | 477490 | 7366090 | 8.57 | <0.01 | 0.11 | <0.004 | 20.3 | 28.39 | <0.10 | <0.003 | 0.017 | 0.12 | <0.10 | 0.44 | | 57.507 |
| TB94082 | dolomite marble | 480670 | 7362770 | 0.69 | <0.01 | 0.22 | <0.004 | 21.67 | 30.25 | <0.10 | <0.003 | 0.009 | 0.13 | <0.10 | 0.46 | | 52.969 |
| TB94083 | dolomite marble | 482210 | 7361250 | 1.02 | 0.24 | 0.09 | 0.013 | 22.09 | 30.73 | <0.10 | 0.014 | <0.002 | 0.12 | <0.10 | 0.48 | | 54.317 |
| TB94087 | dolomite marble | 471010 | 7360710 | 1.23 | 0.06 | 0.35 | <0.004 | 20.97 | 30.23 | <0.10 | <0.003 | 0.128 | 0.31 | <0.10 | 0.5 | | 53.278 |
| TB94092 | dolomite marble | 446220 | 7315190 | 0.29 | 0.1 | 0.1 | 0.008 | 22.96 | 30.44 | <0.10 | 0.056 | <0.002 | 0.13 | <0.10 | 0.46 | | 54.084 |
| TB94093 | dolomite marble | 446410 | 7315440 | 0.22 | 0.04 | 0.04 | <0.004 | 22.23 | 30.59 | <0.10 | 0.005 | <0.002 | 0.14 | <0.10 | 0.47 | | 53.265 |

| Sample | Name | UTM-X | UTM-Y | SiO2 | Al2O3 | Fe2O3 | TiO2 | MgO | CaO | Na2O | K2O | MnO | P2O5 | Cl | F | Gl.tap | Sum |
|---|---|---|---|---|---|---|---|---|---|---|---|---|---|---|---|---|---|
| TB94094 | dolomite marble | 447250 | 7317720 | 0.14 | 0.06 | 0.05 | <0.004 | 21.91 | 30.99 | <0.10 | <0.003 | <0.002 | 0.18 | <0.10 | 0.46 | | 53.33 |
| TB94320 | dolomite marble | 445730 | 7311460 | 0.25 | 0.01 | 0.13 | <0.004 | 22.85 | 30.79 | <0.10 | <0.003 | <0.002 | 0.13 | <0.10 | 0.44 | | 54.16 |
| RBL94071 | dolomite marble | 447820 | 7313450 | 53.86 | 5.92 | 2.29 | 0.29 | 13.06 | 19.45 | 1.62 | 0.09 | 0.02 | 0.47 | <0.10 | 0.23 | 0.53 | 97.62 |
| RBL94063 | garnet gneiss | 456090 | 7330330 | 54.75 | 22.56 | 6.79 | 0.65 | 1.83 | 6.02 | 3.54 | 1.71 | 0.02 | 0.21 | <0.10 | <0.10 | 0.68 | 98.76 |
| RBL94073 | gr-mica quartzite | 450060 | 7314940 | 86.25 | 5.57 | 2.22 | 0.27 | 0.83 | 0.29 | 0.83 | 0.88 | 0.02 | 0.08 | <0.10 | <0.10 | 0.74 | 98 |
| RBL94074 | gr-mica quartzite | 450140 | 7314680 | 81.33 | 8.49 | 4.24 | 0.4 | 1.21 | 0.65 | 0.63 | 1.12 | 0.06 | 0.11 | <0.10 | <0.10 | 0.81 | 99.05 |
| RBL94045 | gr-mica schist | 454810 | 7317790 | 72.12 | 12.18 | 4.9 | 0.79 | 1.38 | 0.89 | 0.51 | 2.74 | 0.02 | 0.12 | <0.10 | <0.10 | 2.72 | 98.38 |
| RBL94046 | gr-mica schist | 459080 | 7317080 | 54.1 | 21.41 | 9.84 | 1.03 | 3.31 | 0.91 | 1.27 | 4.81 | 0.24 | 0.14 | <0.10 | <0.10 | 1.85 | 98.9 |
| RBL94047 | gr-mica schist | 459920 | 7317440 | 52.45 | 18.19 | 8.86 | 1.12 | 4.67 | 1.46 | 0.44 | 3.96 | 0.19 | 0.18 | <0.10 | <0.10 | 7.79 | 99.3 |
| RBL94048 | gr-mica schist | 455300 | 7317175 | 54.19 | 18.49 | 9.15 | 1.15 | 4.97 | 2.48 | 1.5 | 4.1 | 0.08 | 0.25 | <0.10 | <0.10 | 1.73 | 98.09 |
| RBL94094 | gr.-mica schist | 471360 | 7322900 | 59.97 | 18.08 | 8.67 | 0.85 | 3.64 | 1.97 | 1 | 3.52 | 0.27 | 0.16 | <0.10 | <0.10 | 1.41 | 99.54 |
| RBL94098 | gr.-mica schist | 449550 | 7.7E+07 | 64.49 | 16.54 | 8.16 | 0.96 | 2.51 | 1.33 | 0.37 | 3.17 | 0.14 | 0.17 | <0.10 | <0.10 | 1.82 | 99.65 |
| RBL94099 | gr.-mica schist | 449540 | 7311250 | 58.88 | 16.12 | 8 | 0.99 | 3.8 | 3.64 | 0.27 | 3.76 | 0.23 | 0.18 | <0.10 | <0.10 | 2.36 | 98.22 |
| RBL94100 | gr.-mica schist | 449510 | 7311300 | 75.29 | 13.41 | 1.03 | 0.11 | 1.36 | 0.66 | 0.26 | 4.04 | 0.01 | 0.02 | <0.10 | <0.10 | 2.36 | 98.54 |
| RBL94101 | gr.-mica schist | 449510 | 7311390 | 58.5 | 16.68 | 8.38 | 0.96 | 4.6 | 3.76 | 0.5 | 3.81 | 0.16 | 0.18 | <0.10 | <0.10 | 1.29 | 98.83 |
| RBL94102 | gr.-mica schist | 449510 | 7311460 | 58.09 | 15.98 | 8.59 | 0.91 | 4.8 | 3.79 | 0.39 | 3.34 | 0.19 | 0.19 | <0.10 | <0.10 | 2.85 | 99.13 |
| RBL94103 | gr.-mica schist | 449420 | 7311560 | 54.05 | 17.6 | 10.82 | 1.07 | 6.05 | 7.83 | 0.59 | 2.99 | 0.24 | 0.22 | <0.10 | 0.13 | -2.38 | 99.08 |
| RBL94104 | gr.-mica schist | 449280 | 7311620 | 60.26 | 15.64 | 8.36 | 0.9 | 4.8 | 2.99 | 0.55 | 3.92 | 0.18 | 0.19 | <0.10 | <0.10 | 1.34 | 99.12 |
| TB94015 | graphite schist | 462060 | 7319780 | 84.61 | 6.39 | 0.7 | 0.31 | 0.73 | 0.15 | 0.42 | 1.63 | <0.01 | 0.02 | <0.10 | <0.10 | 3.1 | 98.06 |
| RBL94068 | graphite schist | 455760 | 7330690 | 46.59 | 20.5 | 8.7 | 0.62 | 1.98 | 10.13 | 3.02 | 1.33 | 0.08 | 0.16 | <0.10 | 0.12 | 4.28 | 97.39 |
| TB94006 | graphitic schist | 449900 | 7309300 | 49.74 | 17.53 | 10.6 | 0.93 | 8.03 | 1.9 | 1.59 | 6.02 | 0.15 | 0.14 | <0.10 | 0.19 | 1.88 | 98.5 |
| TB94007 | graphitic schist | 449900 | 7309300 | 66.07 | 10.82 | 2.43 | 0.82 | 2.84 | 2.94 | 1.64 | 2.47 | 0.05 | 0.35 | <0.10 | <0.10 | 7.94 | 98.36 |
| RBL94072 | graphitic schist | 448850 | 7314110 | 65.8 | 12.38 | 7.38 | 0.65 | 2.4 | 2.72 | 0.72 | 3.09 | 0.03 | 0.09 | <0.10 | 0.21 | 3.33 | 98.59 |
| RBL94087 | graphitic schist | 464350 | 7327970 | 46.46 | 21.02 | 8.54 | 1.3 | 4.03 | 6.41 | 1.8 | 4.68 | 0.04 | 0.45 | <0.10 | 0.21 | 3.47 | 98.21 |
| TB94012a | gt-mica schist | 457870 | 7319900 | 59.98 | 18.21 | 7.71 | 0.94 | 2.89 | 0.47 | 0.83 | 4.17 | 0.07 | 0.16 | <0.10 | <0.10 | 3.52 | 98.93 |
| TB94012b | gt-mica schist | 457870 | 7319900 | 59.87 | 18.25 | 9.21 | 0.94 | 3.14 | 0.5 | 0.64 | 4.62 | 0.1 | 0.18 | <0.10 | <0.10 | 1.92 | 99.37 |
| TB94013 | gt-mica schist | 462470 | 7319780 | 62.18 | 17.42 | 8.04 | 0.9 | 2.98 | 0.44 | 0.54 | 4.07 | 0.03 | 0.14 | <0.10 | <0.10 | 2.09 | 98.83 |
| TB94017 | gt-mica schist | 462040 | 7320740 | 65.03 | 15.36 | 6.21 | 0.84 | 2.82 | 0.54 | 0.61 | 4.25 | 0.02 | 0.13 | <0.10 | <0.10 | 3.28 | 99.08 |
| TB94021 | gt-mica schist | 453750 | 7321940 | 51.58 | 13.16 | 16.9 | 1.7 | 4.75 | 6.43 | 4.5 | 0.47 | 0.26 | 0.2 | <0.10 | <0.10 | 0.23 | 100.17 |
| TB94026 | gt-mica schist | 459370 | 7323100 | 69.11 | 13.84 | 6.59 | 0.8 | 2.54 | 0.89 | 0.45 | 2.93 | 0.04 | 0.15 | <0.10 | <0.10 | 1.22 | 98.57 |
| TB94040 | gt-mica schist | 466200 | 7320220 | 63.46 | 16.38 | 8.6 | 0.91 | 3.21 | 1.29 | 0.43 | 3.37 | 0.16 | 0.15 | <0.10 | <0.10 | 1.19 | 99.15 |
| TB94041 | gt-mica schist | 466660 | 7321340 | 56.47 | 18.43 | 8.68 | 0.94 | 3.6 | 2.41 | 0.46 | 5.54 | 0.11 | 0.23 | <0.10 | 0.21 | 1.97 | 98.85 |
| TB94049 | gt-mica schist | 471210 | 7324760 | 60.53 | 16.13 | 7.71 | 0.88 | 4.59 | 3.49 | 0.37 | 3.92 | 0.16 | 0.22 | <0.10 | <0.10 | 1.54 | 99.54 |
| TB94090 | gt-mica schist | 453660 | 7326460 | 61.22 | 14.52 | 7.47 | 0.91 | 3.84 | 4.53 | 1.63 | 2.92 | 0.23 | 0.21 | <0.10 | <0.10 | 1.34 | 98.82 |
| RBL94086 | kyanite schist | 462840 | 7329040 | 80.48 | 10.28 | 1.15 | 0.09 | 1.64 | 1.03 | 2.03 | 0.86 | 0.01 | 0.01 | <0.10 | <0.10 | 0.84 | 98.43 |
| RBL94096 | kyanite schist | 472190 | 7321300 | 75.54 | 13.03 | 2.33 | 0.11 | 3.12 | 0.67 | 1.12 | 1.98 | 0.03 | 0.01 | <0.10 | <0.10 | 0.94 | 98.9 |
| RBL94105 | kyanite schist | 449280 | 7311720 | 64.21 | 19.31 | 2.23 | 0.13 | 3.89 | 0.45 | 1.75 | 5.12 | 0.02 | 0.04 | <0.10 | 0.16 | 2.34 | 99.48 |
| RBL94106 | kyanite schist | 449160 | 7311840 | 73.18 | 14.04 | 1.6 | 0.1 | 2.75 | 0.9 | 3.34 | 2.35 | 0.02 | 0.04 | <0.10 | <0.10 | 1.19 | 99.5 |
| RBL94078 | mantle gr achist | 451180 | 7332320 | 64.91 | 14.34 | 7.04 | 0.84 | 3.55 | 2.97 | 1.79 | 2.75 | 0.12 | 0.14 | <0.10 | <0.10 | 0.72 | 99.16 |

| Sample | Name | UTM-X | UTM-Y | SiO2 | Al2O3 | Fe2O3 | TiO2 | MgO | CaO | Na2O | K2O | MnO | P2O5 | Cl | F | Gl.tap | Sum |
|---|---|---|---|---|---|---|---|---|---|---|---|---|---|---|---|---|---|
| RBL94069 | mantle gr schist | 455760 | 7330690 | 54.24 | 19.57 | 8.08 | 0.61 | 2.54 | 8.3 | 3.83 | 0.45 | 0.13 | 0.18 | <0.10 | <0.10 | 0.26 | 98.19 |
| RBL94088 | mantle gr. schist | 463800 | 7328000 | 55.41 | 19.82 | 7.11 | 0.88 | 3.4 | 5.75 | 2.29 | 2.34 | 0.11 | 0.13 | <0.10 | <0.10 | 0.64 | 97.89 |
| RBL94049b | marble w. graphit | 455760 | 7314380 | 0.11 | 0.07 | 0.1 | <0.01 | 22.99 | 30.71 | <0.10 | 0.02 | <0.01 | 0.04 | <0.10 | 0.42 | 46.4 | 100.32 |
| RBL94050 | marble w. graphit | 455820 | 7314360 | 2.77 | 0.58 | 0.22 | 0.04 | 0.35 | 52.96 | <0.10 | 0.14 | <0.01 | 0.12 | <0.10 | 0.75 | 42.12 | 99.24 |
| RBL94003 | massive ore | 430240 | 7383200 | 18.08 | 1.64 | 29.9 | 0.03 | <0.01 | 0.05 | 0.55 | 0.54 | 0.01 | <0.01 | <0.10 | 0.59 | 34.03 | 84.48 |
| TB94042 | metagabbro | 466480 | 7321670 | 47.52 | 15.12 | 14.65 | 3.01 | 5.02 | 6.43 | 3.46 | 1.63 | 0.3 | 0.39 | <0.10 | 0.19 | 1.19 | 98.72 |
| TB94028 | mica schist | 452910 | 7325170 | 57.79 | 17.01 | 7.23 | 0.91 | 2.18 | 4.36 | 4.31 | 3.13 | 0.12 | 0.23 | <0.10 | <0.10 | 1.5 | 98.77 |
| TB94071 | mica schist | 466430 | 7331000 | 71.44 | 11.47 | 3.17 | 0.79 | 1.87 | 2.96 | 0.9 | 3.54 | 0.03 | 0.13 | <0.10 | <0.10 | 2.08 | 98.39 |
| TB94072 | mica schist | 466800 | 7331020 | 71.69 | 11.19 | 5.86 | 0.88 | 2.28 | 1.38 | 2.14 | 2.66 | 0.05 | 0.07 | <0.10 | <0.10 | 0.78 | 98.96 |
| RBL94077 | micrcline gneiss | 448980 | 7332630 | 67.12 | 17.49 | 2.39 | 0.43 | 1.22 | 3.68 | 5.42 | 1.39 | 0.02 | 0.12 | <0.10 | <0.10 | 0.54 | 99.82 |
| RBL94107A | microcline gneis | 430240 | 7383200 | 68 | 8.39 | 1.21 | 0.04 | 0.05 | 0.14 | 0.97 | 5 | <0.01 | 0.02 | <0.10 | <0.10 | 1.12 | 84.95 |
| RBL94108 | microcline gneis | 430240 | 7383200 | 65.47 | 17.13 | 2.86 | 0.47 | 0.32 | 1.18 | 4.08 | 7.34 | 0.02 | 0.18 | <0.10 | <0.10 | 0.5 | 99.55 |
| RBL94005 | microcline gneiss | 430240 | 7383200 | 67.64 | 17.3 | 1.73 | 0.22 | 1.73 | 0.59 | 2.46 | 5.25 | <0.01 | 0.05 | <0.10 | <0.10 | 1.82 | 98.79 |
| RBL94006 | microcline gneiss | 430240 | 7383200 | 72.11 | 14.47 | 1.59 | 0.19 | 2.61 | 0.47 | 1.31 | 4.82 | <0.01 | 0.04 | <0.10 | <0.10 | 1.7 | 99.32 |
| RBL94007 | microcline gneiss | 430240 | 7383200 | 68.22 | 17.19 | 2.75 | 0.42 | 0.45 | 1.02 | 6.15 | 3.11 | 0.02 | 0.14 | <0.10 | <0.10 | 0.57 | 100.03 |
| RBL94008 | microcline gneiss | 430240 | 7383200 | 62.63 | 18.1 | 4.2 | 0.43 | 0.9 | 0.76 | 2.76 | 8.61 | 0.02 | 0.17 | <0.10 | <0.10 | 0.91 | 99.48 |
| RBL94009 | microcline gneiss | 430240 | 7383200 | 61.25 | 18.83 | 4.77 | 0.44 | 2.15 | 1.66 | 2 | 6.46 | 0.02 | 0.15 | <0.10 | <0.10 | 1.86 | 99.58 |
| RBL94010 | microcline gneiss | 430240 | 7383200 | 58.82 | 18.7 | 4.7 | 0.43 | 2.54 | 1.3 | 2.49 | 8.89 | 0.02 | 0.16 | <0.10 | 0.1 | 0.96 | 99.02 |
| RBL94011 | microcline gneiss | 430240 | 7383200 | 60.52 | 18.66 | 4.13 | 0.43 | 1.73 | 0.91 | 1.94 | 8.69 | 0.01 | 0.16 | <0.10 | <0.10 | 1.38 | 98.56 |
| RBL94012 | microcline gneiss | 430240 | 7383200 | 60.66 | 18.71 | 3.9 | 0.44 | 1.25 | 0.84 | 2.21 | 9.38 | 0.02 | 0.16 | <0.10 | <0.10 | 1.15 | 98.72 |
| RBL94013 | microcline gneiss | 430240 | 7383200 | 65.2 | 16.85 | 2.99 | 0.35 | 0.3 | 0.79 | 3.48 | 8.45 | 0.02 | 0.16 | <0.10 | <0.10 | 0.49 | 99.08 |
| RBL94014 | microcline gneiss | 430240 | 7383200 | 64.91 | 17.72 | 2.65 | 0.42 | 0.33 | 0.85 | 3.57 | 9.23 | 0.02 | 0.17 | <0.10 | <0.10 | 0.32 | 100.19 |
| RBL94015 | microcline gneiss | 430240 | 7383200 | 66.23 | 16.54 | 2.43 | 0.4 | 0.3 | 0.96 | 3.55 | 8.11 | 0.02 | 0.16 | <0.10 | <0.10 | 0.31 | 98.98 |
| RBL94016 | microcline gneiss | 430240 | 7383200 | 66.81 | 16.54 | 2.08 | 0.4 | 0.28 | 1.09 | 3.48 | 8.11 | 0.02 | 0.18 | <0.10 | <0.10 | 0.3 | 99.29 |
| RBL94017 | microcline gneiss | 430240 | 7383200 | 63.9 | 17.43 | 2.25 | 0.45 | 0.28 | 0.97 | 3.03 | 9.62 | 0.02 | 0.18 | <0.10 | <0.10 | 0.31 | 98.45 |
| RBL94018 | microcline gneiss | 430240 | 7383200 | 63.27 | 17.63 | 2.39 | 0.38 | 0.28 | 1 | 3.06 | 9.72 | 0.02 | 0.16 | <0.10 | <0.10 | 0.29 | 98.19 |
| RBL94019 | microcline gneiss | 430240 | 7383200 | 61.63 | 18.26 | 2.92 | 0.45 | 0.43 | 1.29 | 3.2 | 9.81 | 0.02 | 0.19 | <0.10 | <0.10 | 0.4 | 98.61 |
| RBL94020 | microcline gneiss | 430240 | 7383200 | 63.17 | 17.89 | 2.27 | 0.38 | 0.25 | 1.09 | 3.37 | 9.43 | 0.02 | 0.15 | <0.10 | <0.10 | 0.4 | 98.43 |
| RBL94021 | microcline gneiss | 430240 | 7383200 | 63.66 | 17.69 | 2.6 | 0.38 | 0.26 | 1.17 | 3.79 | 8.74 | 0.02 | 0.16 | <0.10 | <0.10 | 0.34 | 98.8 |
| RBL94022 | microcline gneiss | 430240 | 7383200 | 62.88 | 17.64 | 2.63 | 0.38 | 0.28 | 1.24 | 3.47 | 8.99 | 0.02 | 0.16 | <0.10 | <0.10 | 0.68 | 98.37 |
| RBL94023 | microcline gneiss | 430240 | 7383200 | 66.87 | 15.98 | 2.04 | 0.35 | 0.24 | 1.29 | 3.51 | 7.51 | 0.01 | 0.13 | <0.10 | <0.10 | 0.7 | 98.62 |
| RBL94024 | microcline gneiss | 430240 | 7383200 | 66.37 | 16.37 | 2.02 | 0.36 | 0.25 | 1.3 | 3.51 | 7.83 | 0.02 | 0.13 | <0.10 | <0.10 | 0.69 | 98.85 |
| RBL94025 | microcline gneiss | 430240 | 7383200 | 67.2 | 16.3 | 2.02 | 0.32 | 0.23 | 1.2 | 3.71 | 7.28 | 0.01 | 0.11 | <0.10 | <0.10 | 0.69 | 99.07 |
| RBL94026 | microcline gneiss | 430240 | 7383200 | 66.44 | 16.43 | 2.05 | 0.33 | 0.26 | 1.16 | 3.49 | 7.85 | 0.02 | 0.12 | <0.10 | <0.10 | 0.75 | 98.89 |
| RBL94027 | microcline gneiss | 430240 | 7383200 | 67.04 | 16.82 | 1.97 | 0.34 | 0.25 | 0.54 | 3.14 | 8.7 | <0.01 | 0.15 | <0.10 | <0.10 | 0.51 | 99.45 |
| RBL94028 | microcline gneiss | 430240 | 7383200 | 66.23 | 16.61 | 2.38 | 0.4 | 0.33 | 0.8 | 3.67 | 7.73 | 0.02 | 0.15 | <0.10 | <0.10 | 0.54 | 98.86 |
| RBL94029 | microcline gneiss | 430380 | 7382935 | 65.34 | 16.6 | 3.28 | 0.39 | 0.61 | 0.61 | 3.19 | 7.96 | 0.02 | 0.16 | <0.10 | <0.10 | 0.51 | 98.67 |
| RBL94030 | microcline gneiss | 430270 | 7383175 | 66.06 | 16.86 | 2.29 | 0.37 | 0.31 | 0.67 | 3.34 | 8.14 | 0.02 | 0.13 | <0.10 | <0.10 | 0.6 | 98.79 |
| RBL94031 | microcline gneiss | 430295 | 7383165 | 61.48 | 19.07 | 3.43 | 0.45 | 1.96 | 1.85 | 3.96 | 5.51 | 0.03 | 0.17 | <0.10 | <0.10 | 1.11 | 99.02 |

| Sample | Name | UTM-X | UTM-Y | SiO2 | Al2O3 | Fe2O3 | TiO2 | MgO | CaO | Na2O | K2O | MnO | P2O5 | Cl | F | Gl.tap | Sum |
|---|---|---|---|---|---|---|---|---|---|---|---|---|---|---|---|---|---|
| RBL94032 | microcline gneiss | 430300 | 7383140 | 67.9 | 16.04 | 1.69 | 0.34 | 0.22 | 0.51 | 2.96 | 8.54 | 0.01 | 0.11 | <0.10 | <0.10 | 0.37 | 98.68 |
| RBL94033 | microcline gneiss | 430310 | 7383130 | 77.05 | 12.06 | 0.69 | 0.16 | 0.13 | 0.62 | 3.6 | 4.16 | <0.01 | 0.05 | <0.10 | <0.10 | 0.28 | 98.81 |
| RBL94034 | microcline gneiss | 430300 | 7383110 | 63.69 | 17.27 | 3.5 | 0.4 | 0.39 | 0.86 | 3.13 | 9.1 | 0.02 | 0.17 | <0.10 | <0.10 | 0.33 | 98.85 |
| RBL94035 | microcline gneiss | 430305 | 7383090 | 64.22 | 17.76 | 2.28 | 0.34 | 0.27 | 0.86 | 3.78 | 8.7 | 0.02 | 0.12 | <0.10 | <0.10 | 0.36 | 98.71 |
| RBL94036 | microcline gneiss | 430305 | 7383060 | 66.06 | 16.69 | 2.37 | 0.36 | 0.27 | 0.49 | 3.33 | 8.49 | 0.01 | 0.13 | <0.10 | <0.10 | 0.43 | 98.62 |
| RBL94037 | microcline gneiss | 430300 | 7383050 | 63.86 | 18.18 | 1.3 | 0.39 | 0.74 | 1.27 | 2.47 | 9.03 | 0.03 | 0.16 | <0.10 | <0.10 | 1.15 | 98.58 |
| RBL94038 | microcline gneiss | 430355 | 7382970 | 78.19 | 11.2 | 1.92 | 0.08 | 0.24 | 0.22 | 2.28 | 3.06 | <0.01 | 0.02 | <0.10 | <0.10 | 1.32 | 98.54 |
| RBL94039 | microcline gneiss | 430380 | 7382935 | 62.94 | 18.4 | 3.02 | 0.34 | 1.52 | 0.94 | 1.76 | 8.62 | 0.01 | 0.11 | <0.10 | <0.10 | 1.39 | 99.06 |
| RBL94058 | microcline gneiss | 430305 | 7383060 | 65.05 | 17.13 | 2.25 | 0.38 | 0.3 | 1.1 | 3.66 | 8.35 | 0.02 | 0.18 | <0.10 | <0.10 | 0.69 | 99.1 |
| RBL94059 | microcline gneiss | 430305 | 7383060 | 65.54 | 17.27 | 1.35 | 0.29 | 0.23 | 0.66 | 2.96 | 9.78 | <0.01 | 0.14 | <0.10 | <0.10 | 0.48 | 98.71 |
| RBL94060 | microcline gneiss | 430305 | 7383060 | 64.35 | 17.28 | 2.16 | 0.42 | 0.33 | 1.32 | 3.36 | 8.46 | 0.02 | 0.19 | <0.10 | <0.10 | 0.85 | 98.73 |
| RBL94001 | muscovite schist | 430240 | 7383200 | 70.53 | 15.81 | 2.24 | 0.21 | 1.4 | 0.25 | 2.48 | 4.23 | <0.01 | 0.04 | <0.10 | <0.10 | 2.12 | 99.31 |
| RBL94002 | muscovite schist | 430240 | 7383200 | 72.67 | 14.4 | 1.62 | 0.18 | 2.18 | 0.29 | 2.4 | 3.95 | <0.01 | 0.03 | <0.10 | <0.10 | 1.63 | 99.35 |
| RBL94004 | muscovite schist | 430240 | 7383200 | 68.5 | 13.77 | 3.95 | 0.16 | 0.84 | 1.1 | 2.23 | 3.29 | <0.01 | 0.03 | <0.10 | <0.10 | 2.93 | 96.82 |
| RBL94259 | ortho gneiss | | | 77.37 | 12.28 | 0.91 | 0.07 | 0.21 | 0.21 | 5.97 | 1.5 | 0.02 | 0.01 | <0.10 | <0.10 | 0.42 | 98.99 |
| RBL94260 | ortho gneiss | | | 71.99 | 15.09 | 2.34 | 0.11 | 0.15 | 1.12 | 3.7 | 3.73 | 0.04 | 0.04 | <0.10 | <0.10 | 1.23 | 99.54 |
| RBL94261 | ortho gneiss | | | 77.06 | 11.94 | 0.28 | 0.06 | 0.17 | 1.01 | 2.39 | 4.19 | 0.01 | 0.01 | <0.10 | <0.10 | 1.3 | 98.43 |
| RBL94076 | po-skarn | 447770 | 7332010 | 53.58 | 14.75 | 10.6 | 0.7 | 2.13 | 9.02 | 4.43 | 1 | 0.08 | 0.37 | <0.10 | 0.11 | 1.51 | 98.17 |
| RBL94097 | psammitic schist | 473460 | 7321400 | 82.56 | 7.72 | 3.92 | 0.55 | 0.63 | 0.13 | 0.27 | 1.6 | 0.07 | 0.09 | <0.10 | <0.10 | 1.19 | 98.73 |
| TB94303 | quartz-mica schis | 467360 | 7332160 | 88.3 | 4.4 | 1.88 | 0.24 | 0.91 | 0.2 | 0.23 | 1.31 | 0.05 | 0.04 | <0.10 | <0.10 | 0.85 | 98.41 |
| TB94027 | quartzite | 452350 | 7325440 | 92.05 | 2.62 | 0.9 | 0.16 | 0.31 | 0.39 | 0.2 | 0.95 | <0.01 | 0.14 | <0.10 | <0.10 | 0.53 | 98.24 |
| RBL94079 | quartzite | 451420 | 7332680 | 78.03 | 11.4 | 1.84 | 0.12 | 0.48 | 1.42 | 0.92 | 3.16 | 0.02 | 0.03 | <0.10 | <0.10 | 1.89 | 99.32 |
| RBL94040 | qz-fld schist | 451625 | 7309650 | 70.03 | 14.14 | 2.81 | 0.12 | 4.33 | 1.85 | 1.66 | 3.17 | 0.03 | 0.03 | <0.10 | <0.10 | 1.21 | 99.38 |
| RBL94041 | qz-fld schist | 451625 | 7309650 | 78.6 | 11.7 | 0.87 | 0.08 | 0.57 | 0.76 | 2.56 | 2.45 | 0.01 | 0.01 | <0.10 | <0.10 | 1.22 | 98.83 |
| RBL94042 | qz-fld schist | 451625 | 7309650 | 75.32 | 12.29 | 1.78 | 0.08 | 2.12 | 0.91 | 2.7 | 2.43 | 0.02 | 0.01 | <0.10 | <0.10 | 1.09 | 98.77 |
| RBL94043 | qz-fld schist | 451625 | 7309650 | 68.54 | 14.75 | 3.96 | 0.1 | 3.52 | 1.24 | 3.99 | 2.46 | 0.02 | 0.02 | <0.10 | <0.10 | 1 | 99.6 |
| RBL94044 | qz-fld schist | 449900 | 7309300 | 73.96 | 14.74 | 1.73 | 0.18 | 1.08 | 0.2 | 0.66 | 4.07 | 0.04 | 0.03 | <0.10 | <0.10 | 1.96 | 98.65 |
| RBL94082 | qz-fld schist | 464300 | 7329260 | 73.57 | 12.94 | 2.52 | 0.28 | 1.09 | 3.54 | 2 | 2.15 | 0.09 | 0.13 | <0.10 | <0.10 | 0.82 | 99.12 |
| RBL94084 | qz-fld schist | 462890 | 7329040 | 75.94 | 13.12 | 1.29 | 0.11 | 1.22 | 1.6 | 2.89 | 2.24 | 0.03 | 0.02 | <0.10 | <0.10 | 1.06 | 99.52 |
| RBL94089 | qz-fld schist | 462950 | 7324330 | 77.09 | 11.56 | 1.43 | 0.1 | 0.4 | 1.25 | 1.15 | 4.87 | 0.02 | 0.02 | <0.10 | <0.10 | 0.79 | 98.68 |
| RBL94092 | qz-fld schist | 462260 | 7329570 | 69.65 | 17.32 | 1.17 | 0.14 | 0.69 | 0.2 | 4.18 | 3.66 | 0.01 | 0.01 | <0.10 | <0.10 | 1.62 | 98.66 |
| RBL94093 | qz-fld schist | 472140 | 7322780 | 70.34 | 15.85 | 2.46 | 0.22 | 1.38 | 0.5 | 3.2 | 4.58 | 0.05 | 0.03 | <0.10 | <0.10 | 1.21 | 99.81 |
| TB94018 | qz-fsp gneiss | 456640 | 7324190 | 76.8 | 14.22 | 0.65 | 0.05 | 0.48 | 0.12 | 0.43 | 3.75 | <0.01 | 0.03 | <0.10 | <0.10 | 1.96 | 98.48 |
| TB94023 | qz-fsp gneiss | 460600 | 7322660 | 78.01 | 12.66 | 1.24 | 0.08 | 0.19 | 0.3 | 3.82 | 2.05 | 0.05 | 0.02 | <0.10 | <0.10 | 1.08 | 99.48 |
| TB94037 | qz-fsp gneiss | 463750 | 7325640 | 77.54 | 12.62 | 1.19 | 0.08 | 0.16 | 0.93 | 2.93 | 2.37 | 0.06 | 0.02 | <0.10 | <0.10 | 0.89 | 98.79 |
| TB94304 | qz-fsp gneiss | 467100 | 7333150 | 75.16 | 11.06 | 5.89 | 1.29 | 0.99 | 0.29 | 0.21 | 2.46 | 0.09 | 0.06 | <0.10 | <0.10 | 1.13 | 98.63 |
| TB94001 | qz-fsp schist | 449900 | 7309300 | 74.16 | 11.61 | 1.44 | 0.09 | 1.05 | 1.34 | 1.09 | 5.97 | 0.04 | 0.02 | <0.10 | <0.10 | 1.74 | 98.56 |
| TB94000 | qz-fsp schist | 449900 | 7309300 | 70.86 | 12.28 | 1.59 | 0.1 | 1.38 | 1.77 | 0.57 | 7.31 | 0.04 | 0.03 | <0.10 | <0.10 | 2.17 | 98.11 |
| TB94003 | qz-fsp schist | 449900 | 7309300 | 72.83 | 12.17 | 1.44 | 0.12 | 0.78 | 1.06 | 0.56 | 7.84 | 0.03 | 0.03 | <0.10 | <0.10 | 1.24 | 98.1 |

| Sample | Name | UTM-X | UTM-Y | SiO2 | Al2O3 | Fe2O3 | TiO2 | MgO | CaO | Na2O | K2O | MnO | P2O5 | Cl | F | Gl.tap | Sum |
|---|---|---|---|---|---|---|---|---|---|---|---|---|---|---|---|---|---|
| TB94004 | qz-fsp schist | 449900 | 7309300 | 50.58 | 16.77 | 10.98 | 1.39 | 5.95 | 4.78 | 2.64 | 4.13 | 0.15 | 0.5 | <0.10 | 0.17 | 0.76 | 98.64 |
| TB94005 | qz-fsp schist | 449900 | 7309300 | 66.69 | 15.77 | 3.14 | 0.36 | 3.06 | 2.81 | 4.26 | 2.19 | 0.05 | 0.11 | <0.10 | <0.10 | 0.63 | 99.07 |
| TB94008 | qz-fsp schist | 449900 | 7309300 | 71.82 | 15.28 | 1.98 | 0.16 | 1.1 | 0.39 | <0.10 | 5.87 | 0.04 | 0.03 | <0.10 | <0.10 | 2.04 | 98.78 |
| TB94009 | qz-fsp schist | 449900 | 7309300 | 73.57 | 13.81 | 1.97 | 0.15 | 1.42 | 0.77 | 0.28 | 4.85 | 0.05 | 0.03 | <0.10 | <0.10 | 1.82 | 98.71 |
| TB94010 | qz-fsp schist | 449900 | 7309300 | 73.95 | 13.79 | 1.85 | 0.15 | 0.51 | 1.3 | 1.39 | 3.73 | 0.07 | 0.03 | <0.10 | <0.10 | 1.32 | 98.08 |
| TB94011 | qz-fsp schist | 449900 | 7309300 | 71.85 | 15.82 | 2.04 | 0.16 | 1.02 | 0.39 | 0.15 | 5.07 | 0.04 | 0.02 | <0.10 | <0.10 | 2.32 | 98.9 |
| TB94046 | qz-fsp schist | 473090 | 7326590 | 65.88 | 12.26 | 5.04 | 0.86 | 3.3 | 5 | 1.28 | 2.67 | 0.09 | 0.14 | <0.10 | <0.10 | 1.59 | 98.11 |
| TB94073 | qz-fsp schist | 467980 | 7331410 | 71.34 | 13.99 | 3.02 | 0.37 | 0.85 | 0.57 | 1.89 | 5.19 | 0.03 | 0.09 | <0.10 | <0.10 | 1.18 | 98.52 |
| TB94074 | qz-fsp schist | 468110 | 7332830 | 68.59 | 12.8 | 6 | 1.16 | 2.18 | 1.71 | 2.29 | 2.97 | 0.07 | 0.21 | <0.10 | <0.10 | 0.94 | 98.93 |
| TB94301 | qz-fsp schist | 467590 | 7332280 | 60 | 18.56 | 8.54 | 0.95 | 2.71 | 0.96 | 1.3 | 4.02 | 0.14 | 0.13 | <0.10 | <0.10 | 1.87 | 99.19 |
| TB94305 | qz-fsp schist | 466880 | 7332960 | 76.27 | 13.05 | 1.41 | 0.08 | 0.58 | 0.55 | 1.09 | 4.17 | 0.01 | 0.02 | <0.10 | <0.10 | 1.49 | 98.71 |
| TB94034 | qz-mica schist | 463460 | 7322470 | 79.68 | 7.13 | 4.27 | 0.43 | 1.28 | 0.56 | 0.28 | 2.05 | 0.02 | 0.09 | <0.10 | <0.10 | 2.39 | 98.18 |
| TB94035 | qz-mica schist | 462290 | 7323900 | 84.63 | 4.31 | 3.39 | 0.22 | 0.85 | 0.56 | 0.61 | 1.02 | 0.03 | 0.04 | <0.10 | <0.10 | 3.06 | 98.72 |
| RBL94085 | toumalinit | 462840 | 7329040 | 67.72 | 17.41 | 1.19 | 0.17 | 4.26 | 1.74 | 2.07 | 0.29 | 0.02 | 0.02 | <0.10 | <0.10 | 1.9 | 96.78 |

| Sample | Name | S | Ba | Sb | Sn | Cd | Ag | Ga | Zn | Cu | Ni | Yb | Co | Ce | La | Nd |
|---|---|---|---|---|---|---|---|---|---|---|---|---|---|---|---|---|
| TB94019 | amphibolite | <0.10 | 31 | < 10 | < 10 | < 10 | < 10 | 21 | 116 | 61 | 21 | < 10 | 37 | 63 | 14 | < 10 |
| TB94020 | amphibolite | <0.10 | 78 | < 10 | < 10 | < 10 | < 10 | 20 | 128 | 59 | 27 | < 10 | 46 | 88 | 21 | < 10 |
| TB94024 | amphibolite | <0.10 | 246 | < 10 | < 10 | < 10 | < 10 | 22 | 109 | 62 | 39 | < 10 | 40 | 57 | 18 | 11 |
| TB94029 | amphibolite | <0.10 | 587 | < 10 | < 10 | < 10 | < 10 | 23 | 106 | 30 | 58 | < 10 | 26 | 80 | 46 | 39 |
| TB94031 | amphibolite | <0.10 | 45 | < 10 | < 10 | < 10 | < 10 | 17 | 70 | 100 | 327 | < 10 | 59 | < 10 | < 10 | < 10 |
| TB94036 | amphibolite | <0.10 | 156 | < 10 | < 10 | < 10 | < 10 | 15 | 69 | 87 | 89 | < 10 | 44 | 14 | < 10 | < 10 |
| TB94039 | amphibolite | <0.10 | 84 | < 10 | < 10 | < 10 | < 10 | 16 | 67 | 12 | 69 | < 10 | 37 | < 10 | 15 | < 10 |
| TB94051 | amphibolite | <0.10 | 1014 | < 10 | < 10 | < 10 | < 10 | 23 | 112 | 48 | 20 | < 10 | 40 | 19 | < 10 | < 10 |
| TB94057 | amphibolite | <0.10 | 36 | < 10 | < 10 | < 10 | < 10 | 26 | 108 | 27 | 58 | < 10 | 52 | 30 | < 10 | < 10 |
| TB94062 | amphibolite | <0.10 | 308 | < 10 | < 10 | < 10 | < 10 | 17 | 172 | 100 | 103 | < 10 | 42 | 57 | 27 | 12 |
| TB94066 | amphibolite | <0.10 | 365 | < 10 | < 10 | < 10 | < 10 | 22 | 110 | < 5 | 73 | < 10 | 40 | 78 | 35 | 37 |
| TB94302 | amphibolite | <0.10 | 78 | < 10 | < 10 | < 10 | < 10 | 13 | 113 | 88 | 74 | < 10 | 50 | 18 | 12 | < 10 |
| RBL94049a | amphibolite | <0.10 | 47 | < 10 | < 10 | < 10 | < 10 | 21 | 101 | 90 | 22 | < 10 | 44 | 24 | 14 | < 10 |
| RBL94051 | amphibolite | <0.10 | 37 | < 10 | < 10 | < 10 | < 10 | 16 | 108 | < 5 | 23 | < 10 | 42 | 22 | < 10 | < 10 |
| RBL94052 | amphibolite | <0.10 | 41 | < 10 | < 10 | < 10 | < 10 | 17 | 93 | 21 | 17 | < 10 | 43 | 27 | < 10 | < 10 |
| RBL94053 | amphibolite | <0.10 | 47 | < 10 | < 10 | < 10 | < 10 | 19 | 78 | 82 | 41 | < 10 | 39 | 21 | < 10 | < 10 |
| RBL94054 | amphibolite | <0.10 | 120 | < 10 | < 10 | < 10 | < 10 | 16 | 36 | < 5 | 40 | < 10 | 29 | 25 | < 10 | < 10 |
| RBL94055 | amphibolite | <0.10 | 86 | < 10 | < 10 | < 10 | < 10 | 15 | 42 | 150 | 39 | < 10 | 36 | 51 | 26 | < 10 |
| RBL94056 | amphibolite | <0.10 | 41 | < 10 | < 10 | < 10 | < 10 | 16 | 113 | 184 | 50 | < 10 | 48 | 38 | < 10 | < 10 |
| RBL94057 | amphibolite | <0.10 | 48 | < 10 | < 10 | < 10 | < 10 | 19 | 76 | 57 | 11 | < 10 | 41 | 37 | 11 | < 10 |
| RBL94061 | amphibolite | <0.10 | 235 | < 10 | < 10 | < 10 | < 10 | 14 | 118 | < 5 | 50 | < 10 | 45 | 69 | 19 | < 10 |
| RBL94064 | amphibolite | <0.10 | 174 | < 10 | < 10 | < 10 | < 10 | 16 | 84 | 15 | < 5 | < 10 | 26 | 24 | < 10 | < 10 |
| RBL94065 | amphibolite | <0.10 | 118 | < 10 | < 10 | < 10 | < 10 | 16 | 88 | 21 | < 5 | < 10 | 26 | 20 | 12 | < 10 |
| RBL94080 | amphibolite | <0.10 | 145 | < 10 | < 10 | < 10 | < 10 | 14 | 59 | 40 | 136 | < 10 | 39 | 21 | 14 | < 10 |
| RBL94090 | amphibolite | <0.10 | 318 | < 10 | < 10 | < 10 | < 10 | 13 | 61 | 134 | 25 | < 10 | 18 | 51 | 15 | 18 |
| RBL94091 | amphibolite | <0.10 | 189 | < 10 | < 10 | < 10 | < 10 | 16 | 81 | 87 | 106 | < 10 | 41 | 36 | 19 | < 10 |
| RBL94070 | calc silicate | <0.10 | 243 | < 10 | < 10 | < 10 | < 10 | 12 | 95 | < 5 | 30 | < 10 | 15 | 61 | 32 | 20 |
| RBL94075 | calc silicate | 1.18 | 168 | < 10 | < 10 | < 10 | < 10 | 20 | 114 | 83 | 58 | < 10 | 20 | 94 | 46 | 29 |
| RBL94095 | calc silicate | <0.10 | 94 | < 10 | < 10 | < 10 | < 10 | 24 | 193 | 20 | 6 | < 10 | 40 | 148 | 59 | 57 |
| TB94014 | calc. schist | <0.10 | 488 | < 10 | < 10 | < 10 | < 10 | 15 | 102 | 26 | 83 | < 10 | 25 | 85 | 46 | 35 |
| TB94016 | calc. schist | <0.10 | 521 | < 10 | < 10 | < 10 | < 10 | 18 | 106 | 41 | 85 | < 10 | 22 | 68 | 43 | 33 |
| TB94022 | calc. schist | 0.49 | 298 | < 10 | < 10 | < 10 | < 10 | 12 | 87 | 32 | 38 | < 10 | 12 | 43 | 28 | 21 |
| TB94032 | calc. schist | <0.10 | 460 | < 10 | < 10 | < 10 | < 10 | 18 | 101 | 10 | 71 | < 10 | 23 | 74 | 42 | 31 |
| TB94038 | calc. schist | <0.10 | 357 | < 10 | < 10 | < 10 | < 10 | 15 | 83 | 38 | 71 | < 10 | 17 | 51 | 36 | 27 |
| TB94050 | calc. schist | <0.10 | 192 | < 10 | < 10 | < 10 | < 10 | 11 | 53 | 48 | 52 | < 10 | 11 | 42 | 25 | 20 |
| TB94058 | calc. schist | <0.10 | 318 | < 10 | < 10 | < 10 | < 10 | 13 | 76 | 23 | 52 | < 10 | 11 | 36 | 24 | 22 |
| TB94063 | calc. schist | <0.10 | 462 | < 10 | < 10 | < 10 | < 10 | 17 | 86 | 13 | 85 | < 10 | 21 | 61 | 37 | 26 |
| TB94064 | calc. schist | <0.10 | 393 | < 10 | < 10 | < 10 | < 10 | 14 | 85 | 44 | 74 | < 10 | 16 | 51 | 46 | 26 |
| TB94089 | calc. schist | 0.67 | 805 | < 10 | < 10 | < 10 | < 10 | 19 | 90 | 86 | 82 | < 10 | 33 | < 10 | 12 | < 10 |

| Sample | Name | S | Ba | Sb | Sn | Cd | Ag | Ga | Zn | Cu | Ni | Yb | Co | Ce | La | Nd |
|---|---|---|---|---|---|---|---|---|---|---|---|---|---|---|---|---|
| TB94097 | calc. schist | <0.10 | 312 | < 10 | < 10 | < 10 | < 10 | 18 | 79 | 43 | 35 | < 10 | 14 | 56 | 29 | 24 |
| RBL94062 | calcareous mica s | 0.19 | 293 | < 10 | < 10 | < 10 | < 10 | 19 | 103 | 37 | 41 | < 10 | 27 | 77 | 39 | 24 |
| RBL94081 | calcareous schist | <0.10 | 343 | < 10 | < 10 | < 10 | < 10 | 14 | 68 | 24 | 54 | < 10 | 14 | 52 | 34 | 27 |
| TB94025 | calcite marble | <0.10 | 260 | < 10 | < 10 | < 10 | < 10 | < 10 | 53 | 6 | 6 | 16 | < 10 | < 10 | < 10 | < 10 |
| TB94043 | calcite marble | <0.10 | 36 | < 10 | < 10 | < 10 | < 10 | < 10 | 10 | 8 | < 5 | 16 | < 10 | < 10 | < 10 | < 10 |
| TB94044 | calcite marble | <0.10 | 35 | < 10 | < 10 | < 10 | < 10 | < 10 | 9 | 6 | < 5 | < 10 | < 10 | < 10 | < 10 | < 10 |
| TB94045 | calcite marble | 0.41 | 175 | < 10 | < 10 | < 10 | < 10 | < 10 | 8 | 6 | 7 | < 10 | < 10 | < 10 | < 10 | 13 |
| TB94052 | calcite marble | <0.10 | 44 | < 10 | < 10 | < 10 | < 10 | < 10 | < 5 | < 5 | < 5 | 19 | < 10 | < 10 | < 10 | < 10 |
| TB94053 | calcite marble | <0.10 | 35 | < 10 | < 10 | < 10 | < 10 | < 10 | < 5 | < 5 | < 5 | 11 | < 10 | < 10 | < 10 | < 10 |
| TB94054 | calcite marble | <0.10 | 37 | < 10 | < 10 | < 10 | < 10 | < 10 | < 5 | < 5 | < 5 | 10 | < 10 | < 10 | < 10 | < 10 |
| TB94055 | calcite marble | <0.10 | 50 | < 10 | < 10 | < 10 | < 10 | < 10 | < 5 | < 5 | < 5 | 10 | < 10 | < 10 | < 10 | < 10 |
| TB94056 | calcite marble | <0.10 | 74 | < 10 | < 10 | < 10 | < 10 | < 10 | 6 | < 5 | < 5 | < 10 | < 10 | < 10 | < 10 | < 10 |
| TB94065 | calcite marble | <0.10 | 48 | < 10 | < 10 | < 10 | < 10 | < 10 | < 5 | < 5 | < 5 | < 10 | < 10 | < 10 | < 10 | < 10 |
| TB94067 | calcite marble | <0.10 | 28 | < 10 | < 10 | < 10 | < 10 | < 10 | < 5 | < 5 | < 5 | 11 | < 10 | < 10 | < 10 | < 10 |
| TB94068 | calcite marble | <0.10 | 34 | < 10 | < 10 | < 10 | < 10 | < 10 | < 5 | < 5 | < 5 | < 10 | < 10 | < 10 | < 10 | < 10 |
| TB94076 | calcite marble | <0.10 | 45 | < 10 | < 10 | < 10 | < 10 | < 10 | < 5 | < 5 | < 5 | 18 | < 10 | < 10 | < 10 | < 10 |
| TB94077 | calcite marble | <0.10 | 39 | < 10 | < 10 | < 10 | < 10 | < 10 | < 5 | < 5 | 5 | < 10 | < 10 | < 10 | < 10 | < 10 |
| TB94084 | calcite marble | <0.10 | 96 | < 10 | < 10 | < 10 | < 10 | < 10 | < 5 | < 5 | < 5 | < 10 | < 10 | < 10 | < 10 | < 10 |
| TB94085 | calcite marble | <0.10 | 63 | < 10 | < 10 | < 10 | < 10 | < 10 | < 5 | 6 | 7 | 12 | < 10 | < 10 | < 10 | < 10 |
| TB94088 | calcite marble | <0.10 | 54 | < 10 | < 10 | < 10 | < 10 | < 10 | < 5 | < 5 | < 5 | < 10 | < 10 | < 10 | < 10 | < 10 |
| TB94096 | calcite marble | <0.10 | 50 | < 10 | < 10 | < 10 | < 10 | < 10 | < 5 | < 5 | < 5 | < 10 | < 10 | < 10 | < 10 | < 10 |
| TB94098 | calcite marble | <0.10 | 39 | < 10 | < 10 | < 10 | < 10 | < 10 | < 5 | < 5 | < 5 | < 10 | < 10 | < 10 | < 10 | < 10 |
| TB94075 | calcite-dolomite m | <0.10 | 41 | < 10 | < 10 | < 10 | < 10 | < 10 | < 5 | < 5 | < 5 | 12 | < 10 | < 10 | < 10 | < 10 |
| TB94095 | calcite-dolomite m | <0.10 | 38 | < 10 | < 10 | < 10 | < 10 | < 10 | < 5 | 5 | 5 | 16 | < 10 | < 10 | < 10 | < 10 |
| TB94099 | calcite-dolomite m | <0.10 | 36 | < 10 | < 10 | < 10 | < 10 | < 10 | < 5 | < 5 | < 5 | 12 | < 10 | < 10 | < 10 | < 10 |
| TB94033 | chert | <0.10 | 383 | < 10 | < 10 | < 10 | < 10 | 18 | 72 | 13 | < 5 | < 10 | < 10 | 117 | 51 | 43 |
| TB94047 | dolomite marble | <0.10 | 22 | < 10 | < 10 | < 10 | < 10 | < 10 | < 5 | < 5 | < 5 | < 10 | < 10 | < 10 | < 10 | < 10 |
| TB94048 | dolomite marble | <0.10 | 21 | < 10 | < 10 | < 10 | < 10 | < 10 | < 5 | < 5 | < 5 | < 10 | < 10 | < 10 | < 10 | < 10 |
| TB94069 | dolomite marble | <0.10 | 19 | < 10 | < 10 | < 10 | < 10 | < 10 | < 5 | < 5 | < 5 | < 10 | < 10 | < 10 | < 10 | < 10 |
| TB94070 | dolomite marble | <0.10 | 22 | < 10 | < 10 | < 10 | < 10 | < 10 | < 5 | < 5 | < 5 | < 10 | < 10 | < 10 | < 10 | < 10 |
| TB94078 | dolomite marble | <0.10 | 22 | < 10 | < 10 | < 10 | < 10 | < 10 | < 5 | < 5 | < 5 | < 10 | < 10 | < 10 | < 10 | < 10 |
| TB94079 | dolomite marble | <0.10 | 26 | < 10 | < 10 | < 10 | < 10 | < 10 | < 5 | < 5 | 6 | < 10 | < 10 | < 10 | < 10 | < 10 |
| TB94080 | dolomite marble | <0.10 | 27 | < 10 | < 10 | < 10 | < 10 | < 10 | < 5 | < 5 | < 5 | < 10 | < 10 | < 10 | < 10 | < 10 |
| TB94081 | dolomite marble | <0.10 | 23 | < 10 | < 10 | < 10 | < 10 | < 10 | < 5 | < 5 | < 5 | < 10 | < 10 | < 10 | < 10 | < 10 |
| TB94082 | dolomite marble | <0.10 | 20 | < 10 | < 10 | < 10 | < 10 | < 10 | < 5 | < 5 | < 5 | < 10 | < 10 | < 10 | < 10 | < 10 |
| TB94083 | dolomite marble | <0.10 | 25 | < 10 | < 10 | < 10 | < 10 | < 10 | < 5 | < 5 | < 5 | < 10 | < 10 | < 10 | < 10 | < 10 |
| TB94087 | dolomite marble | <0.10 | 23 | < 10 | < 10 | < 10 | < 10 | < 10 | < 5 | < 5 | < 5 | < 10 | < 10 | < 10 | < 10 | < 10 |
| TB94092 | dolomite marble | <0.10 | 24 | < 10 | < 10 | < 10 | < 10 | < 10 | < 5 | < 5 | < 5 | < 10 | < 10 | < 10 | < 10 | < 10 |
| TB94093 | dolomite marble | <0.10 | 22 | < 10 | < 10 | < 10 | < 10 | < 10 | < 5 | < 5 | < 5 | < 10 | < 10 | < 10 | < 10 | < 10 |

| Sample | Name | S | Ba | Sb | Sn | Cd | Ag | Ga | Zn | Cu | Ni | Yb | Co | Ce | La | Nd |
|---|---|---|---|---|---|---|---|---|---|---|---|---|---|---|---|---|
| TB94094 | dolomite marble | <0.10 | 22 | < 10 | < 10 | < 10 | < 10 | < 10 | < 5 | < 5 | < 5 | < 10 | < 10 | < 10 | < 10 | < 10 |
| TB94320 | dolomite marble | <0.10 | 18 | < 10 | < 10 | < 10 | < 10 | < 10 | < 5 | < 5 | < 5 | < 10 | < 10 | < 10 | < 10 | < 10 |
| RBL94071 | dolomite marble | <0.10 | 83 | < 10 | < 10 | < 10 | < 10 | < 10 | 84 | 8 | 30 | < 10 | < 10 | < 10 | 17 | 16 |
| RBL94063 | garnet gneiss | <0.10 | 1378 | < 10 | < 10 | < 10 | < 10 | 21 | 69 | 9 | 29 | < 10 | < 10 | 36 | 24 | 13 |
| RBL94073 | gr-mica quartzite | <0.10 | 274 | < 10 | < 10 | < 10 | < 10 | < 10 | 30 | 15 | 9 | < 10 | < 10 | 12 | < 10 | < 10 |
| RBL94074 | gr-mica quartzite | <0.10 | 523 | < 10 | < 10 | < 10 | < 10 | 13 | 46 | 10 | 17 | < 10 | < 10 | 23 | 18 | 12 |
| RBL94045 | gr-mica schist | 0.22 | 407 | < 10 | < 10 | < 10 | < 10 | 15 | 60 | 10 | 6 | < 10 | < 10 | 51 | 31 | 25 |
| RBL94046 | gr-mica schist | <0.10 | 628 | < 10 | < 10 | < 10 | < 10 | 29 | 136 | 9 | 65 | < 10 | 32 | 138 | 72 | 49 |
| RBL94047 | gr-mica schist | <0.10 | 476 | < 10 | < 10 | < 10 | < 10 | 22 | 124 | < 5 | 52 | < 10 | 30 | 123 | 70 | 45 |
| RBL94048 | gr-mica schist | <0.10 | 505 | < 10 | < 10 | < 10 | < 10 | 23 | 126 | 63 | 36 | < 10 | 20 | 70 | 32 | 23 |
| RBL94094 | gr.-mica schist | <0.10 | 473 | < 10 | < 10 | < 10 | < 10 | 21 | 98 | 7 | 47 | < 10 | 30 | 92 | 51 | 28 |
| RBL94098 | gr.-mica schist | <0.10 | 530 | < 10 | < 10 | < 10 | < 10 | 20 | 117 | 12 | 27 | < 10 | 12 | 11 | < 10 | < 10 |
| RBL94099 | gr.-mica schist | 0.16 | 771 | < 10 | < 10 | < 10 | < 10 | 18 | 112 | 30 | 35 | < 10 | 17 | 93 | 55 | 37 |
| RBL94100 | gr.-mica schist | <0.10 | 421 | < 10 | 12 | < 10 | < 10 | 15 | 57 | < 5 | < 5 | < 10 | < 10 | 116 | 60 | 62 |
| RBL94101 | gr.-mica schist | <0.10 | 503 | < 10 | < 10 | < 10 | < 10 | 17 | 112 | 53 | 51 | < 10 | 31 | 105 | 53 | 42 |
| RBL94102 | gr.-mica schist | <0.10 | 646 | < 10 | < 10 | < 10 | < 10 | 19 | 103 | 25 | 48 | < 10 | 23 | 79 | 43 | 32 |
| RBL94103 | gr.-mica schist | <0.10 | 491 | < 10 | < 10 | < 10 | < 10 | 20 | 109 | 110 | 56 | < 10 | 28 | 118 | 61 | 34 |
| RBL94104 | gr.-mica schist | <0.10 | 721 | < 10 | < 10 | < 10 | < 10 | 23 | 100 | 9 | 49 | < 10 | 26 | 115 | 68 | 52 |
| TB94015 | graphite schist | 0.1 | 291 | < 10 | < 10 | < 10 | < 10 | < 10 | 6 | < 5 | < 5 | < 10 | < 10 | < 10 | < 10 | < 10 |
| RBL94068 | graphite schist | 5.01 | 1477 | < 10 | < 10 | < 10 | < 10 | 18 | 97 | 40 | 7 | < 10 | 18 | 22 | 11 | < 10 |
| TB94006 | graphitic schist | 0.85 | 1037 | < 10 | < 10 | < 10 | < 10 | 25 | 464 | 147 | 37 | < 10 | 44 | 45 | 32 | 19 |
| TB94007 | graphitic schist | 0.31 | 1020 | < 10 | < 10 | < 10 | < 10 | 10 | 46 | 10 | 5 | < 10 | < 10 | < 10 | 11 | 12 |
| RBL94072 | graphitic schist | 3.37 | 455 | < 10 | < 10 | < 10 | < 10 | 20 | 116 | 124 | 35 | < 10 | 18 | 103 | 61 | 39 |
| RBL94087 | graphitic schist | 4.68 | 1281 | < 10 | < 10 | < 10 | < 10 | 22 | 132 | 45 | 18 | < 10 | 28 | 63 | 31 | 35 |
| TB94012a | gt-mica schist | <0.10 | 515 | < 10 | < 10 | < 10 | < 10 | 21 | 86 | 26 | 39 | < 10 | 18 | 117 | 102 | 69 |
| TB94012b | gt-mica schist | <0.10 | 607 | < 10 | < 10 | < 10 | < 10 | 26 | 112 | 50 | 45 | < 10 | 26 | 77 | 22 | 23 |
| TB94013 | gt-mica schist | <0.10 | 424 | < 10 | < 10 | < 10 | < 10 | 24 | 98 | 60 | 32 | < 10 | 18 | 47 | 36 | 30 |
| TB94017 | gt-mica schist | 1.56 | 415 | < 10 | < 10 | < 10 | < 10 | 17 | 124 | 40 | 37 | < 10 | 15 | < 10 | < 10 | 14 |
| TB94021 | gt-mica schist | <0.10 | 394 | < 10 | < 10 | < 10 | < 10 | 14 | 63 | 17 | 15 | < 10 | < 10 | 28 | < 10 | 11 |
| TB94026 | gt-mica schist | 0.16 | 349 | < 10 | < 10 | < 10 | < 10 | 20 | 96 | 32 | 27 | < 10 | 14 | 79 | 43 | 31 |
| TB94040 | gt-mica schist | <0.10 | 553 | < 10 | < 10 | < 10 | < 10 | 19 | 122 | 17 | 34 | < 10 | 20 | < 10 | < 10 | < 10 |
| TB94041 | gt-mica schist | <0.10 | 659 | < 10 | < 10 | < 10 | < 10 | 25 | 128 | 5 | 42 | < 10 | 23 | 102 | 62 | 46 |
| TB94049 | gt-mica schist | <0.10 | 525 | < 10 | < 10 | < 10 | < 10 | 21 | 85 | < 5 | 37 | < 10 | 20 | 103 | 54 | 44 |
| TB94090 | gt-mica schist | <0.10 | 354 | < 10 | < 10 | < 10 | < 10 | 15 | 96 | 23 | 46 | < 10 | 24 | 57 | 30 | 23 |
| RBL94086 | kyanite schist | <0.10 | 423 | < 10 | < 10 | < 10 | < 10 | 13 | 59 | < 5 | < 5 | < 10 | < 10 | < 10 | < 10 | < 10 |
| RBL94096 | kyanite schist | <0.10 | 105 | < 10 | < 10 | < 10 | < 10 | 15 | 78 | < 5 | < 5 | < 10 | < 10 | 134 | 42 | 38 |
| RBL94105 | kyanite schist | <0.10 | 159 | < 10 | 16 | < 10 | < 10 | 21 | 108 | < 5 | < 5 | < 10 | < 10 | 65 | 19 | 28 |
| RBL94106 | kyanite schist | <0.10 | 68 | < 10 | < 10 | < 10 | < 10 | 14 | 95 | < 5 | < 5 | < 10 | < 10 | 63 | 20 | 23 |
| RBL94078 | mantle gr achist | <0.10 | 486 | < 10 | < 10 | < 10 | < 10 | 14 | 87 | 11 | 63 | < 10 | 20 | 74 | 27 | 23 |

| Sample | Name | S | Ba | Sb | Sn | Cd | Ag | Ga | Zn | Cu | Ni | Yb | Co | Ce | La | Nd |
|---|---|---|---|---|---|---|---|---|---|---|---|---|---|---|---|---|
| RBL94069 | mantle gr schist | <0.10 | 226 | < 10 | < 10 | < 10 | < 10 | 19 | 67 | 7 | 7 | < 10 | 19 | 21 | 14 | < 10 |
| RBL94088 | mantle gr. schist | <0.10 | 7535 | < 10 | < 10 | < 10 | < 10 | 17 | 98 | 43 | 29 | < 10 | 34 | < 10 | 24 | < 10 |
| RBL94049b | marble w. graphit | <0.10 | 20 | < 10 | < 10 | < 10 | < 10 | < 10 | < 5 | < 5 | < 5 | < 10 | < 10 | < 10 | < 10 | < 10 |
| RBL94050 | marble w. graphit | <0.10 | 55 | < 10 | < 10 | < 10 | < 10 | < 10 | < 5 | < 5 | 6 | < 10 | < 10 | < 10 | < 10 | < 10 |
| RBL94003 | massive ore | 36.4 | < 10 | 29 | 168 | 220 | < 10 | 50 | 91000 | 588 | 21 | < 10 | 35 | 138 | 44 | 31 |
| TB94042 | metagabbro | <0.10 | 904 | < 10 | < 10 | < 10 | < 10 | 23 | 124 | 19 | 21 | < 10 | 38 | 88 | 32 | 35 |
| TB94028 | mica schist | <0.10 | 767 | < 10 | < 10 | < 10 | < 10 | 21 | 115 | 7 | < 5 | < 10 | < 10 | 115 | 47 | 47 |
| TB94071 | mica schist | <0.10 | 607 | < 10 | < 10 | < 10 | < 10 | 13 | 19 | 10 | 10 | < 10 | < 10 | 62 | 39 | 43 |
| TB94072 | mica schist | <0.10 | 720 | < 10 | < 10 | < 10 | < 10 | 15 | 65 | 27 | 20 | < 10 | 11 | 51 | 23 | 26 |
| RBL94077 | micrcline gneiss | <0.10 | 249 | < 10 | < 10 | < 10 | < 10 | 14 | 60 | 10 | < 5 | < 10 | < 10 | < 10 | < 10 | < 10 |
| RBL94107A | microcline gneis | 2.49 | 257 | 64 | < 10 | 16 | 198 | 83 | 103 | 12000 | < 5 | < 10 | < 10 | 81 | 15 | 64 |
| RBL94108 | microcline gneis | <0.10 | 534 | < 10 | < 10 | < 10 | < 10 | 17 | 50 | 36 | < 5 | < 10 | < 10 | 207 | 137 | 113 |
| RBL94005 | microcline gneiss | 0.15 | 278 | < 10 | 11 | < 10 | < 10 | 19 | 318 | 40 | < 5 | < 10 | < 10 | 166 | 94 | 82 |
| RBL94006 | microcline gneiss | <0.10 | 147 | < 10 | < 10 | < 10 | < 10 | 16 | 184 | < 5 | < 5 | < 10 | < 10 | 53 | 27 | 33 |
| RBL94007 | microcline gneiss | <0.10 | 250 | < 10 | < 10 | < 10 | < 10 | 16 | 67 | < 5 | 15 | < 10 | < 10 | 238 | 131 | 81 |
| RBL94008 | microcline gneiss | <0.10 | 564 | < 10 | < 10 | < 10 | < 10 | 21 | 69 | < 5 | 16 | < 10 | < 10 | 239 | 175 | 129 |
| RBL94009 | microcline gneiss | <0.10 | 510 | < 10 | < 10 | < 10 | < 10 | 20 | 273 | < 5 | 6 | < 10 | < 10 | 188 | 124 | 85 |
| RBL94010 | microcline gneiss | <0.10 | 739 | < 10 | < 10 | < 10 | < 10 | 18 | 121 | 29 | 6 | < 10 | < 10 | 208 | 145 | 117 |
| RBL94011 | microcline gneiss | <0.10 | 674 | < 10 | < 10 | < 10 | < 10 | 19 | 89 | < 5 | 14 | < 10 | < 10 | 224 | 156 | 125 |
| RBL94012 | microcline gneiss | <0.10 | 652 | < 10 | < 10 | < 10 | < 10 | 18 | 97 | < 5 | 10 | < 10 | < 10 | 265 | 200 | 159 |
| RBL94013 | microcline gneiss | <0.10 | 513 | < 10 | < 10 | < 10 | < 10 | 17 | 88 | 12 | < 5 | < 10 | < 10 | 213 | 154 | 129 |
| RBL94014 | microcline gneiss | <0.10 | 618 | < 10 | < 10 | < 10 | < 10 | 15 | 80 | < 5 | 15 | < 10 | < 10 | 215 | 174 | 139 |
| RBL94015 | microcline gneiss | <0.10 | 515 | < 10 | < 10 | < 10 | < 10 | 16 | 71 | < 5 | < 5 | < 10 | < 10 | 194 | 139 | 112 |
| RBL94016 | microcline gneiss | <0.10 | 563 | < 10 | < 10 | < 10 | < 10 | 17 | 35 | < 5 | 18 | < 10 | < 10 | 204 | 147 | 123 |
| RBL94017 | microcline gneiss | <0.10 | 645 | < 10 | 13 | < 10 | < 10 | 16 | 41 | < 5 | < 5 | < 10 | < 10 | 209 | 161 | 142 |
| RBL94018 | microcline gneiss | <0.10 | 619 | < 10 | < 10 | < 10 | < 10 | 15 | 48 | 7 | < 5 | 11 | < 10 | 189 | 145 | 120 |
| RBL94019 | microcline gneiss | <0.10 | 617 | < 10 | < 10 | < 10 | < 10 | 21 | 80 | < 5 | < 5 | < 10 | < 10 | 219 | 170 | 145 |
| RBL94020 | microcline gneiss | <0.10 | 563 | < 10 | < 10 | < 10 | < 10 | 16 | 48 | < 5 | 18 | < 10 | < 10 | 204 | 155 | 133 |
| RBL94021 | microcline gneiss | <0.10 | 496 | < 10 | < 10 | < 10 | < 10 | 17 | 50 | < 5 | < 5 | < 10 | < 10 | 211 | 152 | 129 |
| RBL94022 | microcline gneiss | <0.10 | 542 | < 10 | < 10 | < 10 | < 10 | 17 | 46 | < 5 | < 5 | < 10 | < 10 | 203 | 144 | 123 |
| RBL94023 | microcline gneiss | <0.10 | 466 | < 10 | < 10 | < 10 | < 10 | 18 | 42 | < 5 | 16 | < 10 | < 10 | 199 | 134 | 112 |
| RBL94024 | microcline gneiss | <0.10 | 469 | < 10 | < 10 | < 10 | < 10 | 15 | 47 | < 5 | 12 | < 10 | < 10 | 202 | 142 | 116 |
| RBL94025 | microcline gneiss | <0.10 | 430 | < 10 | < 10 | < 10 | < 10 | 15 | 40 | < 5 | < 5 | < 10 | < 10 | 200 | 141 | 111 |
| RBL94026 | microcline gneiss | <0.10 | 494 | < 10 | < 10 | < 10 | < 10 | 17 | 37 | < 5 | 10 | 14 | < 10 | 216 | 161 | 120 |
| RBL94027 | microcline gneiss | <0.10 | 590 | < 10 | < 10 | < 10 | < 10 | 18 | 26 | < 5 | < 5 | < 10 | < 10 | 104 | 68 | 69 |
| RBL94028 | microcline gneiss | <0.10 | 628 | < 10 | < 10 | < 10 | < 10 | 17 | 45 | < 5 | 13 | < 10 | < 10 | 217 | 167 | 133 |
| RBL94029 | microcline gneiss | <0.10 | 904 | < 10 | < 10 | < 10 | < 10 | 17 | 26 | < 5 | < 5 | < 10 | < 10 | 164 | 57 | 56 |
| RBL94030 | microcline gneiss | <0.10 | 584 | < 10 | < 10 | < 10 | < 10 | 15 | 55 | < 5 | < 5 | < 10 | < 10 | 231 | 224 | 154 |
| RBL94031 | microcline gneiss | <0.10 | 624 | < 10 | < 10 | < 10 | < 10 | 17 | 87 | < 5 | 15 | 11 | < 10 | 298 | 206 | 136 |

*Major elements in %, minor in ppm*

| Sample | Name | S | Ba | Sb | Sn | Cd | Ag | Ga | Zn | Cu | Ni | Yb | Co | Ce | La | Nd |
|---|---|---|---|---|---|---|---|---|---|---|---|---|---|---|---|---|
| RBL94032 | microcline gneiss | <0.10 | 884 | < 10 | < 10 | < 10 | < 10 | 14 | 45 | < 5 | 9 | < 10 | < 10 | 152 | 122 | 98 |
| RBL94033 | microcline gneiss | <0.10 | 227 | < 10 | < 10 | < 10 | < 10 | 15 | 29 | 5 | 6 | < 10 | < 10 | 44 | 27 | 28 |
| RBL94034 | microcline gneiss | <0.10 | 623 | < 10 | < 10 | < 10 | < 10 | 19 | 46 | < 5 | 12 | < 10 | < 10 | 87 | 51 | 44 |
| RBL94035 | microcline gneiss | <0.10 | 506 | < 10 | < 10 | < 10 | < 10 | 20 | 47 | < 5 | 9 | < 10 | < 10 | 170 | 90 | 67 |
| RBL94036 | microcline gneiss | <0.10 | 587 | < 10 | < 10 | < 10 | < 10 | 16 | 49 | < 5 | 11 | < 10 | < 10 | 214 | 115 | 108 |
| RBL94037 | microcline gneiss | <0.10 | 1118 | < 10 | < 10 | < 10 | < 10 | 13 | 43 | 18 | 12 | < 10 | < 10 | 80 | 67 | 56 |
| RBL94038 | microcline gneiss | <0.10 | 175 | < 10 | 13 | < 10 | < 10 | 14 | < 5 | < 5 | < 5 | < 10 | < 10 | 22 | 13 | 12 |
| RBL94039 | microcline gneiss | <0.10 | 540 | < 10 | < 10 | < 10 | < 10 | 19 | 45 | < 5 | < 5 | < 10 | < 10 | 156 | 106 | 72 |
| RBL94058 | microcline gneiss | <0.10 | 501 | < 10 | < 10 | < 10 | < 10 | 17 | 23 | < 5 | < 5 | < 10 | < 10 | 209 | 148 | 126 |
| RBL94059 | microcline gneiss | <0.10 | 740 | < 10 | < 10 | < 10 | < 10 | 14 | 14 | < 5 | 7 | < 10 | < 10 | 105 | 82 | 70 |
| RBL94060 | microcline gneiss | <0.10 | 637 | < 10 | < 10 | < 10 | < 10 | 16 | 35 | 6 | 8 | < 10 | < 10 | 201 | 158 | 125 |
| RBL94001 | muscovite schist | 0.2 | 155 | < 10 | 49 | < 10 | < 10 | 20 | 838 | 32 | 6 | < 10 | < 10 | 68 | 39 | 34 |
| RBL94002 | muscovite schist | <0.10 | 132 | < 10 | 24 | < 10 | < 10 | 14 | 117 | 15 | < 5 | < 10 | < 10 | 81 | 42 | 42 |
| RBL94004 | muscovite schist | 0.59 | 252 | 25 | 36 | < 10 | 30 | 30 | 3669 | 199 | 7 | < 10 | < 10 | 69 | 39 | 34 |
| RBL94259 | ortho gneiss | <0.10 | 55 | < 10 | < 10 | 12 | < 10 | 13 | 13 | 18 | < 5 | < 10 | < 10 | 23 | < 10 | 13 |
| RBL94260 | ortho gneiss | <0.10 | 479 | < 10 | < 10 | < 10 | < 10 | 15 | 71 | 5 | < 5 | < 10 | < 10 | 73 | 44 | 38 |
| RBL94261 | ortho gneiss | <0.10 | 593 | < 10 | < 10 | < 10 | < 10 | < 10 | 5 | < 5 | < 5 | < 10 | < 10 | 44 | 36 | 28 |
| RBL94076 | po-skarn | 4.53 | 413 | < 10 | < 10 | < 10 | < 10 | 19 | 48 | 434 | 14 | < 10 | 45 | 122 | 58 | 18 |
| RBL94097 | psammitic schist | <0.10 | 1149 | < 10 | < 10 | < 10 | < 10 | 10 | 37 | < 5 | 6 | < 10 | < 10 | 28 | 16 | 13 |
| TB94303 | quartz-mica schis | <0.10 | 160 | < 10 | < 10 | < 10 | < 10 | < 10 | 22 | 6 | 6 | < 10 | < 10 | < 10 | < 10 | < 10 |
| TB94027 | quartzite | <0.10 | 686 | < 10 | < 10 | < 10 | < 10 | < 10 | < 5 | < 5 | < 5 | < 10 | < 10 | < 10 | 11 | < 10 |
| RBL94079 | quartzite | 0.81 | 817 | < 10 | < 10 | < 10 | < 10 | 13 | 117 | < 5 | < 5 | < 10 | < 10 | 25 | 16 | 18 |
| RBL94040 | qz-fld schist | <0.10 | 200 | < 10 | < 10 | < 10 | < 10 | 15 | 76 | < 5 | < 5 | < 10 | < 10 | 169 | 72 | 61 |
| RBL94041 | qz-fld schist | <0.10 | 128 | < 10 | < 10 | < 10 | < 10 | 13 | 36 | < 5 | < 5 | < 10 | < 10 | 70 | 35 | 33 |
| RBL94042 | qz-fld schist | <0.10 | 51 | < 10 | < 10 | < 10 | < 10 | 14 | 194 | 7 | 9 | < 10 | < 10 | 99 | 46 | 39 |
| RBL94043 | qz-fld schist | <0.10 | 123 | < 10 | < 10 | < 10 | < 10 | 21 | 82 | 7 | < 5 | < 10 | < 10 | 36 | 15 | 13 |
| RBL94044 | qz-fld schist | <0.10 | 1039 | < 10 | < 10 | < 10 | < 10 | 13 | 69 | < 5 | < 5 | < 10 | < 10 | 18 | 16 | 14 |
| RBL94082 | qz-fld schist | <0.10 | 659 | < 10 | < 10 | < 10 | < 10 | 11 | 61 | < 5 | < 5 | < 10 | < 10 | 38 | 26 | 17 |
| RBL94084 | qz-fld schist | <0.10 | 594 | < 10 | < 10 | < 10 | < 10 | 15 | 49 | < 5 | < 5 | < 10 | < 10 | 28 | 16 | 19 |
| RBL94089 | qz-fld schist | <0.10 | 2410 | < 10 | < 10 | < 10 | < 10 | 13 | 78 | 11 | < 5 | < 10 | < 10 | 79 | 46 | 46 |
| RBL94092 | qz-fld schist | <0.10 | 1066 | < 10 | < 10 | < 10 | < 10 | 19 | 63 | < 5 | < 5 | < 10 | < 10 | 82 | 49 | 46 |
| RBL94093 | qz-fld schist | <0.10 | 265 | < 10 | 11 | < 10 | < 10 | 18 | 67 | < 5 | < 5 | < 10 | < 10 | 160 | 77 | 62 |
| TB94018 | qz-fsp gneiss | <0.10 | 367 | < 10 | < 10 | < 10 | < 10 | 11 | 33 | < 5 | < 5 | < 10 | < 10 | < 10 | 10 | < 10 |
| TB94023 | qz-fsp gneiss | <0.10 | 480 | < 10 | < 10 | < 10 | < 10 | < 10 | 33 | < 5 | < 5 | < 10 | < 10 | 31 | 25 | 21 |
| TB94037 | qz-fsp gneiss | <0.10 | 528 | < 10 | < 10 | < 10 | < 10 | < 10 | 31 | < 5 | < 5 | < 10 | < 10 | 40 | 39 | 24 |
| TB94304 | qz-fsp gneiss | <0.10 | 674 | < 10 | 69 | < 10 | < 10 | 17 | 57 | 9 | 12 | < 10 | 12 | 30 | < 10 | 13 |
| TB94001 | qz-fsp schist | <0.10 | 194 | < 10 | < 10 | < 10 | < 10 | 16 | 52 | 7 | < 5 | < 10 | < 10 | 80 | 52 | 54 |
| TB94000 | qz-fsp schist | <0.10 | 190 | < 10 | < 10 | < 10 | < 10 | 14 | 47 | 9 | < 5 | < 10 | < 10 | 113 | 90 | 85 |
| TB94003 | qz-fsp schist | <0.10 | 281 | < 10 | < 10 | < 10 | < 10 | 12 | 27 | < 5 | 7 | < 10 | < 10 | 97 | 76 | 80 |

| Sample | Name | S | Ba | Sb | Sn | Cd | Ag | Ga | Zn | Cu | Ni | Yb | Co | Ce | La | Nd |
|---|---|---|---|---|---|---|---|---|---|---|---|---|---|---|---|---|
| TB94004 | qz-fsp schist | <0.10 | 1334 | < 10 | < 10 | < 10 | < 10 | 16 | 90 | 10 | 19 | < 10 | 37 | 119 | 71 | 41 |
| TB94005 | qz-fsp schist | <0.10 | 656 | < 10 | < 10 | < 10 | < 10 | 15 | 42 | 14 | 13 | < 10 | < 10 | 116 | 55 | 48 |
| TB94008 | qz-fsp schist | <0.10 | 951 | < 10 | < 10 | < 10 | < 10 | 17 | 46 | < 5 | < 5 | < 10 | < 10 | 61 | 48 | 44 |
| TB94009 | qz-fsp schist | <0.10 | 615 | < 10 | < 10 | < 10 | < 10 | 12 | 33 | < 5 | < 5 | < 10 | < 10 | 63 | 55 | 43 |
| TB94010 | qz-fsp schist | <0.10 | 900 | < 10 | < 10 | < 10 | < 10 | 16 | 49 | < 5 | < 5 | < 10 | < 10 | 57 | 39 | 31 |
| TB94011 | qz-fsp schist | <0.10 | 851 | < 10 | < 10 | < 10 | < 10 | 12 | 65 | 8 | < 5 | < 10 | < 10 | 67 | 51 | 41 |
| TB94046 | qz-fsp schist | 0.62 | 785 | < 10 | < 10 | < 10 | < 10 | 16 | 74 | 27 | 22 | < 10 | 13 | 20 | 11 | 21 |
| TB94073 | qz-fsp schist | <0.10 | 576 | < 10 | < 10 | < 10 | < 10 | 20 | 10 | 7 | 5 | < 10 | < 10 | 91 | 35 | 41 |
| TB94074 | qz-fsp schist | <0.10 | 840 | < 10 | < 10 | < 10 | < 10 | 16 | 43 | 11 | 8 | < 10 | < 10 | < 10 | < 10 | < 10 |
| TB94301 | qz-fsp schist | <0.10 | 540 | < 10 | < 10 | < 10 | < 10 | 21 | 107 | 38 | 18 | < 10 | 11 | 52 | 22 | 20 |
| TB94305 | qz-fsp schist | <0.10 | 139 | < 10 | < 10 | < 10 | < 10 | 17 | < 5 | < 5 | < 5 | < 10 | < 10 | 32 | < 10 | 16 |
| TB94034 | qz-mica schist | 0.59 | 243 | < 10 | < 10 | < 10 | < 10 | 10 | 55 | 28 | 50 | < 10 | < 10 | < 10 | < 10 | < 10 |
| TB94035 | qz-mica schist | 0.45 | 179 | < 10 | < 10 | < 10 | < 10 | < 10 | 29 | 49 | 52 | < 10 | < 10 | < 10 | 11 | 12 |
| RBL94085 | toumalinit | <0.10 | 120 | < 10 | 10 | < 10 | < 10 | 24 | 76 | < 5 | < 5 | < 10 | < 10 | 12 | < 10 | < 10 |

| Sample | Name | W | Mo | Nb | Zr | Y | Sr | Rb | U | Th | Pb | Cr | V | As | Sc |
|---|---|---|---|---|---|---|---|---|---|---|---|---|---|---|---|
| TB94019 | amphibolite | < 30 | < 5 | 9 | 177 | 65 | 94 | < 5 | < 10 | < 10 | < 10 | 37 | 191 | < 10 | 35 |
| TB94020 | amphibolite | < 30 | < 5 | < 5 | 153 | 54 | 55 | 9 | < 10 | < 10 | < 10 | 61 | 351 | < 10 | 44 |
| TB94024 | amphibolite | < 30 | < 5 | 37 | 154 | 44 | 268 | 5 | < 10 | < 10 | < 10 | 79 | 336 | < 10 | 41 |
| TB94029 | amphibolite | < 30 | < 5 | 14 | 227 | 38 | 120 | 183 | < 10 | 14 | 30 | 118 | 146 | < 10 | 19 |
| TB94031 | amphibolite | < 30 | < 5 | 7 | 52 | 28 | 137 | 9 | < 10 | < 10 | < 10 | 671 | 205 | < 10 | 38 |
| TB94036 | amphibolite | < 30 | < 5 | 20 | 75 | 26 | 203 | < 5 | 10 | < 10 | < 10 | 304 | 240 | < 10 | 31 |
| TB94039 | amphibolite | < 30 | < 5 | 27 | 96 | 36 | 281 | < 5 | 12 | < 10 | < 10 | 222 | 249 | < 10 | 33 |
| TB94051 | amphibolite | < 30 | < 5 | < 5 | 92 | 35 | 204 | 7 | < 10 | < 10 | < 10 | 40 | 359 | < 10 | 47 |
| TB94057 | amphibolite | < 30 | < 5 | 12 | 164 | 50 | 169 | < 5 | < 10 | < 10 | < 10 | 98 | 380 | < 10 | 40 |
| TB94062 | amphibolite | < 30 | < 5 | 12 | 168 | 60 | 95 | 116 | < 10 | < 10 | 25 | 231 | 209 | < 10 | 35 |
| TB94066 | amphibolite | < 30 | < 5 | 32 | 231 | 36 | 191 | 139 | < 10 | < 10 | 23 | 180 | 210 | < 10 | 24 |
| TB94302 | amphibolite | < 30 | < 5 | < 5 | 57 | 37 | 148 | < 5 | < 10 | < 10 | < 10 | 141 | 275 | < 10 | 43 |
| RBL94049a | amphibolite | < 30 | < 5 | < 5 | 62 | 32 | 173 | < 5 | < 10 | < 10 | < 10 | 34 | 346 | < 10 | 48 |
| RBL94051 | amphibolite | < 30 | < 5 | < 5 | 47 | 26 | 170 | < 5 | < 10 | < 10 | < 10 | 43 | 389 | < 10 | 45 |
| RBL94052 | amphibolite | < 30 | < 5 | < 5 | 63 | 29 | 174 | < 5 | < 10 | < 10 | < 10 | 16 | 299 | < 10 | 43 |
| RBL94053 | amphibolite | < 30 | < 5 | < 5 | 50 | 26 | 144 | < 5 | < 10 | < 10 | < 10 | 97 | 319 | < 10 | 42 |
| RBL94054 | amphibolite | < 30 | < 5 | < 5 | 20 | 16 | 219 | < 5 | < 10 | < 10 | < 10 | 179 | 229 | < 10 | 42 |
| RBL94055 | amphibolite | < 30 | < 5 | < 5 | 40 | 22 | 116 | < 5 | < 10 | < 10 | 11 | 110 | 246 | < 10 | 41 |
| RBL94056 | amphibolite | < 30 | < 5 | < 5 | 95 | 43 | 129 | < 5 | < 10 | < 10 | < 10 | 97 | 377 | < 10 | 56 |
| RBL94057 | amphibolite | < 30 | < 5 | < 5 | 51 | 26 | 132 | < 5 | < 10 | < 10 | < 10 | 12 | 354 | < 10 | 50 |
| RBL94061 | amphibolite | < 30 | < 5 | < 5 | 116 | 38 | 71 | 83 | < 10 | < 10 | < 10 | 152 | 286 | < 10 | 42 |
| RBL94064 | amphibolite | < 30 | < 5 | < 5 | 44 | 16 | 294 | 13 | < 10 | < 10 | 19 | 13 | 136 | < 10 | 23 |
| RBL94065 | amphibolite | < 30 | < 5 | < 5 | 41 | 24 | 213 | 21 | < 10 | < 10 | 10 | < 5 | 157 | < 10 | 27 |
| RBL94080 | amphibolite | < 30 | < 5 | 20 | 77 | 26 | 236 | < 5 | < 10 | < 10 | < 10 | 364 | 221 | < 10 | 33 |
| RBL94090 | amphibolite | < 30 | < 5 | 5 | 102 | 20 | 246 | 40 | < 10 | < 10 | 19 | 68 | 202 | < 10 | 19 |
| RBL94091 | amphibolite | < 30 | < 5 | 9 | 97 | 28 | 295 | 12 | 13 | < 10 | < 10 | 356 | 223 | < 10 | 31 |
| RBL94070 | calc silicate | < 30 | < 5 | 14 | 174 | 36 | 282 | 12 | < 10 | < 10 | < 10 | 43 | 79 | < 10 | 19 |
| RBL94075 | calc silicate | < 30 | < 5 | 38 | 213 | 51 | 367 | 32 | 15 | < 10 | < 10 | 121 | 124 | < 10 | 27 |
| RBL94095 | calc silicate | < 30 | < 5 | 35 | 352 | 56 | 48 | 29 | < 10 | < 10 | < 10 | 11 | 216 | < 10 | 32 |
| TB94014 | calc. schist | < 30 | < 5 | 15 | 250 | 32 | 262 | 130 | 12 | 16 | 27 | 158 | 130 | < 10 | 22 |
| TB94016 | calc. schist | < 30 | < 5 | 14 | 186 | 30 | 190 | 139 | < 10 | 16 | 24 | 143 | 133 | < 10 | 19 |
| TB94022 | calc. schist | < 30 | 6 | 11 | 156 | 26 | 102 | 99 | 11 | 17 | 18 | 76 | 123 | < 10 | 16 |
| TB94032 | calc. schist | < 30 | < 5 | 14 | 201 | 32 | 216 | 134 | 13 | 17 | 17 | 129 | 128 | < 10 | 19 |
| TB94038 | calc. schist | < 30 | < 5 | 9 | 176 | 34 | 217 | 85 | < 10 | < 10 | 29 | 146 | 105 | < 10 | 16 |
| TB94050 | calc. schist | < 30 | < 5 | 7 | 168 | 38 | 228 | 21 | 10 | < 10 | 24 | 121 | 82 | < 10 | 16 |
| TB94058 | calc. schist | < 30 | < 5 | 10 | 166 | 32 | 214 | 84 | 13 | 10 | 26 | 114 | 99 | < 10 | 15 |
| TB94063 | calc. schist | < 30 | < 5 | 15 | 168 | 30 | 202 | 112 | < 10 | 11 | 19 | 138 | 114 | < 10 | 17 |
| TB94064 | calc. schist | < 30 | < 5 | 13 | 184 | 38 | 226 | 93 | 17 | 13 | 18 | 126 | 112 | < 10 | 19 |
| TB94089 | calc. schist | < 30 | 7 | 15 | 223 | 16 | 166 | 120 | < 10 | < 10 | 14 | 128 | 154 | < 10 | 15 |

| Sample | Name | W | Mo | Nb | Zr | Y | Sr | Rb | U | Th | Pb | Cr | V | As | Sc |
|---|---|---|---|---|---|---|---|---|---|---|---|---|---|---|---|
| TB94097 | calc. schist | < 30 | < 5 | 12 | 182 | 28 | 88 | 117 | < 10 | 10 | 14 | 73 | 103 | < 10 | 13 |
| RBL94062 | calcareous mica s | < 30 | < 5 | 9 | 163 | 33 | 130 | 88 | < 10 | < 10 | 18 | 146 | 190 | < 10 | 24 |
| RBL94081 | calcareous schist | < 30 | < 5 | 6 | 144 | 33 | 230 | 84 | 21 | < 10 | 15 | 119 | 101 | < 10 | 17 |
| TB94025 | calcite marble | < 30 | < 5 | < 5 | 23 | 21 | 399 | 18 | 24 | < 10 | 98 | 9 | 27 | < 10 | < 10 |
| TB94043 | calcite marble | < 30 | 6 | < 5 | 22 | 17 | 434 | < 5 | 61 | < 10 | 20 | < 5 | 17 | < 10 | < 10 |
| TB94044 | calcite marble | < 30 | < 5 | < 5 | 8 | 15 | 805 | < 5 | 65 | < 10 | < 10 | < 5 | 14 | < 10 | < 10 |
| TB94045 | calcite marble | < 30 | < 5 | 7 | 48 | 35 | 198 | 39 | 40 | < 10 | < 10 | 19 | 55 | < 10 | < 10 |
| TB94052 | calcite marble | < 30 | < 5 | < 5 | 34 | 9 | 2178 | < 5 | 78 | < 10 | < 10 | < 5 | 18 | < 10 | < 10 |
| TB94053 | calcite marble | < 30 | < 5 | < 5 | 29 | 15 | 1677 | < 5 | 45 | < 10 | < 10 | < 5 | 12 | < 10 | < 10 |
| TB94054 | calcite marble | < 30 | < 5 | < 5 | 12 | < 5 | 1021 | < 5 | 36 | < 10 | < 10 | < 5 | 14 | < 10 | < 10 |
| TB94055 | calcite marble | < 30 | < 5 | < 5 | < 5 | 7 | 511 | < 5 | 57 | < 10 | 11 | < 5 | 15 | < 10 | < 10 |
| TB94056 | calcite marble | < 30 | < 5 | < 5 | 15 | 12 | 841 | < 5 | 22 | < 10 | 74 | < 5 | 13 | < 10 | < 10 |
| TB94065 | calcite marble | < 30 | < 5 | < 5 | 20 | < 5 | 997 | < 5 | 92 | < 10 | < 10 | < 5 | 20 | < 10 | < 10 |
| TB94067 | calcite marble | < 30 | < 5 | < 5 | < 5 | < 5 | 838 | < 5 | 18 | < 10 | < 10 | < 5 | 14 | < 10 | < 10 |
| TB94068 | calcite marble | < 30 | < 5 | < 5 | 13 | 8 | 1051 | < 5 | 90 | < 10 | < 10 | < 5 | 14 | < 10 | < 10 |
| TB94076 | calcite marble | < 30 | < 5 | < 5 | 12 | < 5 | 950 | < 5 | 57 | < 10 | < 10 | < 5 | 12 | < 10 | < 10 |
| TB94077 | calcite marble | < 30 | < 5 | < 5 | 13 | < 5 | 931 | < 5 | 41 | 11 | < 10 | < 5 | 14 | < 10 | < 10 |
| TB94084 | calcite marble | < 30 | < 5 | < 5 | 33 | < 5 | 1571 | < 5 | 108 | < 10 | < 10 | < 5 | 17 | < 10 | < 10 |
| TB94085 | calcite marble | < 30 | < 5 | < 5 | 40 | 5 | 2269 | < 5 | 49 | < 10 | < 10 | < 5 | 11 | < 10 | < 10 |
| TB94088 | calcite marble | < 30 | < 5 | < 5 | 26 | 7 | 1622 | < 5 | 36 | < 10 | < 10 | < 5 | 18 | < 10 | < 10 |
| TB94096 | calcite marble | < 30 | < 5 | < 5 | 32 | 11 | 1704 | < 5 | 60 | < 10 | < 10 | < 5 | 14 | < 10 | < 10 |
| TB94098 | calcite marble | < 30 | < 5 | < 5 | 18 | 11 | 982 | < 5 | 36 | < 10 | < 10 | < 5 | 16 | < 10 | < 10 |
| TB94075 | calcite-dolomite m | < 30 | < 5 | < 5 | 16 | < 5 | 1150 | < 5 | 109 | < 10 | < 10 | < 5 | 13 | < 10 | < 10 |
| TB94095 | calcite-dolomite m | < 30 | < 5 | < 5 | 27 | < 5 | 1589 | < 5 | 53 | < 10 | < 10 | < 5 | 17 | < 10 | < 10 |
| TB94099 | calcite-dolomite m | < 30 | < 5 | < 5 | < 5 | < 5 | 308 | < 5 | 28 | < 10 | < 10 | < 5 | 13 | < 10 | < 10 |
| TB94033 | chert | < 30 | < 5 | 34 | 489 | 80 | 188 | 76 | < 10 | 14 | 13 | < 5 | 5 | < 10 | 14 |
| TB94047 | dolomite marble | < 30 | < 5 | < 5 | < 5 | < 5 | 45 | < 5 | 18 | 13 | < 10 | < 5 | 8 | < 10 | < 10 |
| TB94048 | dolomite marble | < 30 | < 5 | < 5 | < 5 | 9 | 78 | < 5 | 42 | < 10 | < 10 | < 5 | 10 | < 10 | < 10 |
| TB94069 | dolomite marble | < 30 | < 5 | < 5 | < 5 | < 5 | 69 | < 5 | 48 | < 10 | < 10 | < 5 | 7 | < 10 | < 10 |
| TB94070 | dolomite marble | < 30 | < 5 | < 5 | < 5 | 5 | 58 | < 5 | 43 | < 10 | < 10 | < 5 | 7 | < 10 | < 10 |
| TB94078 | dolomite marble | < 30 | < 5 | < 5 | < 5 | 6 | 60 | < 5 | < 10 | < 10 | < 10 | < 5 | 8 | < 10 | 10 |
| TB94079 | dolomite marble | < 30 | < 5 | < 5 | < 5 | < 5 | 69 | < 5 | 20 | < 10 | < 10 | < 5 | 11 | < 10 | < 10 |
| TB94080 | dolomite marble | < 30 | < 5 | < 5 | < 5 | < 5 | 132 | < 5 | 31 | < 10 | < 10 | < 5 | 11 | < 10 | < 10 |
| TB94081 | dolomite marble | < 30 | < 5 | < 5 | < 5 | < 5 | 128 | < 5 | < 10 | < 10 | < 10 | < 5 | 7 | < 10 | 10 |
| TB94082 | dolomite marble | < 30 | < 5 | < 5 | < 5 | 6 | 135 | < 5 | 30 | < 10 | < 10 | < 5 | 9 | < 10 | < 10 |
| TB94083 | dolomite marble | < 30 | < 5 | < 5 | < 5 | 6 | 104 | < 5 | 49 | < 10 | < 10 | < 5 | 9 | < 10 | < 10 |
| TB94087 | dolomite marble | < 30 | < 5 | < 5 | < 5 | 5 | 101 | < 5 | 47 | < 10 | < 10 | < 5 | 8 | < 10 | < 10 |
| TB94092 | dolomite marble | < 30 | < 5 | < 5 | < 5 | < 5 | 53 | < 5 | 37 | < 10 | < 10 | < 5 | 10 | < 10 | < 10 |
| TB94093 | dolomite marble | < 30 | < 5 | < 5 | < 5 | < 5 | 82 | < 5 | 46 | 11 | < 10 | < 5 | 9 | < 10 | < 10 |

| Sample | Name | W | Mo | Nb | Zr | Y | Sr | Rb | U | Th | Pb | Cr | V | As | Sc |
|---|---|---|---|---|---|---|---|---|---|---|---|---|---|---|---|
| TB94094 | dolomite marble | < 30 | < 5 | < 5 | < 5 | 6 | 73 | < 5 | 35 | < 10 | < 10 | < 5 | 12 | < 10 | < 10 |
| TB94320 | dolomite marble | < 30 | < 5 | < 5 | < 5 | < 5 | 56 | < 5 | 33 | < 10 | < 10 | < 5 | 12 | < 10 | < 10 |
| RBL94071 | dolomite marble | < 30 | < 5 | 8 | 93 | 29 | 575 | < 5 | 25 | < 10 | < 10 | 35 | 52 | < 10 | 16 |
| RBL94063 | garnet gneiss | < 30 | < 5 | < 5 | 63 | 30 | 490 | 27 | < 10 | < 10 | < 10 | 45 | 182 | < 10 | 27 |
| RBL94073 | gr-mica quartzite | < 30 | < 5 | 6 | 39 | 10 | 18 | 30 | < 10 | < 10 | < 10 | 28 | 28 | < 10 | 15 |
| RBL94074 | gr-mica quartzite | < 30 | < 5 | 10 | 72 | 27 | 74 | 37 | < 10 | < 10 | 12 | 39 | 37 | < 10 | 18 |
| RBL94045 | gr-mica schist | < 30 | < 5 | 16 | 252 | 19 | 49 | 112 | < 10 | < 10 | 24 | 62 | 77 | < 10 | 14 |
| RBL94046 | gr-mica schist | < 30 | < 5 | 22 | 202 | 39 | 92 | 207 | < 10 | < 10 | 38 | 110 | 146 | < 10 | 23 |
| RBL94047 | gr-mica schist | < 30 | < 5 | 18 | 237 | 28 | 78 | 173 | < 10 | 15 | 28 | 139 | 144 | < 10 | 20 |
| RBL94048 | gr-mica schist | < 30 | < 5 | 13 | 211 | 21 | 87 | 173 | < 10 | 13 | 28 | 125 | 146 | < 10 | 27 |
| RBL94094 | gr.-mica schist | < 30 | < 5 | 17 | 160 | 31 | 106 | 157 | < 10 | 14 | 29 | 89 | 110 | < 10 | 24 |
| RBL94098 | gr.-mica schist | < 30 | < 5 | 15 | 202 | 17 | 93 | 106 | < 10 | < 10 | 18 | 99 | 117 | < 10 | 23 |
| RBL94099 | gr.-mica schist | < 30 | < 5 | 19 | 220 | 29 | 105 | 177 | < 10 | 12 | 58 | 111 | 125 | < 10 | 23 |
| RBL94100 | gr.-mica schist | < 30 | < 5 | 33 | 164 | 48 | 72 | 178 | 18 | 92 | 59 | 5 | 10 | < 10 | < 10 |
| RBL94101 | gr.-mica schist | < 30 | < 5 | 15 | 195 | 31 | 112 | 143 | < 10 | < 10 | 20 | 99 | 124 | < 10 | 18 |
| RBL94102 | gr.-mica schist | < 30 | < 5 | 15 | 165 | 29 | 142 | 154 | < 10 | < 10 | 16 | 113 | 127 | < 10 | 22 |
| RBL94103 | gr.-mica schist | < 30 | < 5 | 19 | 227 | 41 | 297 | 125 | < 10 | 12 | 32 | 95 | 124 | < 10 | 26 |
| RBL94104 | gr.-mica schist | < 30 | < 5 | 16 | 183 | 33 | 100 | 183 | < 10 | 12 | 18 | 94 | 119 | < 10 | 20 |
| TB94015 | graphite schist | < 30 | 15 | 14 | 75 | 12 | 41 | 75 | < 10 | 12 | 13 | 57 | 191 | < 10 | < 10 |
| RBL94068 | graphite schist | < 30 | < 5 | < 5 | 53 | 27 | 329 | 23 | 15 | < 10 | 10 | 11 | 203 | < 10 | 27 |
| TB94006 | graphitic schist | < 30 | < 5 | 19 | 225 | 18 | 134 | 251 | < 10 | 24 | 82 | 84 | 140 | < 10 | 18 |
| TB94007 | graphitic schist | < 30 | 51 | 9 | 136 | 39 | 139 | 80 | 19 | 15 | 40 | 111 | 477 | < 10 | 12 |
| RBL94072 | graphitic schist | < 30 | < 5 | 12 | 115 | 44 | 318 | 97 | < 10 | 11 | < 10 | 70 | 88 | < 10 | 17 |
| RBL94087 | graphitic schist | < 30 | < 5 | 7 | 182 | 45 | 225 | 64 | < 10 | < 10 | 20 | < 5 | 238 | < 10 | 24 |
| TB94012a | gt-mica schist | < 30 | < 5 | 18 | 237 | 34 | 66 | 183 | < 10 | 19 | 21 | 96 | 124 | < 10 | 18 |
| TB94012b | gt-mica schist | < 30 | < 5 | 15 | 180 | 23 | 54 | 188 | < 10 | 23 | 27 | 110 | 163 | < 10 | 23 |
| TB94013 | gt-mica schist | < 30 | < 5 | 15 | 188 | 31 | 68 | 165 | < 10 | 16 | 29 | 103 | 150 | < 10 | 22 |
| TB94017 | gt-mica schist | < 30 | < 5 | 16 | 179 | 16 | 86 | 166 | < 10 | 18 | 22 | 90 | 142 | < 10 | 18 |
| TB94021 | gt-mica schist | < 30 | < 5 | 15 | 302 | 24 | 48 | 112 | < 10 | 18 | 20 | 67 | 78 | < 10 | 15 |
| TB94026 | gt-mica schist | < 30 | < 5 | 13 | 218 | 31 | 84 | 128 | < 10 | 18 | 14 | 81 | 117 | < 10 | 13 |
| TB94040 | gt-mica schist | < 30 | < 5 | 18 | 207 | 32 | 124 | 173 | < 10 | 16 | 12 | 105 | 112 | < 10 | 20 |
| TB94041 | gt-mica schist | < 30 | < 5 | 18 | 198 | 36 | 141 | 359 | < 10 | 19 | 55 | 86 | 112 | < 10 | 22 |
| TB94049 | gt-mica schist | < 30 | < 5 | 18 | 204 | 31 | 139 | 209 | < 10 | 22 | 37 | 72 | 108 | < 10 | 15 |
| TB94090 | gt-mica schist | < 30 | < 5 | 16 | 200 | 31 | 126 | 110 | < 10 | 26 | 14 | 101 | 115 | < 10 | 21 |
| RBL94086 | kyanite schist | < 30 | 7 | 13 | 143 | 32 | 278 | 62 | < 10 | < 10 | 22 | 8 | 8 | < 10 | < 10 |
| RBL94096 | kyanite schist | 31 | < 5 | 15 | 178 | 29 | 182 | 85 | < 10 | 57 | 35 | < 5 | 9 | < 10 | < 10 |
| RBL94105 | kyanite schist | < 30 | < 5 | 57 | 242 | 68 | 82 | 153 | 10 | 93 | 44 | 14 | 12 | < 10 | < 10 |
| RBL94106 | kyanite schist | < 30 | < 5 | 37 | 179 | 57 | 102 | 98 | < 10 | 28 | 54 | 18 | 9 | < 10 | < 10 |
| RBL94078 | mantle gr achist | < 30 | < 5 | 11 | 188 | 27 | 111 | 118 | < 10 | < 10 | 14 | 155 | 115 | < 10 | 16 |

| Sample | Name | W | Mo | Nb | Zr | Y | Sr | Rb | U | Th | Pb | Cr | V | As | Sc |
|---|---|---|---|---|---|---|---|---|---|---|---|---|---|---|---|
| RBL94069 | mantle gr schist | < 30 | < 5 | < 5 | 50 | 22 | 455 | 6 | < 10 | < 10 | < 10 | 7 | 219 | < 10 | 32 |
| RBL94088 | mantle gr. schist | < 30 | < 5 | 8 | 175 | 16 | 316 | 35 | < 10 | < 10 | 14 | 78 | 266 | < 10 | 29 |
| RBL94049b | marble w. graphit | < 30 | < 5 | < 5 | < 5 | < 5 | 46 | < 5 | < 10 | < 10 | < 10 | < 5 | 7 | < 10 | < 10 |
| RBL94050 | marble w. graphit | < 30 | < 5 | < 5 | 25 | < 5 | 1138 | < 5 | 65 | < 10 | < 10 | < 5 | 17 | < 10 | < 10 |
| RBL94003 | massive ore | 143 | 29 | 6 | 42 | 7 | 7 | 22 | 12 | 56 | 15900 | 58 | 179 | < 10 | < 10 |
| TB94042 | metagabbro | < 30 | < 5 | 21 | 236 | 49 | 234 | 45 | < 10 | < 10 | 10 | 26 | 358 | 70 | 37 |
| TB94028 | mica schist | < 30 | < 5 | 88 | 667 | 58 | 465 | 40 | < 10 | < 10 | < 10 | < 5 | 17 | < 10 | 12 |
| TB94071 | mica schist | < 30 | < 5 | 13 | 686 | 35 | 54 | 133 | < 10 | 14 | < 10 | 49 | 57 | < 10 | < 10 |
| TB94072 | mica schist | < 30 | 5 | 14 | 363 | 31 | 132 | 139 | < 10 | < 10 | 19 | 50 | 93 | < 10 | 18 |
| RBL94077 | micrcline gneiss | < 30 | < 5 | 9 | 126 | 6 | 524 | 65 | < 10 | < 10 | 13 | 5 | 32 | < 10 | < 10 |
| RBL94107A | microcline gneis | 79 | < 5 | < 5 | 91 | < 5 | 43 | 90 | < 10 | 535 | 136000 | < 5 | 8 | < 10 | < 10 |
| RBL94108 | microcline gneis | < 30 | < 5 | 24 | 455 | 33 | 173 | 202 | 11 | 47 | 169 | < 5 | 30 | 26 | < 10 |
| RBL94005 | microcline gneiss | < 30 | < 5 | 32 | 238 | 40 | 76 | 171 | 17 | 60 | 329 | < 5 | 12 | 12 | < 10 |
| RBL94006 | microcline gneiss | 31 | < 5 | 29 | 202 | 11 | 53 | 158 | < 10 | 59 | 116 | < 5 | 11 | < 10 | < 10 |
| RBL94007 | microcline gneiss | < 30 | < 5 | 26 | 429 | 42 | 199 | 94 | < 10 | < 10 | 53 | < 5 | 25 | 16 | < 10 |
| RBL94008 | microcline gneiss | < 30 | < 5 | 26 | 442 | 39 | 206 | 211 | < 10 | 64 | 43 | < 5 | 23 | 29 | 10 |
| RBL94009 | microcline gneiss | < 30 | < 5 | 26 | 444 | 41 | 189 | 143 | 17 | 57 | 30 | < 5 | 39 | 11 | < 10 |
| RBL94010 | microcline gneiss | < 30 | < 5 | 26 | 471 | 39 | 226 | 162 | 19 | 82 | 61 | < 5 | 37 | 17 | < 10 |
| RBL94011 | microcline gneiss | < 30 | < 5 | 26 | 455 | 37 | 166 | 161 | < 10 | 79 | 43 | < 5 | 31 | 12 | < 10 |
| RBL94012 | microcline gneiss | < 30 | < 5 | 24 | 462 | 40 | 194 | 220 | < 10 | 71 | 54 | < 5 | 31 | < 10 | < 10 |
| RBL94013 | microcline gneiss | < 30 | < 5 | 21 | 405 | 35 | 157 | 224 | < 10 | 67 | 40 | < 5 | 26 | < 10 | < 10 |
| RBL94014 | microcline gneiss | < 30 | < 5 | 22 | 447 | 33 | 143 | 251 | < 10 | 59 | 35 | < 5 | 25 | < 10 | 11 |
| RBL94015 | microcline gneiss | < 30 | < 5 | 23 | 434 | 39 | 158 | 251 | < 10 | 45 | 40 | < 5 | 28 | < 10 | 13 |
| RBL94016 | microcline gneiss | < 30 | < 5 | 23 | 430 | 34 | 176 | 245 | < 10 | 59 | 39 | < 5 | 29 | < 10 | 10 |
| RBL94017 | microcline gneiss | < 30 | < 5 | 27 | 465 | 38 | 169 | 280 | < 10 | 77 | 48 | < 5 | 28 | < 10 | 10 |
| RBL94018 | microcline gneiss | < 30 | < 5 | 23 | 435 | 37 | 170 | 281 | < 10 | 62 | 55 | < 5 | 30 | < 10 | 11 |
| RBL94019 | microcline gneiss | < 30 | < 5 | 26 | 504 | 54 | 205 | 308 | 11 | 71 | 71 | < 5 | 32 | < 10 | 11 |
| RBL94020 | microcline gneiss | < 30 | < 5 | 25 | 442 | 39 | 173 | 277 | < 10 | 73 | 35 | < 5 | 25 | < 10 | < 10 |
| RBL94021 | microcline gneiss | < 30 | < 5 | 22 | 440 | 38 | 184 | 282 | < 10 | 64 | 40 | < 5 | 33 | < 10 | < 10 |
| RBL94022 | microcline gneiss | < 30 | < 5 | 22 | 432 | 42 | 165 | 279 | < 10 | 64 | 34 | 6 | 32 | < 10 | < 10 |
| RBL94023 | microcline gneiss | < 30 | < 5 | 22 | 384 | 34 | 158 | 242 | < 10 | 49 | 25 | 6 | 24 | < 10 | 11 |
| RBL94024 | microcline gneiss | < 30 | < 5 | 20 | 401 | 37 | 162 | 255 | 14 | 68 | 38 | < 5 | 31 | < 10 | 11 |
| RBL94025 | microcline gneiss | < 30 | < 5 | 22 | 383 | 37 | 151 | 233 | < 10 | 53 | 33 | < 5 | 22 | < 10 | < 10 |
| RBL94026 | microcline gneiss | < 30 | < 5 | 24 | 384 | 36 | 159 | 248 | < 10 | 58 | 34 | < 5 | 22 | < 10 | < 10 |
| RBL94027 | microcline gneiss | < 30 | < 5 | 22 | 376 | 24 | 170 | 251 | < 10 | 59 | 37 | < 5 | 28 | < 10 | < 10 |
| RBL94028 | microcline gneiss | < 30 | < 5 | 19 | 423 | 34 | 194 | 244 | < 10 | 48 | 34 | < 5 | 27 | < 10 | 10 |
| RBL94029 | microcline gneiss | < 30 | < 5 | 23 | 423 | 27 | 205 | 174 | 12 | 56 | 42 | < 5 | 43 | < 10 | 11 |
| RBL94030 | microcline gneiss | < 30 | < 5 | 24 | 413 | 43 | 164 | 242 | < 10 | 67 | 34 | < 5 | 25 | < 10 | 12 |
| RBL94031 | microcline gneiss | < 30 | < 5 | 25 | 466 | 54 | 209 | 106 | < 10 | 41 | 32 | < 5 | 37 | < 10 | 13 |

| Sample | Name | W | Mo | Nb | Zr | Y | Sr | Rb | U | Th | Pb | Cr | V | As | Sc |
|---|---|---|---|---|---|---|---|---|---|---|---|---|---|---|---|
| RBL94032 | microcline gneiss | < 30 | < 5 | 23 | 386 | 24 | 144 | 181 | < 10 | 70 | 38 | < 5 | 23 | < 10 | < 10 |
| RBL94033 | microcline gneiss | 35 | < 5 | 21 | 187 | 28 | 113 | 109 | < 10 | 26 | 29 | < 5 | 14 | < 10 | < 10 |
| RBL94034 | microcline gneiss | < 30 | < 5 | 22 | 426 | 20 | 160 | 267 | < 10 | 68 | 33 | < 5 | 33 | < 10 | < 10 |
| RBL94035 | microcline gneiss | < 30 | < 5 | 22 | 409 | 25 | 166 | 254 | < 10 | 67 | 59 | < 5 | 24 | < 10 | 12 |
| RBL94036 | microcline gneiss | < 30 | < 5 | 24 | 405 | 26 | 173 | 237 | < 10 | 81 | 31 | < 5 | 22 | < 10 | < 10 |
| RBL94037 | microcline gneiss | < 30 | < 5 | 28 | 452 | 16 | 216 | 125 | 22 | 76 | 78 | < 5 | 36 | < 10 | < 10 |
| RBL94038 | microcline gneiss | < 30 | < 5 | 27 | 157 | 37 | 62 | 117 | < 10 | < 10 | 13 | 9 | 12 | 15 | < 10 |
| RBL94039 | microcline gneiss | < 30 | < 5 | 26 | 408 | 17 | 122 | 152 | < 10 | 64 | 39 | < 5 | 59 | < 10 | < 10 |
| RBL94058 | microcline gneiss | < 30 | < 5 | 23 | 397 | 38 | 155 | 248 | < 10 | 67 | 33 | < 5 | 29 | < 10 | < 10 |
| RBL94059 | microcline gneiss | < 30 | < 5 | 18 | 291 | 27 | 247 | 264 | < 10 | 52 | 39 | < 5 | 23 | < 10 | < 10 |
| RBL94060 | microcline gneiss | < 30 | < 5 | 23 | 455 | 41 | 175 | 251 | < 10 | 68 | 30 | < 5 | 29 | < 10 | 11 |
| RBL94001 | muscovite schist | < 30 | < 5 | 24 | 185 | 23 | 67 | 108 | < 10 | 44 | 282 | < 5 | 11 | 29 | < 10 |
| RBL94002 | muscovite schist | < 30 | < 5 | 24 | 199 | 20 | 82 | 121 | < 10 | 50 | 92 | 6 | 11 | < 10 | 10 |
| RBL94004 | muscovite schist | 41 | < 5 | 12 | 64 | 16 | 42 | 50 | < 10 | 32 | 2827 | < 5 | 16 | 361 | < 10 |
| RBL94259 | ortho gneiss | < 30 | < 5 | 24 | 107 | 36 | 25 | 56 | < 10 | < 10 | 124 | < 5 | 6 | < 10 | < 10 |
| RBL94260 | ortho gneiss | < 30 | < 5 | 16 | 141 | 9 | 128 | 139 | < 10 | < 10 | 21 | 11 | 6 | < 10 | < 10 |
| RBL94261 | ortho gneiss | < 30 | < 5 | 9 | 69 | 19 | 71 | 140 | < 10 | 19 | 33 | 13 | 6 | < 10 | < 10 |
| RBL94076 | po-skarn | < 30 | < 5 | 37 | 172 | 50 | 459 | 9 | < 10 | < 10 | 12 | 26 | 79 | < 10 | 25 |
| RBL94097 | psammitic schist | < 30 | < 5 | 12 | 204 | 17 | 59 | 60 | < 10 | 11 | 14 | 41 | 57 | < 10 | < 10 |
| TB94303 | quartz-mica schis | < 30 | < 5 | 6 | 42 | 9 | 17 | 57 | < 10 | 11 | < 10 | 22 | 36 | < 10 | < 10 |
| TB94027 | quartzite | 32 | < 5 | < 5 | 117 | 14 | 10 | 40 | 17 | 22 | < 10 | 17 | 22 | < 10 | < 10 |
| RBL94079 | quartzite | < 30 | < 5 | 7 | 143 | 23 | 56 | 47 | < 10 | < 10 | 40 | < 5 | 7 | < 10 | 12 |
| RBL94040 | qz-fld schist | < 30 | < 5 | 32 | 215 | 38 | 150 | 99 | 11 | 63 | 49 | 8 | 5 | < 10 | < 10 |
| RBL94041 | qz-fld schist | < 30 | < 5 | 27 | 118 | 30 | 54 | 82 | < 10 | 31 | 23 | < 5 | 6 | < 10 | < 10 |
| RBL94042 | qz-fld schist | < 30 | < 5 | 32 | 136 | 47 | 115 | 102 | < 10 | 36 | 75 | < 5 | 5 | < 10 | < 10 |
| RBL94043 | qz-fld schist | < 30 | 6 | 38 | 172 | 34 | 134 | 108 | < 10 | 18 | 47 | < 5 | 6 | < 10 | < 10 |
| RBL94044 | qz-fld schist | < 30 | < 5 | 19 | 220 | 29 | 63 | 126 | < 10 | 23 | 25 | < 5 | 8 | < 10 | < 10 |
| RBL94082 | qz-fld schist | < 30 | < 5 | 10 | 136 | 28 | 180 | 66 | < 10 | < 10 | 17 | < 5 | 11 | < 10 | 10 |
| RBL94084 | qz-fld schist | < 30 | < 5 | 13 | 138 | 22 | 191 | 125 | < 10 | < 10 | 23 | < 5 | 9 | < 10 | < 10 |
| RBL94089 | qz-fld schist | < 30 | < 5 | 13 | 148 | 39 | 375 | 182 | < 10 | 24 | 36 | < 5 | 11 | < 10 | < 10 |
| RBL94092 | qz-fld schist | < 30 | < 5 | 24 | 142 | 29 | 136 | 167 | < 10 | < 10 | < 10 | < 5 | 10 | < 10 | < 10 |
| RBL94093 | qz-fld schist | < 30 | < 5 | 25 | 291 | 47 | 67 | 189 | < 10 | 43 | 29 | < 5 | 12 | < 10 | < 10 |
| TB94018 | qz-fsp gneiss | 32 | < 5 | 6 | 72 | 6 | 62 | 111 | < 10 | 29 | 14 | < 5 | 9 | < 10 | < 10 |
| TB94023 | qz-fsp gneiss | 31 | < 5 | 13 | 86 | 22 | 52 | 107 | < 10 | 12 | 19 | < 5 | 5 | < 10 | < 10 |
| TB94037 | qz-fsp gneiss | < 30 | < 5 | 10 | 89 | 28 | 98 | 125 | < 10 | 19 | 17 | < 5 | < 5 | < 10 | < 10 |
| TB94304 | qz-fsp gneiss | < 30 | < 5 | 16 | 603 | 33 | 44 | 106 | < 10 | 19 | 27 | 49 | 130 | < 10 | 17 |
| TB94001 | qz-fsp schist | < 30 | < 5 | 29 | 149 | 47 | 41 | 166 | 14 | 86 | 27 | < 5 | < 5 | < 10 | < 10 |
| TB94000 | qz-fsp schist | < 30 | < 5 | 29 | 184 | 62 | 37 | 197 | 18 | 94 | 35 | < 5 | < 5 | < 10 | < 10 |
| TB94003 | qz-fsp schist | < 30 | < 5 | 31 | 167 | 46 | 28 | 192 | 16 | 97 | 29 | < 5 | 6 | < 10 | < 10 |

*Major elements in %, minor in ppm*

XRF, major and minor elements

| Sample | Name | W | Mo | Nb | Zr | Y | Sr | Rb | U | Th | Pb | Cr | V | As | Sc |
|---|---|---|---|---|---|---|---|---|---|---|---|---|---|---|---|
| TB94004 | qz-fsp schist | < 30 | < 5 | 15 | 211 | 35 | 356 | 186 | < 10 | 14 | 15 | 7 | 225 | < 10 | 21 |
| TB94005 | qz-fsp schist | < 30 | < 5 | 24 | 215 | 49 | 304 | 85 | < 10 | 19 | 24 | 31 | 50 | < 10 | 13 |
| TB94008 | qz-fsp schist | 32 | < 5 | 19 | 198 | 37 | 24 | 184 | < 10 | 46 | 14 | 6 | 10 | < 10 | < 10 |
| TB94009 | qz-fsp schist | < 30 | < 5 | 15 | 173 | 33 | 26 | 175 | < 10 | 47 | 21 | 15 | 10 | < 10 | < 10 |
| TB94010 | qz-fsp schist | < 30 | < 5 | 15 | 191 | 34 | 71 | 162 | 11 | 31 | 77 | < 5 | 7 | < 10 | < 10 |
| TB94011 | qz-fsp schist | < 30 | < 5 | 19 | 198 | 41 | 43 | 182 | < 10 | 41 | 24 | < 5 | 6 | < 10 | < 10 |
| TB94046 | qz-fsp schist | < 30 | < 5 | 13 | 290 | 32 | 140 | 95 | < 10 | 28 | 41 | 67 | 90 | < 10 | 22 |
| TB94073 | qz-fsp schist | < 30 | < 5 | 20 | 210 | 27 | 43 | 177 | < 10 | 28 | 10 | < 5 | 36 | < 10 | 12 |
| TB94074 | qz-fsp schist | < 30 | < 5 | 14 | 379 | 21 | 127 | 121 | < 10 | < 10 | 23 | 32 | 84 | < 10 | 11 |
| TB94301 | qz-fsp schist | < 30 | < 5 | 15 | 234 | 37 | 107 | 174 | < 10 | 17 | 22 | 102 | 137 | < 10 | 21 |
| TB94305 | qz-fsp schist | < 30 | < 5 | 21 | 99 | 30 | 21 | 285 | < 10 | 87 | < 10 | 6 | < 5 | < 10 | < 10 |
| TB94034 | qz-mica schist | < 30 | 16 | 7 | 96 | 6 | 36 | 56 | 14 | 17 | < 10 | 52 | 112 | < 10 | 11 |
| TB94035 | qz-mica schist | < 30 | 28 | < 5 | 43 | 22 | 26 | 36 | 19 | < 10 | < 10 | 27 | 164 | < 10 | < 10 |
| RBL94085 | toumalinit | < 30 | 5 | 5 | 112 | 10 | 252 | 17 | < 10 | < 10 | 29 | < 5 | 20 | < 10 | 12 |

# GEOLOGY OF THE OKSTINDANE AREA, NORDLAND